

Old Dominion University
ODU Digital Commons

OES Theses and Dissertations


Ocean & Earth Sciences

Winter 2009

Biogenic Tracers Through the Holocene on the Alaskan Shelf

Carie A. Curry
Old Dominion University

Follow this and additional works at: https://digitalcommons.odu.edu/oeas_etds

 Part of the [Climate Commons](#), [Geochemistry Commons](#), [Oceanography Commons](#), and the [Paleobiology Commons](#)

Recommended Citation

Curry, Carie A.. "Biogenic Tracers Through the Holocene on the Alaskan Shelf" (2009). Master of Science (MS), Thesis, Ocean & Earth Sciences, Old Dominion University, DOI: 10.25777/015c-rr07
https://digitalcommons.odu.edu/oeas_etds/35

This Thesis is brought to you for free and open access by the Ocean & Earth Sciences at ODU Digital Commons. It has been accepted for inclusion in OES Theses and Dissertations by an authorized administrator of ODU Digital Commons. For more information, please contact digitalcommons@odu.edu.

**BIOGENIC TRACERS THROUGH THE HOLOCENE ON THE
ALASKAN SHELF**

by

Carie A. Curry
B.S. December 2006, Old Dominion University, Norfolk, Virginia


A Thesis Submitted to the Faculty of
Old Dominion University in Partial Fulfillment of the
Requirement for the Degree of

MASTERS OF SCIENCE

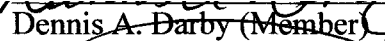
OCEAN AND EARTH SCIENCES

OLD DOMINION UNIVERSITY
December 2009

Approved by:



Gregory A. Cutter (Director)



Dennis A. Darby (Member)



David J. Burdige (Member)

ABSTRACT

BIOGENIC TRACERS THROUGH THE HOLOCENE ON THE ALASKAN SHELF

Carie A. Curry
Old Dominion University, 2009
Director: Dr. Gregory A. Cutter

Dramatic environmental changes in the Arctic Ocean have been observed for the last two decades including changing the amount of sea ice thickness and extent, and increased river discharge. In order to put these and other current day observations into historical context and perhaps reveal mechanisms controlling them, a suite of paleo-proxies were used to analyze two high resolution cores collected on the 2005 HOTRAX expedition. The goals of this research were: (1) develop an analytical method for determining biogenic calcite, (2) identify the major sources of biogenic matter into the system over the Holocene, and (3) assemble the history of depositional events that have occurred in the Alaskan shelf over the Holocene.

The C/N and $\delta^{13}\text{C}$ in the very earliest record at Station 5, 12,000 ybp, suggest marine conditions prior to the inundation of glacial outwash and terrestrial organic matter. From 12,000 to 9600 ybp abundant amounts of terrestrially-derived materials were delivered to the Alaskan shelf, confirmed by dolomite, high C/N ratios, heavy $\delta^{13}\text{C}$ signatures, and low sulfur. Immediately following these terrestrial inputs, a thousand year transition period re-established marine conditions like those found in the late Holocene. In the mid-Holocene, 6000 - 1000 ybp, increased concentrations of pyrite occurred at this time because enough labile organic matter was deposited for anoxic conditions to occur, and sufficient amounts of sulfate and iron were available.

The most recent record, 1000 ybp to present, shows much different biogeochemical conditions than in the mid to early Holocene, organic carbon concentrations are 50% higher, but anoxic conditions do not appear to be present likely due to high amounts of bioturbation, enhancing oxygen penetration into the upper sediments.

In terms of the marine sources of organic matter in the mid and late Holocene, their origin appears to be diatoms or other siliceous organisms. The recent observations of coccolithophores in the Bering Sea suggest that other phytoplankton species could be present in high latitude waters, but they were not found in the Holocene records examined here. With respect to other environmental changes occurring in the Arctic at present, it will interesting to see if increased river discharges shift the Alaskan shelf to a more terrestrially-dominated system as seen in the earliest Holocene.

ACKNOWLEDGMENTS

I am very grateful to Dr. Gregory Cutter and my thesis committee, Dr. Burdige and Dr. Darby, for their support and guidance through this research. Their advice and guidance have been very helpful. Special thanks to Brandon Gipson and other graduate, undergraduate and lab staff that have helped me accomplish this data intensive research. I extend many thanks to all the graduate students for their friendship, conversations, and an outlet for many moments of frustration. Finally, I thank the National Science Foundation for support on this project and several others in which I have been fortunate enough to participate.

This thesis is dedicated to my daughter, Alexandra, who has been my inspiration.

TABLE OF CONTENTS

	Page
LIST OF TABLES	ix
LIST OF FIGURES	x
 Chapter	
1. CHANGES IN THE ARCTIC	1
1.1. INTRODUCTION	1
1.2. BACKGROUND	3
1.3. STATION P1	6
1.4. RESEARCH OBJECTIVES	13
2. SAMPLING AND ANALYTICAL METHODS	14
2.1. SAMPLING	14
2.2. ANALYTICAL METHODS	15
2.3. AGE MODELS	17
2.4. DIAGENETIC CALCULATIONS	17
3. DETERMINATION OF BIOGENIC CARBONATE	19
3.1. BACKGROUND	19
3.2. EXPERIMENTAL SECTION	21
3.2.1. APPARATUS	21
3.2.2. STANDARDS AND REAGENTS	21
3.2.3. PROCEDURE FOR TOTAL CARBONATE	23
3.2.4. PROCEDURE FOR BIOGENIC CARBONATE	23
3.2.5. CALCULATIONS	24
3.2.6. REGRESSIONS TO CALCULATE BIOGENIC CARBONATE	25
3.3. DISCUSSION	27
3.3.1. OPTIMIZATION OF BIOGENIC CARBONATE RECOVERY	27
3.3.2. SEPARATING BIOGENIC FROM REFRACTORY CARBONATE	28
3.3.3. RECOVERIES OF CARBONATE UNDER OPTIMIZED CONDITIONS	31
3.3.4. ANALYTICAL FIGURES OF MERIT	39
3.4. CONCLUSIONS	40

Chapter	Page
4. BIOGENIC MATTER THROUGH THE HOLOCENE	41
4.1. INTRODUCTION	41
4.2. RESULTS	43
4.2.1. AGE MODEL	43
4.2.2. CARBON, NITROGEN AND SULFUR	45
4.2.3. BIOGENIC SILICA	47
4.2.4. BIOGENIC CARBONATE	49
4.2.5. TOTAL CARBONATE	49
4.2.6. CARBON AND NITROGEN ISOTOPES	51
4.2.7. TOTAL SULFUR AND SULFUR SPECIATION	52
4.3. DISCUSSION	55
4.3.1. TEMPORAL AND REGIONAL TRENDS	55
4.3.2. SOURCES OF ORGANIC MATTER	62
4.3.3. INTEGRITY OF THE SEDIMENT RECORDS	65
4.4. SUMMARY	66
 REFERENCES	 69
 APPENDICES	
A. STATION P1 DATA	75
B. MULTICORE 6 DATA	79
C. MULTICORE 8 DATA	81
D. TC05 DATA	82
E. TC08 DATA	83
F. JPC05 DATA	84
G. JPC08 DATA	88
 VITA	 90

LIST OF TABLES

Table	Page
1. CM 5014 Settings for Standard Operating Procedures for Total Carbonate Method	22
2. Autosampler Tray Format	24
3. CM5014 Settings for Standard Operating Procedures for Biogenic Carbonate Method.....	25
4. Linear Regression Results for Black Sea Sediment Analyzed Using the Optimized Conditions of pH 5 1M Sodium Acetate Solution and 10°C.....	27
5. Sample Regression Data Using Biogenic Carbonate Procedures and Linear Regression From 40-60 minutes	31

LIST OF FIGURES

Figure	Page
1. Study area where sediment samples were obtained at Station P1 in 1992 by the USGS, and Stations 5 and 8 from Leg 1 of the HOTRAX cruise, June 2005 [Jakobsson <i>et al.</i> , 2004].....	7
2. Organic carbon, organic nitrogen, total sulfur, and atomic C:N [Darby <i>et al.</i> , 2001] for Station P1.	9
3. Organic carbon, biogenic silica, atomic C:S ratio and atomic Cd:Ca ($\times 10^{-7}$) for Station P1 [Darby <i>et al.</i> , 2001].....	10
4. Evolution of CO ₂ from two carbonate minerals using a pH 5 buffer and 10°C.....	26
5. Varying combinations of temperature and pH used to: (a) minimize recovery of dolomite, (b) optimize the recovery of calcium carbonate.....	29
6. Linear regressions for the CO ₂ evolution from a 10% mixture of Black Sea sediment and pure dolomite to determine analysis time and the time over which the regression is carried out (0-60 min., 10-60 min., 30-60 min., etc).....	30
7. Composite graph showing CO ₂ evolution from different types of carbonate minerals and natural samples using a pH 5 buffer and 10°C	32
8. Calcium carbonate (reagent grade) response to pH 5 and 10°C treatment.....	34
9. Dolomite response to pH 5 and 10° C treatment	35
10. Chalk response to pH 5 and 10° C treatment	36
11. Responses of two Black Sea sediments (light and dark; see text) to pH 5 and 10°C treatment	37
12. Responses of three Black Sea/dolomite mixtures, pure dolomite, and “pure” Black Sea sediment used in the mixtures to pH 5 and 10° C treatment.....	38
13. Analyses of three Black Sea sediment-dolomite mixtures under optimized conditions (including linear regressions of the “dolomite drift” to determine the concentration of biogenic carbonate) at pH 5 and 10°C.	40

Figure	Page
14. Organic carbon, organic nitrogen, and total sulfur versus age at Station 5.....	44
15. Organic carbon, organic nitrogen, and total sulfur versus age at Station 8.....	46
16. Biogenic silica versus age at Stations 5 and 8.....	48
17. Total carbonate versus age at Stations 5 and 8.....	50
18. Organic carbon and nitrogen isotopes versus age at Station 5.....	51
19. Acid volatile sulfide (AVS, primarily FeS), greigite (Fe ₃ S ₄), and pyrite (FeS ₂) versus age in Multicore 6 that is adjacent to Station 5.....	53
20. Total sulfur and pyrite versus age at Station 5.....	54
21. Atomic organic carbon:organic nitrogen ratios versus age at Stations 5, 8, and P1.....	56
22. Overlays of organic carbon, organic nitrogen, total sulfur, and biogenic silica at Stations P1, 5, and 8.....	58
23. Degree of pyritization (calculated at the ratio of pyrite sulfur to total sulfur) as a function of age at Station 5.....	61
24. Known isotopic source materials (boxes) overlying organic carbon and nitrogen isotope data from Station 5.....	62
25. Plots of (a) organic carbon versus age at Station 5 and (b) Atomic C/N versus $\delta^{13}\text{C}$ from Station 5, with known organic matter sources identified.....	64
26. Sources of organic matter (OM) through the Holocene on the Alaskan shelf.....	68

CHAPTER 1

CHANGES IN THE ARCTIC

1.1. Introduction

Dramatic changes in the Arctic Ocean have been observed for the last two decades [Overland *et al.*, 2008]. Warming global temperatures are changing the amount of sea ice thickness and ice extent. Rapid changes in sea ice have been intensely monitored and most recently the lowest ice extent was recorded in September 2007 with 4.2 million km², approximately 23% less ice than the last record low in September 2005 [Strove *et al.*, 2008; Comiso *et al.*, 2008; Perovich and Richter-Menge, 2007]. The loss of sea ice changes the planet's albedo and allows more heating in the Arctic Ocean and increases sea surface temperature. A 4% per year increase of solar heating has occurred in the past decades in the Chukchi and adjacent seas [Pervioch *et al.*, 2007] and sea surface temperatures as high as 5°C during the 2007 record ice minimum [Steele *et al.*, 2008].

Melting sea ice and increased river discharges to the Arctic Ocean lower its salinity. The Pan-Arctic drainage basin covers 22.4 million km² and contributes approximately 128 km³ (0.004 Sv) of freshwater from six major Eurasian rivers [Peterson *et al.*, 2002]. Increasing global temperature and intensification of positive North Atlantic Oscillation (+NAO) has been linked with increased river discharge which suggests that river discharge is responding to large-scale climatic changes [Peterson *et al.*, 2002; Serrez *et al.*, 2000]. The Labrador and Norwegian Seas are

The model journal for this thesis is *Paleoceanography*.

sources of cold water that are major contributors to North Atlantic Deep Water (NADW) [Swift *et al.*, 1980; Aagaard *et al.*, 1991]. The formation of North Atlantic Deep Water is best known for its role as the key link that drives global thermohaline circulation, transferring heat from low to high latitudes and moderating the climate in northern Europe [Seager *et al.*, 2002]. An increase of Pan-Arctic drainage and increased meltwater from glaciers could sufficiently freshen the Labrador and Norwegian Seas that the formation of NADW is disrupted [Teller *et al.*, 2002].

In addition to increasing sea surface temperature and changes in salinity, a decrease in sea ice abundance, more open water, and wave activity have increased the depth of the euphotic zone and increased ventilation that transports nutrients from below the mixed layer. With more nutrients and light available in the surface of the Arctic, the depth at which primary production occurs deepens below the stratified surface layer and into the thermocline [Hill *et al.*, 2005]. Increasing amounts of primary production during the summer months amplifies the amount of biogenic material deposited in the coastal and shelf sediments. Additionally, inputs of terrestrial organic matter from meltwater runoff and coastal erosion are increasing [Belicka *et al.*, 2004]. Events recorded in these coastal sediments can show the dynamic changes that the Arctic Ocean has undergone.

The goal of this research was to establish a Holocene record of biogenic sources in the western Alaskan shelf. Proxies for biogenic sources were used to measure climatic and environmental changes. This research helps elucidate the biogeochemical processes on the Alaskan shelf that have occurred as a function of climate change in the Holocene.

1.2. Background

Biogeochemical processes in the Arctic Ocean have only recently begun to be examined. The Shelf-Basin Interaction (SBI) program was initiated to improve the understanding of the impacts of global change on the physical and biogeochemical interactions among the Arctic shelf, slope, and basins [Grebmeier *et al.*, 1998, 2001; Grebmeier, 2003]. The SBI program focused on the Chukchi and Beaufort Seas from 1998 to 2008. The key efforts of the SBI program were centered on water mass exchange, material fluxes, biogeochemical cycling, and monitoring the responses to rapid climate changes that are anticipated to occur.

The historical work from Phase I of SBI, and surveying and mooring data from Phase II, has provided an extensive data set. *Codispoti et al.* [2005] evaluated physical shelf-basin mixing processes and the impact on nutrients in the upper halocline. The advection of nutrients from the Bering Strait was identified as the source of high rates of productivity on the shelf and limited production within the basin. A report on plankton distribution within the water column [Ashjian *et al.*, 2005] supported the conclusions of *Codispoti et al.* [2005] that both nutrients and particulate material are transported along the shelf rather than basin-ward. Primary production rates were measured by *Hill et al.* [2005] over the shelf, slope, and deeper basin waters. The average annual production was $80 \text{ g C m}^{-2} \text{ yr}^{-1}$ on the shelf and declined to $<20 \text{ g C m}^{-2} \text{ yr}^{-1}$ in the Canada Basin. Very high rates of production were observed in Barrow Canyon ($>400 \text{ g C m}^{-2} \text{ yr}^{-1}$) and the Bering Sea ($>800 \text{ g C m}^{-2} \text{ yr}^{-1}$). The estimate of surface primary production in the Chukchi shelf by $^{234}\text{Th}/^{238}\text{U}$ disequilibrium was 940 g

$\text{C m}^{-2} \text{ yr}^{-1}$, with an export flux of $17 \text{ g C m}^{-2} \text{ yr}^{-1}$, approximately 18% of total surface production [Moran *et al.*, 1997]. Notably, this area of the Arctic is the most biologically active region of any ocean [Springer and McRoy, 1993].

Other work that has been completed in the Arctic Ocean near the Chukchi Sea gives a better understanding of the changes in biogeochemical and physical processes as climate has altered. Changes in overall circulation affect the Arctic Ocean on different time scales. Arctic circulation is mainly driven by inflowing waters from the Atlantic and prevailing winds which drive the Trans Polar Drift System [Mysak, 2001; Rigor *et al.*, 2006]. The observed changes in sea-ice in the past 50 years reveal seasonal changes in circulation on decadal and multi-decadal scales. The circulation of the Arctic Ocean is a complex interaction between the amount of sea ice cover, prevailing winds, and large-scale atmospheric circulation patterns [Mysak, 2001]. The Chukchi shelf has undergone significant change as an extensive system of paleochannels have been cut and subsequently buried with sediment [Hill *et al.*, 2006; Kegwin *et al.*, 2006]. High amounts of outwash from the last glacial maximum have filled paleochannels with a complex stratigraphy of large meltwater events and cyclic changes in sea level. Interestingly, radiometrically-dated peats and storm deposits from northwest Alaska have recorded only a 1.5 m rise in sea level during the past 6000 yrs due to isostatic rebound which is considerably slower compared to other passive margins in North America [Mason and Jordan, 2001].

During the Holocene there have been many events that have been recorded in the marine sediment records in the Arctic Ocean. Large inputs of freshwater have had a major impact on the salinity, nutrients, and eustatic sea level in the Arctic Ocean

[Kegwin *et al.*, 2006]. The initial outburst and draining of Lake Agassiz have been suggested as the major cause of the dramatic cold event, the Younger Dryas, ca. 12.9 kybp [Hillarie-Marcel *et al.*, 2007]. Approximately 9500 km³ of fresh water was discharged through the Great Lakes and St. Lawrence River into the Arctic Ocean during a transitional mode from glacial to interglacial circulation, disrupting thermohaline circulation [Teller *et al.*, 2002]. The final collapse of Lake Agassiz, ca. 8200 ybp, contributed an additional 163,000 km³ of freshwater [Teller *et al.*, 2002] and carbonate-rich turbidite layers [Hillarie-Marcel *et al.*, 2007]. During this time the North Atlantic had stabilized into a strong interglacial circulation pattern and the North Atlantic Deep Water formation did not suffer significant changes [Teller *et al.*, 2002]

Climate change in the Arctic has also been determined to occur in cyclic patterns of warming and cooling. Using Arctic sediments, Bond *et al.* [1997] found that a millennial pacing of climate change, approximately 1470 ± 532 years, occurs independent of the glacial-interglacial climate state. This periodic warming and cooling of the Arctic Ocean is reflected in the timing of major climate events such as the Younger Dryas (12,900 ybp), the 8200 ybp cooling event, the Medieval Warm Period (1300 ybp), and the Little Ice Age (300 ybp).

The timing and effects of the opening of Bering Strait during glacial and interglacial cycles have also imprinted their changes to the Arctic Ocean and are reflected in the sediments. Deep channels have been cut through the Barrow Canyon by scouring flood waters [Phillips *et al.*, 1988]. Increases of $\delta^{18}\text{O}$ in planktonic foraminifera and $\delta^{13}\text{C}$ in carbonaceous mollusc shells are consistent with increase in salinity and transition from estuarine to more open ocean conditions approximately

12,000 ybp [Kegwin *et al.*, 2006]. Variations in chlorite and muscovite minerals deposited in the sediments reflect the inflow of Pacific water through the Bering Strait [Ortiz *et al.*, 2009]. Recent observations (1990-1991) show the overall salinity and ventilation in the Arctic Ocean is set by the inflow of waters through the Bering Strait [Woodgate *et al.*, 2008].

1.3. Station P1

In 1992, the United States Geological Survey (USGS) obtained sediment cores in effort to complete a paleo-environmental profile for the changing climatic conditions in the Chukchi Basin during the Holocene [Polyak *et al.*, 2007]. A core was obtained at Station P1 during Cruise P1-92-AR (hereafter called P1), located on the Chukchi Slope (73.42° N, 162.45° W, 201 m water depth; Figure 1) and subsequently analyzed as part of the SBI Phase I program [Darby *et al.*, 2001]. Core P1 was approximately 429 cm in length, but only 220 cm encompassed the Holocene record. Radiocarbon dating was performed on carbonate shells found in the core. The sedimentation rates at Station P1 were somewhat variable, about 22 cm ky⁻¹ [Darby *et al.*, 2001].

Organic carbon (Org. C) in the core recovered at Station P1 varied between 1 to 2% through the Holocene (Figure 2). A minimum of 1.0% organic carbon occurred at 9600 ybp and a steady increase of organic carbon reached a maximum of 2% by 7500 ybp. Little variation occurred between 7500 to 1100 ybp with an average of 1.6%. Another maximum occurs near the surface, around 700 ybp. Although not much is known about the concentration of organic carbon, burial rates, and rates of remineralization on the Alaskan shelf, these values are typical of other Arctic shelf sediments [Naidu *et al.*, 2004]. In comparison, the organic carbon in the Alaskan shelf

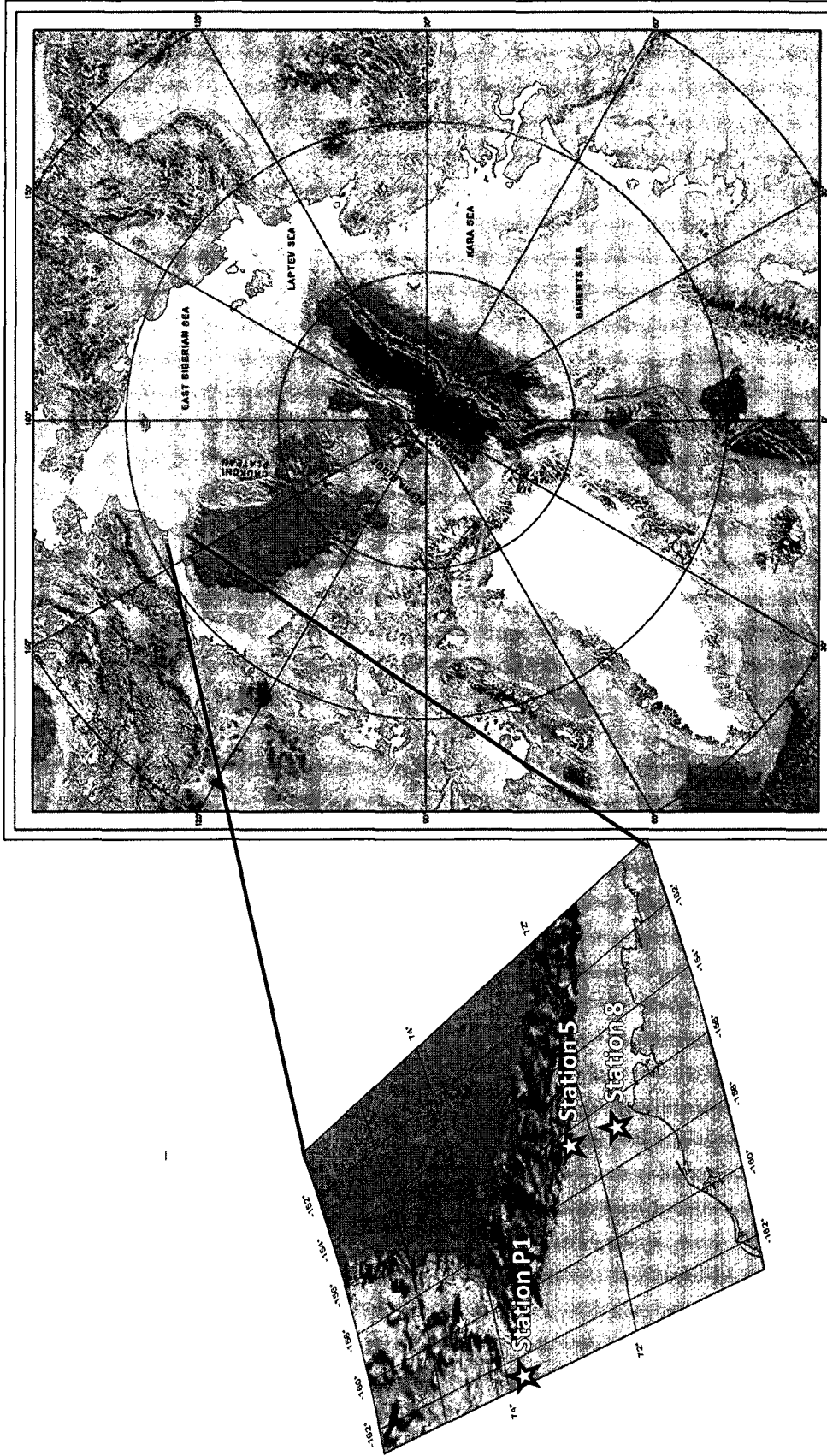


Figure 1. Study area where sediment samples were obtained at Station P1 in 1992 by the USGS, and Stations 5 and 8 from Leg 1 of the HOTRAX cruise, June 2005 [Jakobsson et al., 2004].

is similar to that found in the Mackenzie shelf and the Laptev Sea, ca. 0.5 to 2.0%, and somewhat similar to slightly higher organic carbon concentration in the Kara Sea and Barents Sea [Stein and Fahl, 2004, Stein and Fahl, 2004a, Vertov and Romankevich, 2004, Macdonald et al., 2004].

Organic nitrogen (Org. N) parallels the trends in organic carbon over the Holocene (Figure 2) and varied between 0.08 to 0.24%. In the early Holocene, Org. N values reached their minimum around 9600 ybp. A steady increase of nitrogen to 0.16% occurred, and then constant concentrations were maintained until 1100 ybp. The surface maximum occurred near 600 ybp, with a value of 0.24% nitrogen. The sources of nitrogen and organic carbon can be partially identified by the atomic Org. C:Org. N ratios and compared to that of the Redfield ratio which defines the marine end-member as 6.6 [Redfield et al., 1963]. During the early Holocene C:N values were relatively high, from 15 to 20 (Figure 2). A higher C:N ratio, typically > 15, indicates terrestrially-derived organic matter [Bordovskiy, 1965]. An increase of organic carbon and nitrogen occurred in the last 1000 years, with a lower C:N ratio of 10. This suggests an increase in marine primary production in overlying surface waters.

Total sulfur in P1 also parallels Org. C and Org. N, but with slightly more fluctuations. It has a maximum of 0.4% at 7700 ybp and a minimum of 0.06% at 9600 ybp (Figure 2). An additional sulfur minimum is shown near the surface. This low sulfur event occurs at the same time as an increase of carbon and nitrogen. Preservation of sulfur and organic carbon in sediments is strongly affected by microbial respiration via sulfate reduction [Howarth, 1983]. As bacteria use sulfate as the terminal electron acceptor to anaerobically oxidize organic carbon, sulfate is metabolically reduced to

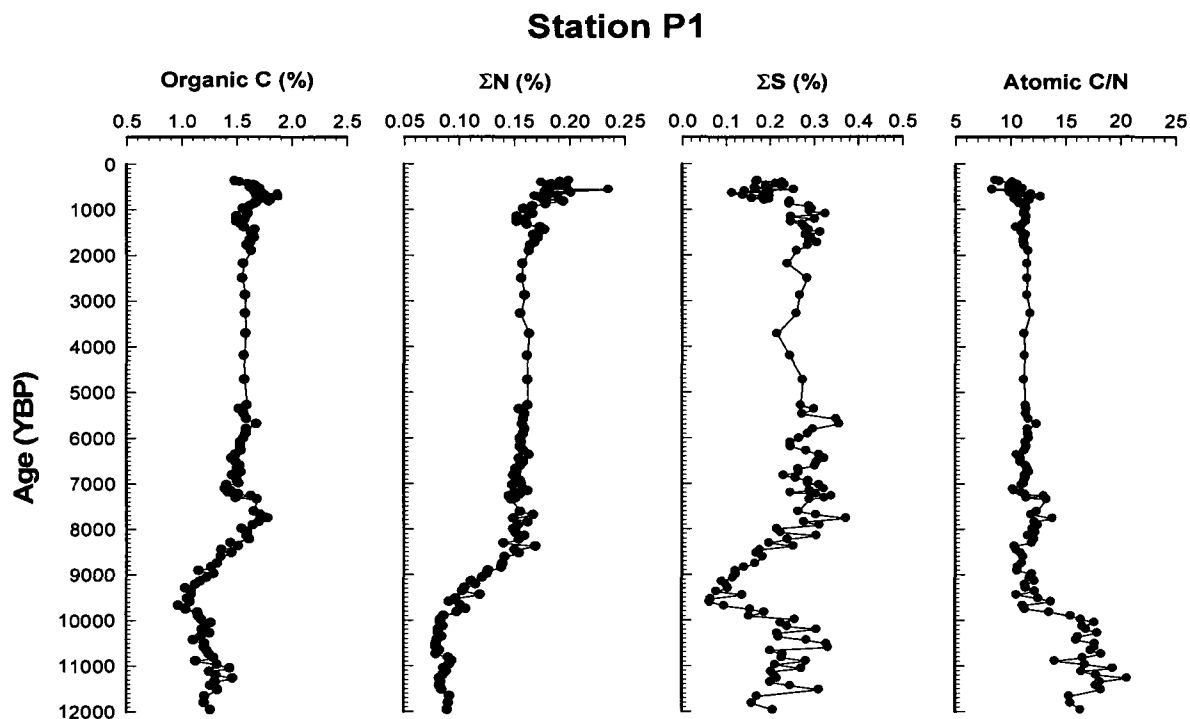


Figure 2. Organic carbon, organic nitrogen, total sulfur, and atomic C:N [Darby *et al.*, 2001] for Station P1.

hydrogen sulfide (and many other intermediate sulfur species), and reacts with iron oxides to form mackinawite (FeS) and eventually pyrite (FeS_2) [Goldhaber, 1974]. The samples from P1 were not analyzed for reduced sulfur constituents, though a considerable amount of sulfur may actually be in these reduced forms. To this end, the organic carbon to pyrite (Org.C:Pyrite) ratio is a useful paleo-environmental indicator of anoxic remineralization of organic carbon [Bernier and Raiswell, 1983]. The organic carbon to total sulfur (Org.C:S) ratios for P1 (Figure 3) show values around 10 to 15 for most of the Holocene. This is typical of a marine environment where seawater-sulfate is ‘recorded’ in the sediments as pyrite. A maximum Org.C:S value of 45 indicates a fresher, less marine environment [Bernier and Raiswell, 1983]. This freshwater input parallels other changes seen in carbon and nitrogen profiles (Figure 3).

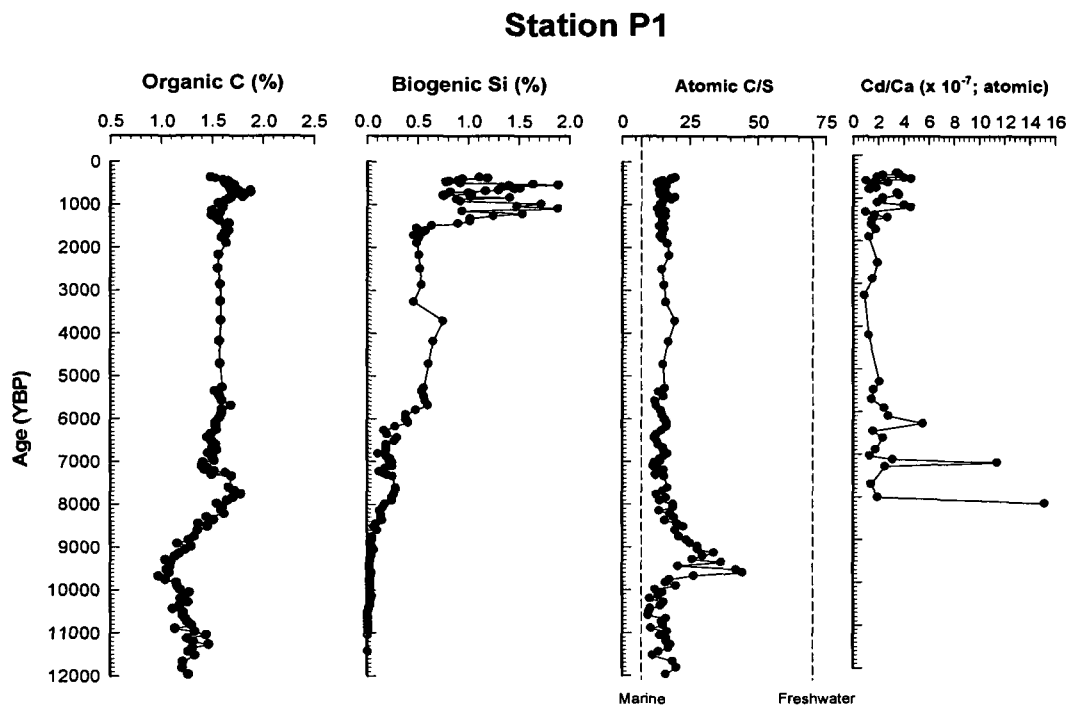


Figure 3. Organic carbon, biogenic silica, atomic C:S ratio and atomic Cd:Ca ($\times 10^{-7}$) for Station P1 [Darby *et al.*, 2001].

This is an important indication of potential climate change where freshwater discharges accompanied the warming temperatures. If a large input of freshwater into the Arctic Ocean could sufficiently dilute seawater-sulfate, would be preserved in the sediment record as a low sulfur event similar to that occurring ca. 9600 years ago (Figure 3).

Although the Org.C:S ratios in Figure 3 seem to show a major event in the Alaskan shelf, total sulfur is not the best indicator of seawater-sulfate. Total sulfur represents many other forms of sulfur such as elemental and organic sulfur. The timing of a freshening event in the Alaskan shelf could be better supported if organic carbon to pyrite-sulfur (Org.C:Pyrite) ratios were generated from a new sediment core from the same region as Station P1. A freshening of the Alaskan shelf would bring waters with low concentrations of sulfate and would not support the formation of pyrite and other reduced forms of sulfur within the sediments. Alternatively, the elevated Org. C:S

ratios (Figure 3) could be attributed to terrestrial/freshwater organic matter that have high Org. C:S ratios. To better support either case, pyrite sulfur values are needed. Therefore, the record observed in P1 indicates either a freshening of the Arctic or freshwater-derived organic material. The Org. C:Pyrite values are needed to determine which occurred.

The biogenic silica records at Station P1 (Figure 3) show several during the Holocene. A considerable input of biogenic silica is found at Station P1 over the last 1600 years (Figure 3). Though biogenic silica suffers diagenetic loss after burial [McManus *et al.*, 1995], a modest amount is preserved. Though the diagenetic loss of silica has attenuated the record, significant inputs also occur at 3700 and 7600 ybp. These events of increased biogenic silica concentrations correspond with elevated levels of carbon and nitrogen as well as minima in Org.C:N ratios. If the diagenetic loss of biogenic silica has occurred at a constant rate, then these apparent maxima are likely underestimating the true inputs and clearly show that siliceous organisms have played an important, but varying, role in primary productivity in the Alaskan shelf. If the rate of diagenetic loss has not been constant, then these observed changes may simply reflect changes in processes that preserve biogenic silica. Additional cores on the Alaskan shelf may help resolve this ambiguity.

Cadmium:Calcium (Cd:Ca) ratios in benthic foraminifera can be used as a proxy for phosphate in the overlying waters [Hester and Boyle, 1982]. Since phosphate is a limiting nutrient for primary productivity, this proxy can help estimate the amounts of nutrients available to drive primary production and resulting biogenic fluxes from surface waters over large time scales. Because of the limited abundance and species of

foraminifera at P1, well-known and well-calibrated foraminifera such as *N. pachyderma* or *C. wuellerstorfi* were not present. Therefore the Cd:Ca record cannot be relied upon to quantify but only estimate amounts of phosphate in the Alaskan shelf during the Holocene. The small quantities of foraminifera, mainly *I. norcrossi*, that were available in core P1 show variable phosphate concentrations in the Alaskan shelf over the Holocene (Figure 3). At 1200 ybp, the increases of biogenic silica, carbon, and nitrogen correlate with large inputs of phosphate (Figure 3). For the middle Holocene, there is a fairly constant input of nutrients, which maintains the fluxes of carbon, nitrogen, and biogenic silica to the sediments. During the mid-Holocene, 8000 to 5500ybp, fluctuations in nutrients again occurred (Figure 3) which correlate with increases of organic carbon and biogenic silica.

Unfortunately, the P1 core was stored at room temperature for several years before analysis. This storage compromised the geochemical composition of labile phases such iron sulfides and even biogenic carbonate. Thus, properly stored cores would yield more data for such constituents. However, the findings from P1 were one catalyst for obtaining more cores in this region with higher sedimentation rates, and proper handling and storage.

There are many things that we do not know about changes in biogeochemical processes in the Arctic Ocean that can be answered using properly-acquired, high resolution cores. The timing of biological productivity and other related events that have occurred in the Holocene, via the P1 core, can be more clearly defined. Comparisons between the P1 core and the Healy Oden Trans Arctic Expedition (HOTRAX) from other sites on the Alaskan shelf could extend the environmental and

climatic records during the Holocene for this region. Finally, a comparison of paleo-productivity records in shelf/slope sediments to the most recently observed surface productivity from the SBI program offer valuable insight to the relative magnitude of the modern fluxes and places them in context with the past.

1.4. Research Objectives

In order to establish the sources and fluxes of biogenic material in the Alaskan shelf through the Holocene, I utilized a suite of paleo-proxies to analyze cores collected recently on the 2005 HOTRAX expedition. The objectives of this research were: (1) Develop an analytical method for determining biogenic carbonate; (2) Identify the major sources of biogenic matter into the system over the Holocene; (3) Assemble the history of depositional events that have occurred on the Alaskan shelf over the Holocene. My research hopefully will help to elucidate the biogeochemical processes on the Alaskan shelf that have occurred as a function of climate change in the Holocene.

CHAPTER 2

SAMPLING AND ANALYTICAL METHODS

2.1. Sampling

The 2005 HOTRAX expedition was a collaborative effort funded by the National Science Foundation and Swedish Polar Secretariate that collected sediment cores for the development of a pan-Arctic stratigraphy and paleoclimate record [Darby *et al.*, 2009]. Leg 1 of the expedition was conducted from 13-26 June 2005 and recovered eight multi-cores (MC), trigger cores (TC), and jumbo piston cores (JPC) along the shelf and continental slope near Barrow, Alaska (Figure 1). The trigger cores and the jumbo piston cores were stored at 4°C and sampled at Ohio State University within 5 months, while the multicores were processed on board ship. Of the eight core locations, two (Stations 5 and 8) were chosen for their high sedimentation rates and detailed record of the Holocene. Core HLY0501-5JPC (hereafter called Station 5) was located on the Alaskan slope (72.69° N, 157.52° W, 410 m water depth), and was the longest core recovered on Leg 1, 16.7 m. Core HLY0501-8JPC (hereafter called Station 8) was located on the edge of the Barrow Canyon (71.63° N, 156.88° W, 89 m water depth) and was 15.2 m in length.

An individual multi-core tube was used for porewater collection via a whole core squeezer [Bender *et al.*, 1987]. A 5 cm (o.d.) acrylic tube was inserted into the sediments of the multicore tube and pistons placed on each end of the tube. The top piston was outfitted with a 70 µm polyethylene frit for filtering the porewater, and 3-way valve to allow the porewater to be collected hermetically using acid-cleaned, gas-

tight syringes. The prepared sub-core was placed in an aluminum rack, that held the core in place as a 1.5 ton hydraulic jack pushed against the bottom piston until the sediment surface reached the top piston, and dewatered the core from the top down [Bender *et al.*, 1987]. Porewater samples were collected in 8-10 mL aliquots. Porewater was then filtered through a 0.4 μm polycarbonate filter into polyethylene vials and stored at $< 20^\circ \text{C}$.

The multi-cores were anaerobically sectioned in a nitrogen-filled glove bag on board in 1cm intervals from the sediment-water interface to 10 cm and then 2 cm intervals from 10 cm to ca. 60 cm. These sections were immediately frozen to preserve the sediment redox conditions. The TC and JPC cores were analyzed using 1cm thick samples at 20 cm intervals from the core top to bottom. All core samples were prepared for bulk biogenic analyses by first obtaining a wet to dry ratio drying a 2 cm^3 sub-sample at 50°C . From this ratio porosity was calculated (1):

$$\phi = ((\text{wet weight g} - \text{dry weight g}) * \rho_w) \div \text{volume } \text{cm}^{-3} \quad (1)$$

where ρ_w is the density of water. Next, approximately 5 g wet sediment was freeze-dried and delicately crushed and sieved with a $<200 \mu\text{m}$ mesh, collecting ca. 1 gram for biogenic silica determinations. The remaining dried sediment was ground with an agate mortar and pestle and homogenized to $<200 \mu\text{m}$. A portion of frozen sediment was retained for the analysis of sedimentary sulfur speciation.

2.2. Analytical Methods

The concentration of total carbon, nitrogen and sulfur were determined by oxidative pyrolysis using a Carlo Erba NA1500 analyzer [Cutter and Radford-Knoery, 1991]. All determinations for each sediment interval were made in triplicate and the

analytical precision was maintained at 5% relative standard deviation (RSD) or better. To ensure accuracy National Institute of Standards and Technology (NIST) Estuarine Sediment (Standard Reference Material 1646) was analyzed.

Total inorganic carbon (TIC) was determined by warm (50°C) 1M perchloric acidification with a UIC CM5420 TIC analyzer. The difference between the total carbon (by oxidative pyrolysis) and inorganic carbon (by TIC) gave the amount of organic carbon in each sample.

Organic carbon and nitrogen isotope samples were prepared at Old Dominion University as described in *Cutter and Radford-Knoery* [1991], but the tin weighing cups were layered inside silver cups (11x8 mm). The prepared samples were sent to the University of California at Davis - Stable Isotope Facility and analyzed by isotope ratio mass spectrometry.

Acid volatile sulfur (AVS or FeS), greigite, and pyrite were determined using selective generation of H₂S, cryotrapping, and gas chromatography-photoionization detection [*Cutter and Oatts*, 1987]. In order to measure AVS, 0.5mg of frozen sediment was placed in a gas stripping vessel, acidified to 0.5M HCl to generate hydrogen sulfide from iron monosulfide (FeS) minerals, cryotrapped to preconcentrate it, and then determined with gas chromatography-photoionization detection. Potassium iodide and sodium borohydride solutions were then added to the gas stripping vessel for the analysis of greigite; the generated H₂S was determined as above. To accurately determine pyrite, ca. 100 mg sample of dried, ground and sieved sediment were extracted using carbon tetrachloride to remove elemental sulfur. A very small (0.1 mg) subsample of the extracted sediment was subjected to the methods above to liberate any

residual AVS and greigite. A reduced chromium (II) reagent was then added to quantitatively generate hydrogen sulfide from pyrite. AVS, greigite, and pyrite concentrations were determined only in the multi-cores because the trigger core and jumbo piston cores were not preserved for their redox conditions as the multicores were. However, pyrite was determined in the trigger and piston cores to give better resolution and timing of reducing conditions throughout the Holocene.

Biogenic silica was determined in all sediment samples that were carefully prepared (as described in Sampling) from 0 to ca.1000 cm. The determination of biogenic silica utilized a timed sodium carbonate leach technique [DeMaster, 1991] and the resulting silicate was determined colorimetrically using a rapid-flow analyzer.

2.3. Age Models

Age models from radiocarbon dating by Accelerator Mass Spectrometry (AMS) and paleomagnetic intensities have previously been determined (HY0501-8JPC and HY0501-5JPC) [Darby *et al.*, 2009A; Lise-Pronovost *et al.*, 2009]. Data for ^{210}Pb in the most recent sediments (MC6) are also available [McKay *et al.*, 2008].

2.4. Diagenetic Calculations

The amounts of biogenic matter obtained in these cores do not represent all the primary production occurring in surface waters. An appreciable amount, ca. 18%, of total biogenic material produced at the surface is lost due to export fluxes and water column regeneration [Moran *et al.*, 1997]. Once buried, more is lost to diagenetic remineralization. Calculations used sedimentary organic carbon data to study the diagenesis of organic matter (2):

$$G = G_{nr} + (G_o - G_{nr}) * e^{-\alpha z} \quad (2)$$

where G_{nr} is the refractory or non-reactive organic carbon at depth, G_o is the total amount of organic carbon at the surface, $(G_o - G_{nr})$ is the concentration of reactive organic carbon at the sediment surface, and α is (3):

$$\alpha = k / \omega \quad (3)$$

with k being the rate constant for organic carbon attenuation, ω is the sedimentation rate, and z is depth in centimeters [*Burdige, 2006*]. The percent of organic matter remineralization within the sediments was calculated by (4):

$$G_{remin} = (G_o - G_{\infty}) / G_o \quad (4)$$

where G_o is the total amount of organic matter at the sediment surface and G_{∞} is the amount of organic matter at depth. Using J_{in} from organic matter flux to sediment surface via sediment trap data from other investigations [e.g., *Baskaran and Naidu, 1995; Moran et al., 1997*], the carbon burial efficiency (BE) was calculated as (5):

$$BE = (J_{bur}) / (J_{in}) \quad (5)$$

where J_{bur} is sedimentation rate (ω) times amount of organic matter at depth (G_{∞}) times dry sediment density (ρ). Obtaining estimates of organic matter remineralization and carbon burial efficiency is important to understanding how the biogeochemical processes on the Alaskan shelf contribute to the overall budget of the Arctic Ocean. Burial rates of organic carbon in the Arctic Ocean are typically high when compared to other oceans, accounting for 7-11% of global carbon budget [*Stein and Macdonald, 2004*].

CHAPTER 3

DETERMINATION OF BIOGENIC CARBONATE

3.1. Background

Carbonate is the most widely found major biogenic component of sediments in the ocean [Kennett, 1982]. Marine sediments contain a wide range of biogenic carbonate depending on their location, water column depth, and surface water conditions that promote primary production from organisms such as coccolithophores and foraminifera. Carbonate-rich sediments (>80% biogenic carbonate) are mainly found in shallow tropical waters, while the continental shelf and slope can contain a variety of biogenic carbonate and terrestrially-derived carbonates (e.g. refractory dolomite) [Morse and Mackenzie, 1990]. The preservation of biogenic carbonate in marine sediments is affected by dissolution in calcium carbonate-undersaturated waters and early diagenetic processes within the sediments [Burdige, 2006]. The accumulation of biogenic carbonate in the sediments has a major role in the complex carbonate system, affecting alkalinity, ΣCO_2 of the ocean, and ultimately the CO_2 content of the atmosphere [Emerson and Hedges, 2003]. The oceanic carbonate system is modified on ocean-circulation time scales (ca. 1,000 yrs) by biological processes [Emerson and Hedges, 2003]. Thus, biogenic carbonate preservation in sediments is important since it provides a record of past ocean conditions.

The determination of sedimentary calcium carbonate (CaCO_3) has evolved from simple phosphoric acidification [Presley, 1975] and vacuum gasometric technique [Jones and Kaiteris, 1983] to modern automated systems using coulometric detection. All these methods utilize the production of carbon dioxide from the acidification of a

known weight of sediment that contains carbonate. The detection of carbonate using phosphoric acidification and vacuum gasometric methods only measures sediment containing at least 5% CaCO_3 , and have 0.1% and 0.25% accuracy respectively [Presley, 1975; Jones and Kaiteris, 1983]. Though these two methods have been proven to be reliable at determining CaCO_3 , they are laborious and time consuming, requiring careful monitoring of pressure, temperature, and the vacuum apparatus. In addition, neither of these methods discriminates between biogenic carbonate and refractory carbonate such as dolomite.

The coulometric determination of CaCO_3 has decreased detection limits and increased accuracy, while reducing analysis time from hours to minutes (UIC Operation Manual, Version 3). The coulometric determination of CaCO_3 is based on the titration of a monoethanolamine and indicator solution with carbon dioxide (CO_2). Acidification of CaCO_3 -containing sediments produces CO_2 that is carried in an inert nitrogen gas stream. The nitrogen and CO_2 gas are then bubbled through monoethanolamine indicator solution, which readily absorbs carbon dioxide and forms a strong acid that causes the indicator color to fade. An electrical current, conducted through a pure silver anode and platinum cathode, automatically increases upon loss of indicator color, and titrates the strong base to return the indicator solution to its original color. The detection limit of coulometric determination of CaCO_3 is $<1 \mu\text{g}$ and has 0.2% accuracy (UIC Operation Manual, Version 3).

Because the standard operating procedures for the coulometric detection of CaCO_3 in sediments (e.g. UIC Operation Manual, Version 3) do not discriminate between biogenic carbonate and refractory dolomites, a modification to these

procedures for the selective analysis of biogenic carbonate was developed. Since temperature and pH can control the dissolution kinetics of different carbonate minerals [Morse and Arvidson, 2002], modifications to the existing coulometric method that include manipulating these two parameters can be used to selectively determine biogenic carbonate.

3.2. Experimental Section

3.2.1. Apparatus

The Total Inorganic Carbon (TIC) coulometric detector (CM5014) is used in conjunction with the auto-acidification module (CM5240) from UIC. The coulometric detector and acidification module are used as described in the instrument literature for standard operating procedures for TIC analysis (UIC Operation Manual, Version 3 and Table 1). A constant-temperature refrigeration-circulator is used with the CM5240's jacketed acidification/condenser column. High purity nitrogen is the carrier gas.

3.2.2. Standards and Reagents

A calcium carbonate standard (Baker Analyzed) and different types of calcium carbonate minerals such as dolomite (Geology Lab, Old Dominion University), and chalk (Wards Scientific), as well as sediment from the Black Sea known to contain biogenic carbonate were used to develop the method. Mineral specimens were finely ground and sieved through a <200 μm mesh screen. In addition to these standards and reagents, several mixtures of dolomite and Black Sea sediments were combined at different concentrations (1%, 5.4%, and 10.9% Black Sea sediment) and used to test the recovery of biogenic carbonate in a refractory carbonate matrix.

Table 1. CM 5014 Settings for Standard Operating Procedure for Total Carbonate Method

Analysis Type = Carbon

Calculation Based On = Weight

Units = Milligrams

Difference Criteria = 0.10% (Default Setting)

Factor = 1.0 (Default Setting)

Number of Readings = 30

Interval in Minutes = 1.0

Timing Method = Fixed Number of Runs Method

Sampling Method = Auto; CM5014 Runs Autosampler Without Pausing

Autosampler = 5240 TIC

Write To Disk Turned ON

Reagent solutions were prepared with doubly deionized water and purged with helium to remove atmospheric carbon dioxide contamination. Perchloric acid (2M) was prepared in 5L batches and purged with helium for 2 hours. The sodium acetate buffer solution was prepared in 1L polyethylene cubitainer whose cap was modified with a swagelock fitting to easily connect to the acid supply line on the CM5240 acidification module. Approximately 750 ml of 1M acetic acid were placed inside of the 1L cubitainer and purged with helium for one hour. Then, while continually being purged, the pH was adjusted to 5 using approximately 75 mL of 10M sodium hydroxide. The cubitainer was then capped and all the helium head space was pushed out of the container. Each resulting cubitainer of sodium acetate/acetic acid buffer was stored at 6°C until use. The weakly acidic buffer solution was found to contain a considerable amount of CO₂ contamination if not prepared and handled carefully. The CO₂ contamination was significant enough to be detrimental to accurate sample analysis. CO₂-free reagent was found to be consistently low over 36 hours of continuous use, with only ca. 2 mg CO₂ per milliliter of sodium acetate solution.

3.2.3. Procedure for Total Carbonate

Using the standard operating procedures for total inorganic carbon (TIC) analysis (Table 1), the reagents and samples were loaded into the autosampler tray in a sequence (Table 2) such that two blanks (empty sample cups) were included at the beginning of each run to determine reagent CO₂ contamination. Next, three Baker CaCO₃ standards (10 ± 0.5mg) were positioned, and one additional Baker CaCO₃ sample was included in the middle of the tray and at the end of every set of analyses to ensure accuracy throughout the run. Samples were weighed out in triplicate (50 ± 0.5mg). Using 2M perchloric acid, the samples were acidified and heated to 50°C for 30 minutes. The constant-temperature refrigeration circulator was cooled to 15°C to limit water vapor from collecting in the gas lines. The complete analysis time is 30 minutes for acidification plus an additional 6 minutes for the rinse/dump cycle between samples, totaling 36 minutes per sample. This TIC method was used to obtain the total amount of carbonate, including biogenic and refractory forms.

3.2.4. Procedure for Biogenic Carbonate

Several modifications were made to the standard operating procedures for total carbonate for the selective determination of biogenic carbonate (Table 3). Sample size was reduced from 50mg to 10mg to limit the amount of refractory dolomite contamination. The pH buffered 1M sodium acetate solution was used in place of the 2M perchloric acid. The constant-temperature refrigeration circulator was set at 9.5°C to cool the acidification chamber and slow the acidification reaction to limit the evolution of CO₂ from refractory dolomite. Using the buffered acetic acid solution and

Table 2. Autosampler Tray Format

Position	Sample ID	Weight (mg)	Position	Sample ID	Weight (mg)
1	Blank	Empty			
2	Blank	Empty			
3	Baker CaCO ₃	50 ± 0.9	24	Baker CaCO ₃	50 ± 0.9
4	Baker CaCO ₃	50 ± 0.9	25	Sample	50 ± 0.9
5	Baker CaCO ₃	50 ± 0.9	26	Sample Dup.	50 ± 0.9
6	Sample	50 ± 0.9	27	Sample Trip.	50 ± 0.9
7	Sample Dup.	50 ± 0.9	28	Sample	50 ± 0.9
8	Sample Trip.	50 ± 0.9	29	Sample Dup.	50 ± 0.9
9	Sample	50 ± 0.9	30	Sample Trip.	50 ± 0.9
10	Sample Dup.	50 ± 0.9	31	Sample	50 ± 0.9
11	Sample Trip.	50 ± 0.9	32	Sample Dup.	50 ± 0.9
12	Sample	50 ± 0.9	33	Sample Trip.	50 ± 0.9
13	Sample Dup.	50 ± 0.9	34	Sample	50 ± 0.9
14	Sample Trip.	50 ± 0.9	35	Sample Dup.	50 ± 0.9
15	Sample	50 ± 0.9	36	Sample Trip.	50 ± 0.9
16	Sample Dup.	50 ± 0.9	37	Sample	50 ± 0.9
17	Sample Trip.	50 ± 0.9	38	Sample Dup.	50 ± 0.9
18	Sample	50 ± 0.9	39	Sample Trip.	50 ± 0.9
19	Sample Dup.	50 ± 0.9	40	Sample	50 ± 0.9
20	Sample Trip.	50 ± 0.9	41	Sample Dup.	50 ± 0.9
21	Sample	50 ± 0.9	42	Sample Trip.	50 ± 0.9
22	Sample Dup.	50 ± 0.9	43	Baker CaCO ₃	50 ± 0.9
23	Sample Trip.	50 ± 0.9			

cooler temperatures, samples were run for 60 minutes with a total analysis time of 66 minutes per sample.

3.2.5. Calculations

The coulometric determination of TIC from CO₂ generated from sediments is automatically calculated and reported by the coulometric detector software. The coulometric response is converted to concentration by (6):

$$(\text{coulometric response} - \text{blank}) / (\text{sample weight}) * 0.1 = \% \text{ carbonate} \quad (6)$$

Table 3. CM 5014 Settings for Standard Operating Procedures for Biogenic Carbonate Method

Analysis Type = Carbon
Calculation Based On = Weight
Units = Milligrams
Difference Criteria = 0.10% (Default Setting)
Factor = 1.0 (Default Setting)
Number of Readings = 60
Interval in Minutes = 1.0
Timing Method = Fixed Number of Runs Method
Sampling Method = Auto; CM5014 Runs Autosampler Without Pausing
Autosampler = 5240 TIC
Write To Disk Turned ON

3.2.6. Regressions to Calculate Biogenic Carbonate

To separate the labile biogenic carbonate from refractory dolomite, a linear regression was used to identify the slow CO₂ production from dolomite compared to the exponential evolution of CO₂ from biogenic carbonate. The many different types of carbonate minerals required a wide range of time to dissolve. To determine the amount of biogenic carbonate in any sediment, the analysis time has to be long enough to recover the labile portion but limit the amount of refractory carbonate contamination. In order to do this, linear regressions were applied to all the different phases of carbonates and carbonate sediments and it was found that the inflection point, where the exponential growth decays to a linear increase, typically falls around 40 minutes, when the change in slope is less than 1% (Figure 4).

As samples are being analyzed the data generated is recorded (printed) at 1 minute intervals (Table 3). The 60 data points generated for each sample were entered into a spreadsheet, graphed (time vs. coulometric response), and data from 40 to 60 min were linearly regressed. The y-intercept from this linear regression was used as the

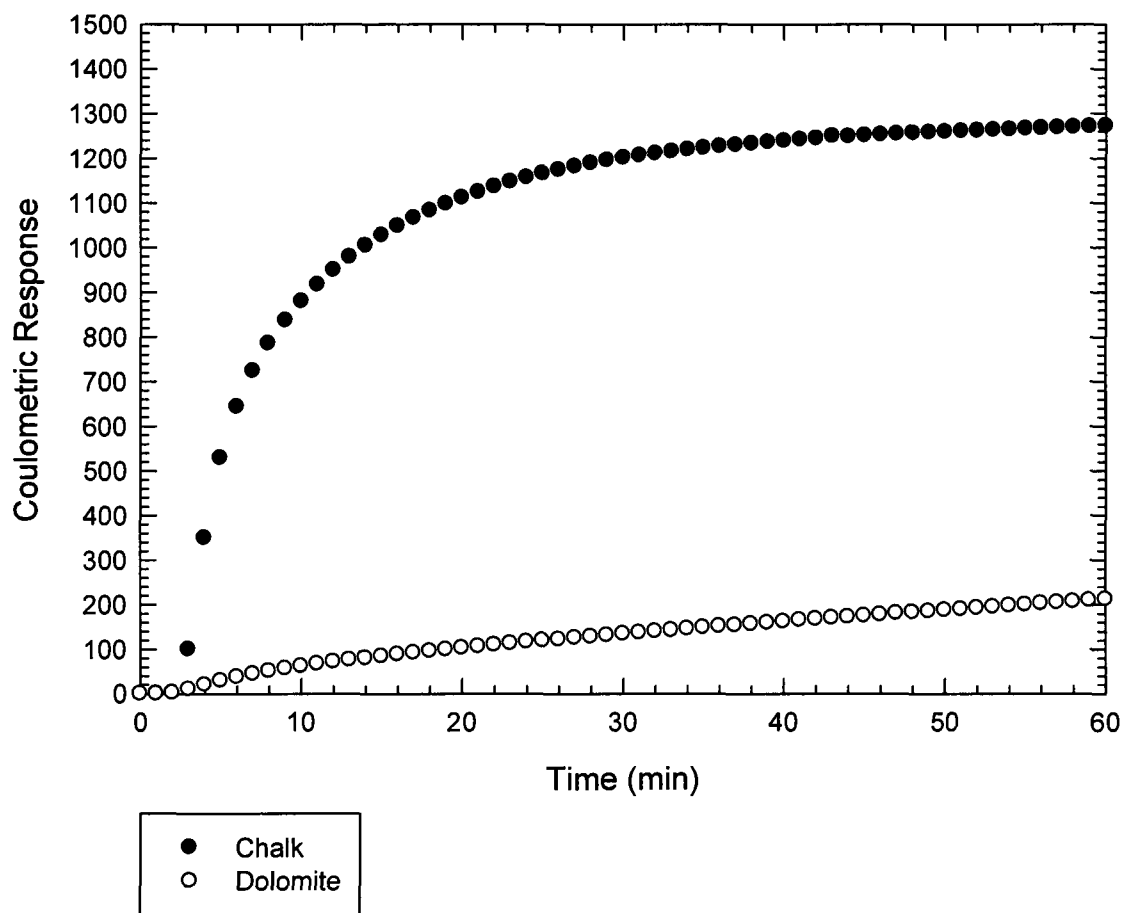


Figure 4. Evolution of CO₂ from two carbonate minerals using a pH 5 buffer and 10°C.

“coulometric response” and placed in equation (1) to determine the concentration of biogenic carbonate. The slope of the line indicates the amount of CO₂ being slowly generated by refractory carbonates.

Table 4. Linear Regression Results for Black Sea Sediment Analyzed Using the Optimized Conditions of pH 5 1M Sodium Acetate Solution and 10°C

Time	Y-Intercept	Slope	R ²	Calculated Concentration	% Recovery
0-60	504	8.8	0.48	4.7	61
5-60	695	4.16	0.63	6.5	84
10-60	757	2.7	0.95	7.1	91
15-60	772	2.37	0.98	7.2	93
20-60	780	2.2	0.99	7.3	94
25-60	786	2.07	0.99	7.4	94
30-60	790	1.99	0.99	7.4	95
35-60	793	1.93	0.99	7.4	95
40-60	795	1.89	0.99	7.5	96
45-60	796	1.89	0.99	7.5	96
50-60	798	1.83	0.99	7.5	96
55-60	799	1.82	0.99	7.5	96

3.3. Discussion

3.3.1. Optimization of Biogenic Carbonate Recovery

The temporal trend of CO₂ evolution from CaCO₃-containing sediments is very different due to several factors, including how strongly the carbonate is mineralized, or pH of the solution in which it dissolves, and the temperature. In Figure 4, chalk shows a rapid exponential growth of CO₂ production and then begins to plateau as the carbonate minerals are exhausted. The well-crystalline dolomite does not show a rapid response to mild acidification (Figure 4). Dolomite slowly evolves CO₂ over time at a consistent and nearly linear rate.

Altering the ambient conditions of the chemical reaction, such as the pH and temperature, shows a dramatic effect on the rate of production of CO₂. Increasing the strength of acid and temperature more quickly liberates CO₂ from mineral chalk and

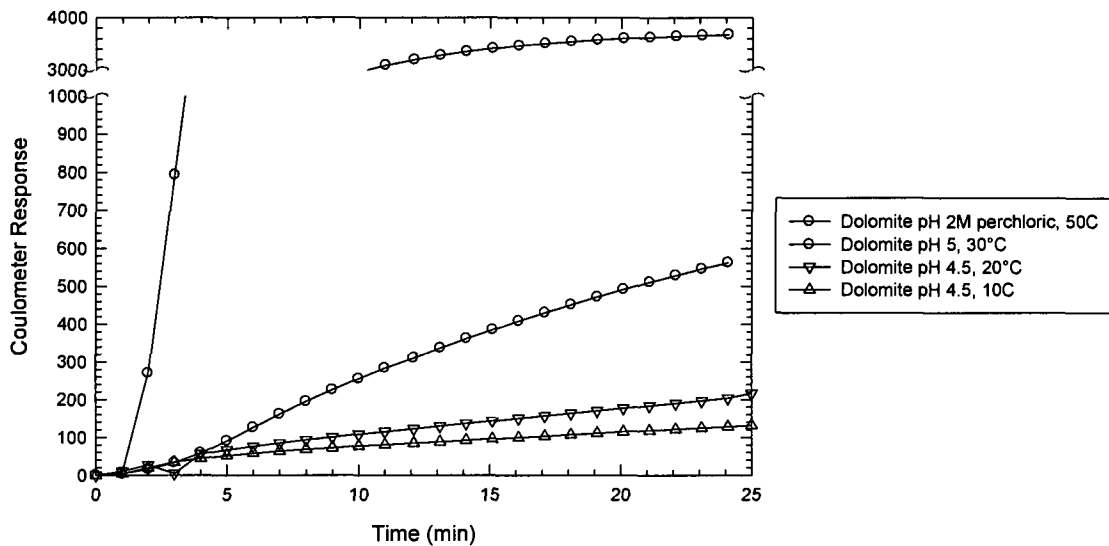
dolomite (Figure 5). Increasing pH and decreasing temperature slows down the evolution of CO₂ (Figure 5) A weak acid-buffer solution was the best reagent as it is mild enough to minimize the dissolution of dolomite to a slow, consistent (linear) production of CO₂, but still rigorous enough to produce a rapid and complete dissolution of weakly-mineralized carbonates like biogenic carbonate (Figure 5). Many samples were run under a variety of pH and temperatures and, it was found that 10°C and pH 5 suit the type of standards and samples being analyzed with good recovery and precision (Table 4).

3.3.2. Separating Biogenic from Refractory Carbonate

The evolution of CO₂ from weakly-mineralized carbonates and refractory carbonates cannot be clearly and fully separated by only optimizing reaction conditions (e.g., Figure 5). The determination of biogenic silicate using a sodium carbonate buffer has essentially the same problem of separating it from aluminosilicates. For the *DeMaster* [1991] method to detect biogenic silica, sediments are leached in a warm alkaline solution, subsamples are taken at 1, 2, 3 and 5 hrs, and then analyzed for their silicate concentrations using standard colorimetric techniques. Typically biogenic silica dissolves quickly under the optimized conditions, 1% sodium carbonate at 85°C. The silicate data is then plotted as a function of time and regressed through the slow linear growth region, excluding the initial exponential increase of biogenic silica, to correct for the simultaneous dissolution of aluminosilicates. Though this technique is not a direct measurement of biogenic silica, it serves as a useful tool to indirectly estimate biogenic silica abundance within 2 to 3% accuracy [*Mortlock and Froelich, 1989*]

Data from the weakly acidic buffered solution for biogenic carbonate were

(a) Evolution of Carbon Dioxide from Dolomite at Varying Temperature and pH



(b) Evolution of Carbon Dioxide from Carbonate Reagent at Varying Temperature and pH

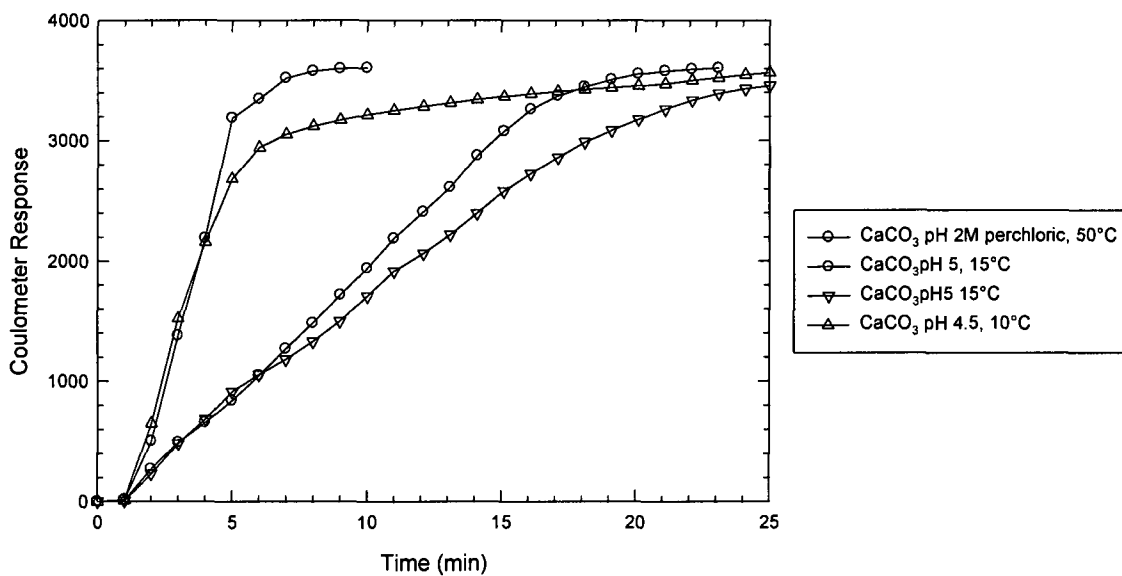


Figure 5. Varying combinations of temperature and pH used to: (a) minimize recovery of dolomite, (b) optimize the recovery of calcium carbonate.

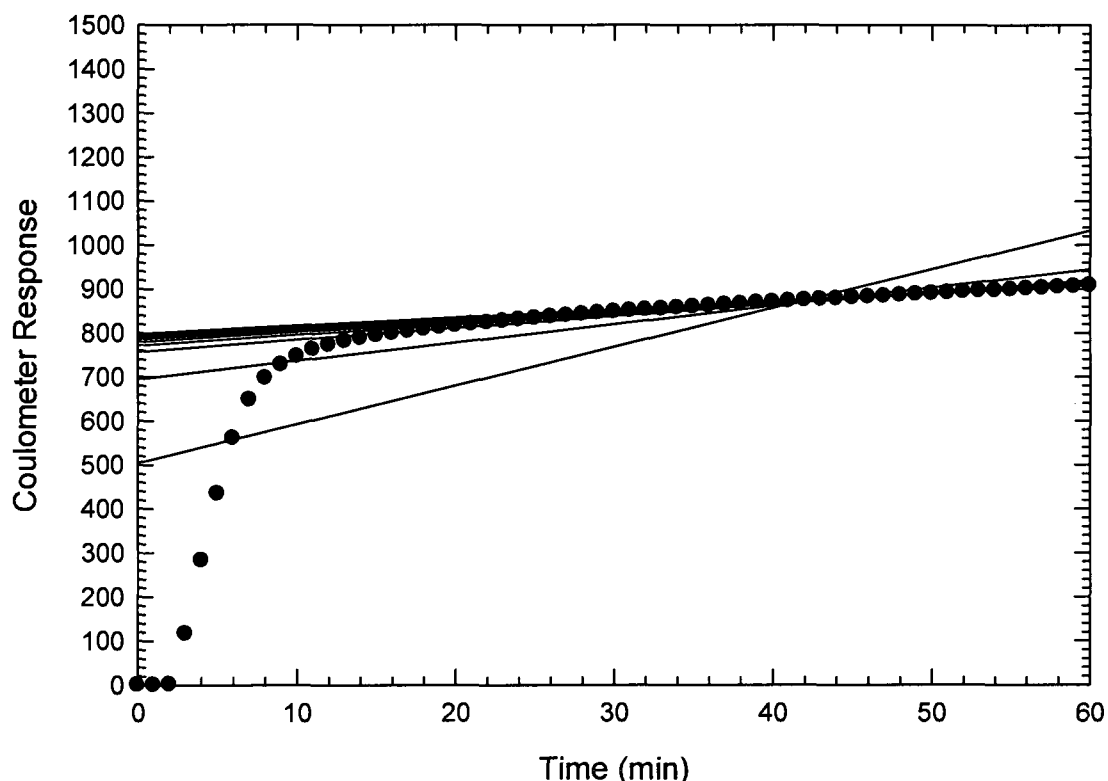


Figure 6. Linear regressions for the CO₂ evolution from a 10% mixture of Black Sea sediment and pure dolomite to determine analysis time and the time over which the regression is carried out (0-60 min., 10-60 min., 30-60 min., etc.).

similarly analyzed. To determine the time in which the fast, asymptotic growth of biogenic carbonate smooths out to the slow, linear evolution of refractory dolomite, a sample containing biogenic carbonate (Black Sea) was analyzed and a series of linear regressions were performed starting from 0-60min, and then decreasing by 5min; 5-60 min, 10-60 min, etc. (Figure 6, Table 4). The slopes of each of the linear regressions after 30 min. converge to 1.85 ± 0.04 , and the y-intercepts converge to 797.7 ± 1.23 at time 45-60 min. The calculated recovery for this sediment is $96 \pm 0.2\%$ ($n = 5$), using TIC and total carbon (via CNS analysis) as the 100% value since there is

Table 5. Sample Regression Data Using Biogenic Carbonate Procedures and Linear Regression From 40-60 Minutes

	Sample Weight	Y-Intercept	Slope	R ²	Calculated Concentration	Average	STD	Theoretical Value
Dolomite	12.71	1.3	29.0	0.998	0.228			
	12.80	1.5	30.9	0.998	0.241			
	12.14	1.5	26.1	0.999	0.215			
	12.05	1.5	24.7	0.998	0.205	0.222	0.016	12.010
1% Black Sea	13.13	1.1	26.6	0.999	0.203			
	12.87	1.4	22.5	0.997	0.175			
	11.55	1.1	26.6	0.999	0.230			
	11.59	1.3	40.1	0.997	0.346			
	12.20	1.4	39.0	0.996	0.320	0.268	0.075	0.103
5% Black Sea	12.75	1.3	75.9	0.993	0.595			
	13.66	1.3	65.0	0.99	0.476			
	13.62	1.3	75.9	0.993	0.557			
	13.89	1.5	54.1	0.995	0.389			
	13.24	1.5	59.1	0.995	0.446			
	13.50	1.3	64.1	0.995	0.475	0.467	0.075	0.461
10% Black Sea	13.95	1.3	136.7	0.991	0.980			
	12.20	1.1	95.9	0.993	0.786			
	12.80	1.2	113.3	0.993	0.885			
	12.84	1.2	105.2	0.993	0.819	0.868	0.086	0.870
100% Black Sea	10.57	0.4	942.4	0.963	8.916			
	10.64	0.5	936.4	0.995	8.801			
	11.27	0.4	942.0	0.964	8.358			
	11.13	0.2	961.9	0.997	8.642			
	11.29	0.3	970.7	0.997	8.598	8.663	0.212	8.700

no dolomite in this sample.

3.3.3. Recoveries of Carbonate Under Optimized Conditions

Using these optimized conditions, a buffered solution at pH 5 and 10°C temperature, a variety of pure carbonate mineral phases and mixtures of refractory and labile carbonates were analyzed. Since natural sediments often contain a mixture of biogenic carbonate and other refractory carbonates, it is important that the method work for a variety of both carbonate and non-carbonate materials. Figure 7 shows a

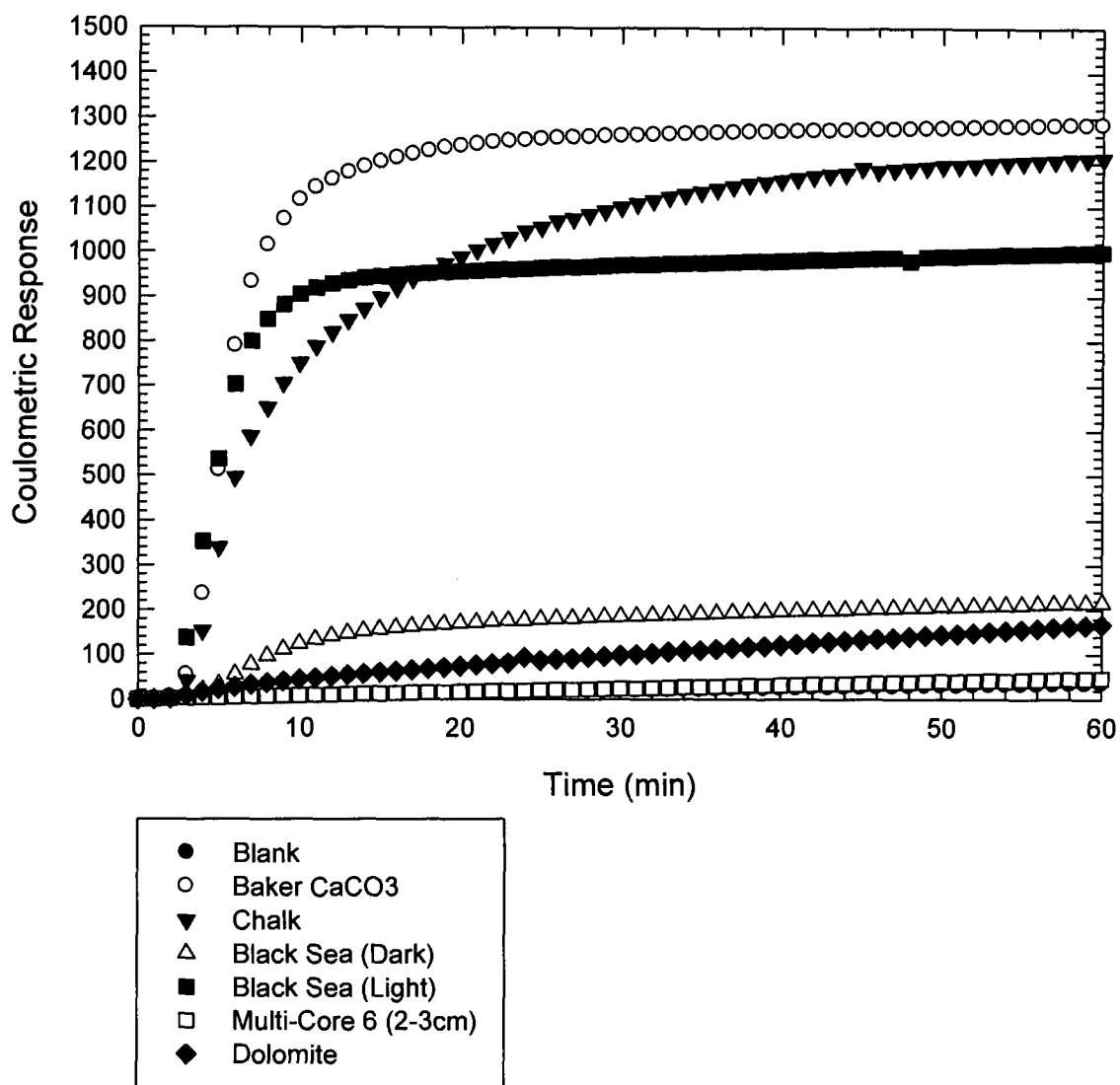


Figure 7. Composite graph showing CO₂ evolution from different types of carbonate minerals and natural samples using a pH 5 buffer and 10°C. A coulometric response of ca. 1200 is complete recovery of CO₂ from the acidification of carbonate minerals, based on formula weight and assuming samples are 100% CaCO₃.

compilation of data for all types of mineral carbonates and natural samples. Well-crystallized dolomite slowly evolves CO₂ at a linear rate when analyzed under these optimized conditions. Other phases of carbonates that were analyzed, CaCO₃ reagent and mineral chalk, show complete recovery within a relatively short amount of time (Figure 7).

Natural biogenic-containing samples that were analyzed show a variety of responses (Figure 7). The light and dark Black Sea sediments show exponential growth of CO₂ from biogenic carbonate, reach a maximum value, and do not continually increase CO₂ production. Surface sediment from the Alaskan shelf (MC6) showed no biogenic carbonate as it has the same coulometric response as the reagent blank (Figure 7). Well-crystalline minerals (e.g., dolomite) generate CO₂ much more slowly and create a general increasing trend over a long period of time (Figure 5). This “dolomite drift” is essentially creating an increasing baseline over the analysis time.

The evolution of CO₂ from the calcium carbonate reagent was quickly completed in approximately 15 minutes (Figure 8). A linear regression of 20 data points (40 to 60min) has a slope, 1.2, and calculated recovery of carbon, using the y-intercept as described above and in equation (6), full carbon recovery based on chemical formula weight, $12.0 \pm 0.3\%$ was achieved with precision of 2.3% RSD.

Knowing the time evolution of CO₂ from dolomite is important for the accurate determination of biogenic carbonate as it potentially can be a major interference. Using the recommended pH 5 solution and cold temperature, the partial dissolution of dolomite produces a remarkably small, but consistent amount of CO₂ over the long analysis time (Figure 9). Using a linear regression to separate the linear CO₂

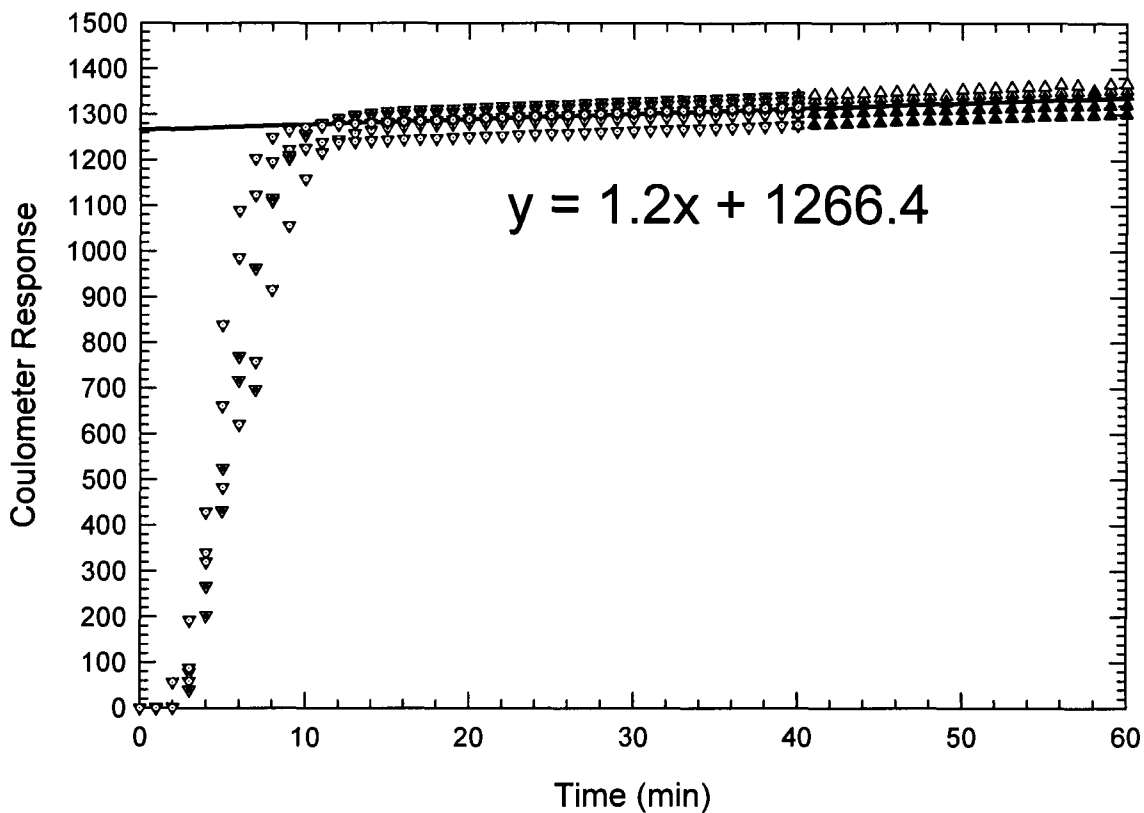


Figure 8. Calcium carbonate (reagent grade) response to pH 5 and 10°C treatment. A linear regression of data from 40 to 60 min. and equation are shown.

production from refractory carbonate from non-linear CO₂ production from biogenic carbonate is an elegantly simple solution for resolving the refractory and labile phases.

Chalk is a sedimentary rock that is typically formed in marine conditions from the accumulation of biogenic carbonate produced by coccolithophores and other calcifying phytoplankton. Once ground and sieved, mineral chalk is potentially as reactive as biogenic carbonate. The analysis of chalk over 60 minutes shows that CO₂ produced

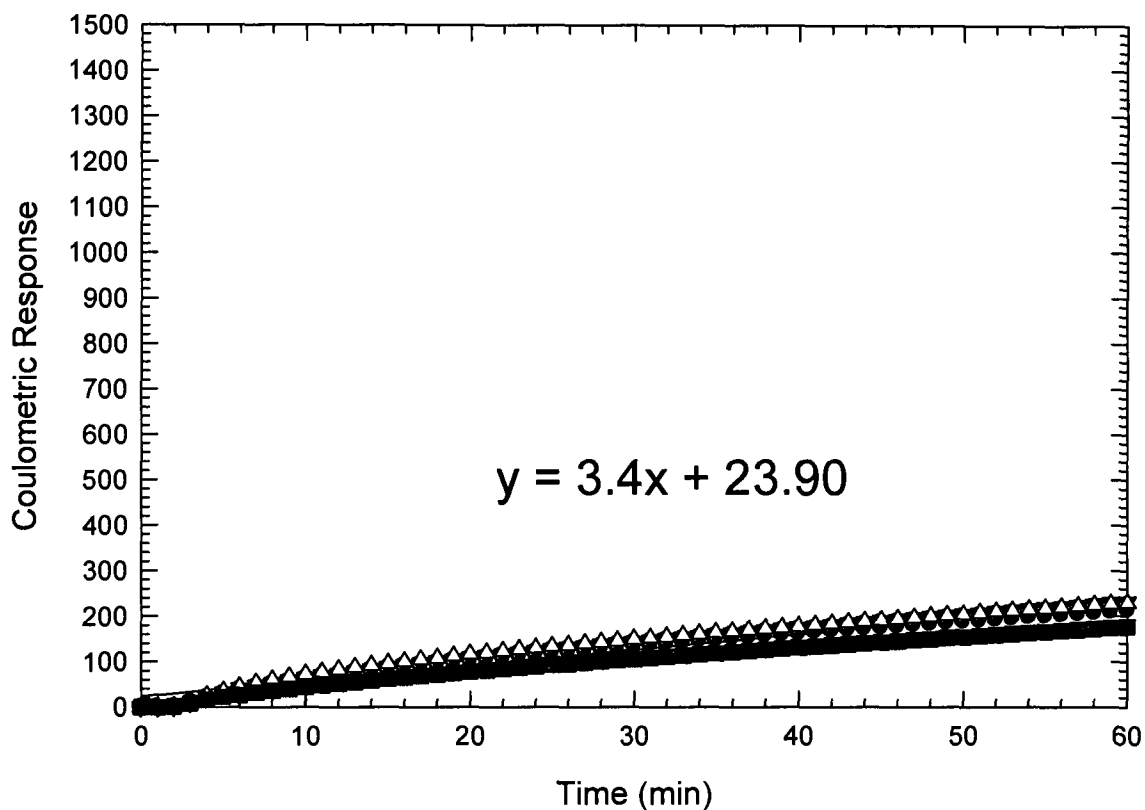


Figure 9. Dolomite response to pH 5 and 10°C treatment. A linear regression of data from 40 to 60 min. and equation are shown.

is nearly complete in ca. 30 min (Figure 10). A linear regression of 20 data points, 40 to 60min has a slightly higher slope than calcium carbonate and dolomite, 2.0, as the labile minerals are still generating some CO₂ for the entire time of analysis. The calculated concentration of chalk is $11.5 \pm 0.2\%$ (2.3% RSD) biogenic carbonate or 96% recovery based on chemical formula weight, assuming it is 100% calcium carbonate.

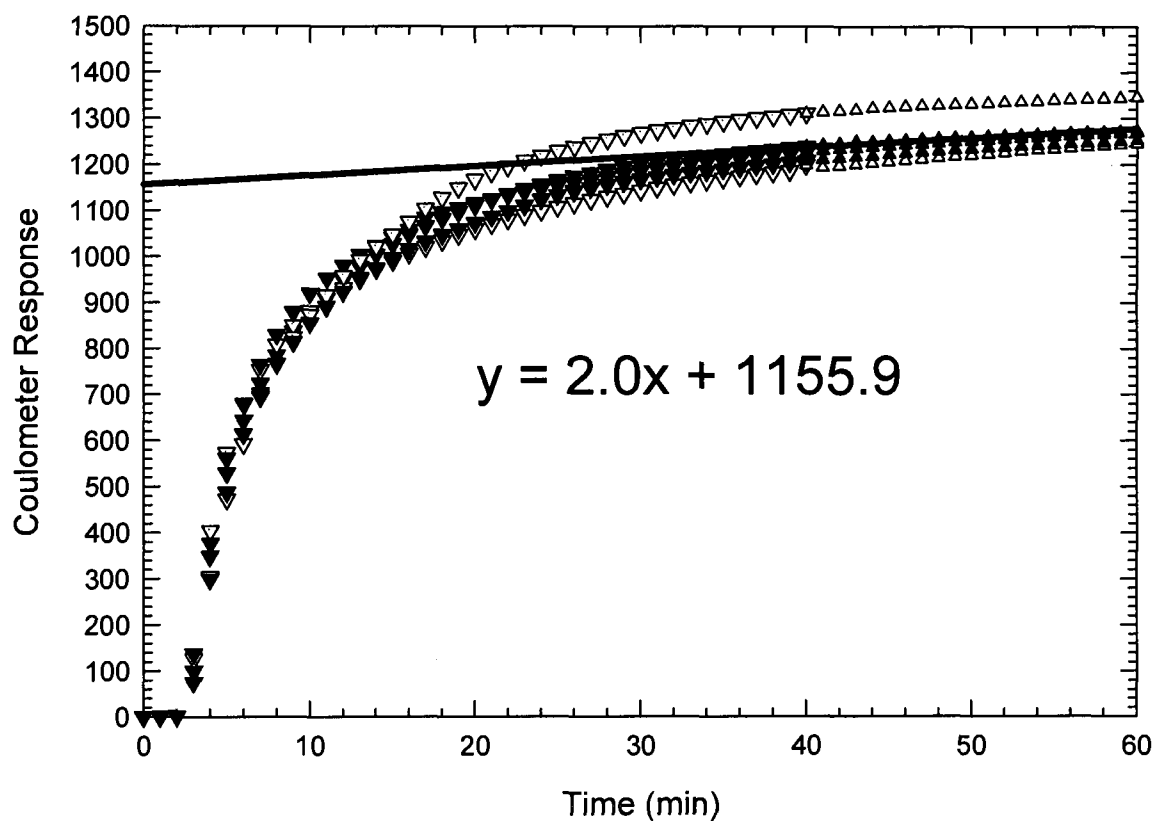


Figure 10. Chalk response to pH 5 and 10°C treatment. A linear regression of data from 40 to 60 min. and equation are shown.

Three different samples of sediment from the Black Sea were used in optimizing the recovery of biogenic carbonate. Natural variations in the sediment of the Black Sea show lighter and darker layers corresponding to annual summer blooms of the coccolithoforid *E. huxleyi* (light layers) and a minimum of blooms during the winter, darker organic layers, [Hey *et al.*, 1991]. The different layers of Black Sea sediment thus show similar trends in the time evolution of CO₂ (Figure 11). At approximately 40 minutes the recovery of biogenic carbonate is complete. Linear regressions for both samples from 40 to 60 minutes (20 data points) show different y-intercepts since they

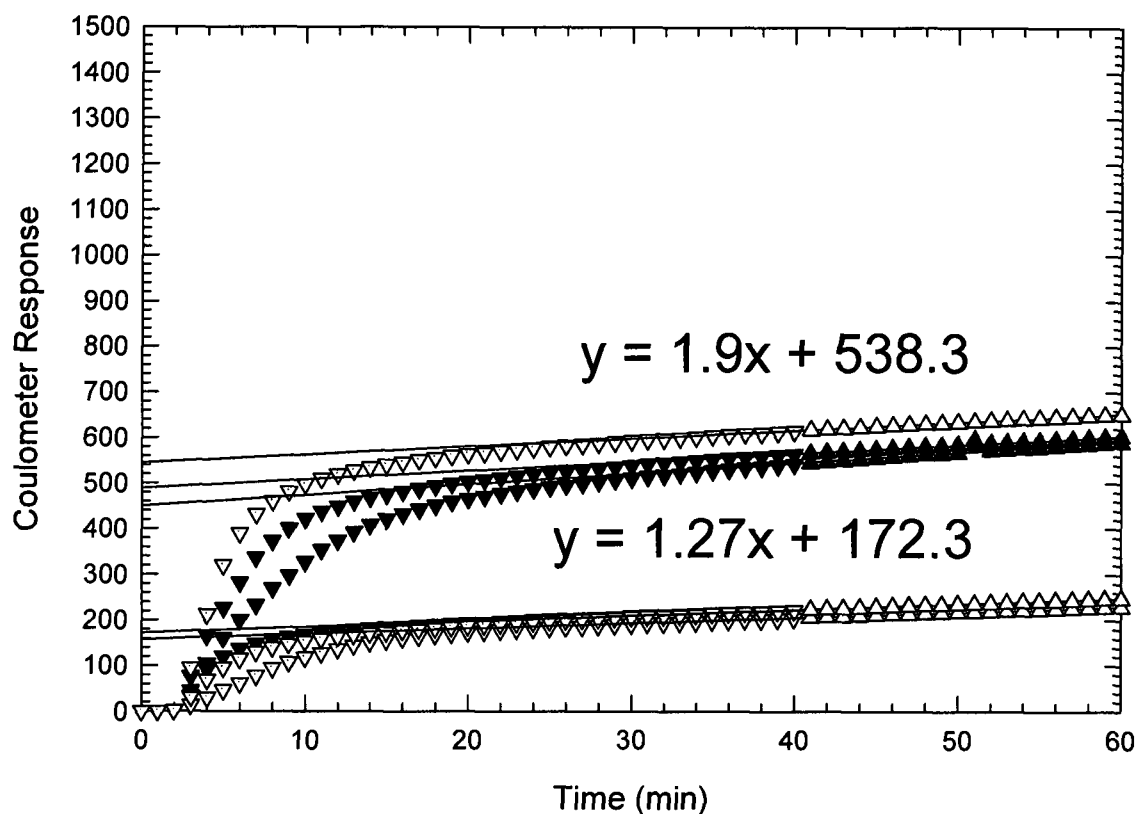


Figure 11. Responses of two Black Sea sediments (light and dark; see text) to pH 5 and 10°C treatment. Sample weights were also varied. A linear regression of data from 40 to 60 min. and equations are shown.

have differing amounts of biogenic carbonate. The lighter layer has $5.4 \pm 0.3\%$ biogenic carbonate (2.3% RSD) and darker layer has $1.9 \pm 0.1\%$ (2.8% RSD) biogenic carbonate. The detection of trace amounts of biogenic carbonate in a refractory carbonate matrix is probably the “worst-case scenario” for analysis. Since the time evolution of dolomite and biogenic carbonate-containing sediments has been individually identified (as above), a series of dolomite samples with Black Sea additions were analyzed. Three mixtures were made gravimetrically with 10.0%, 5.4%

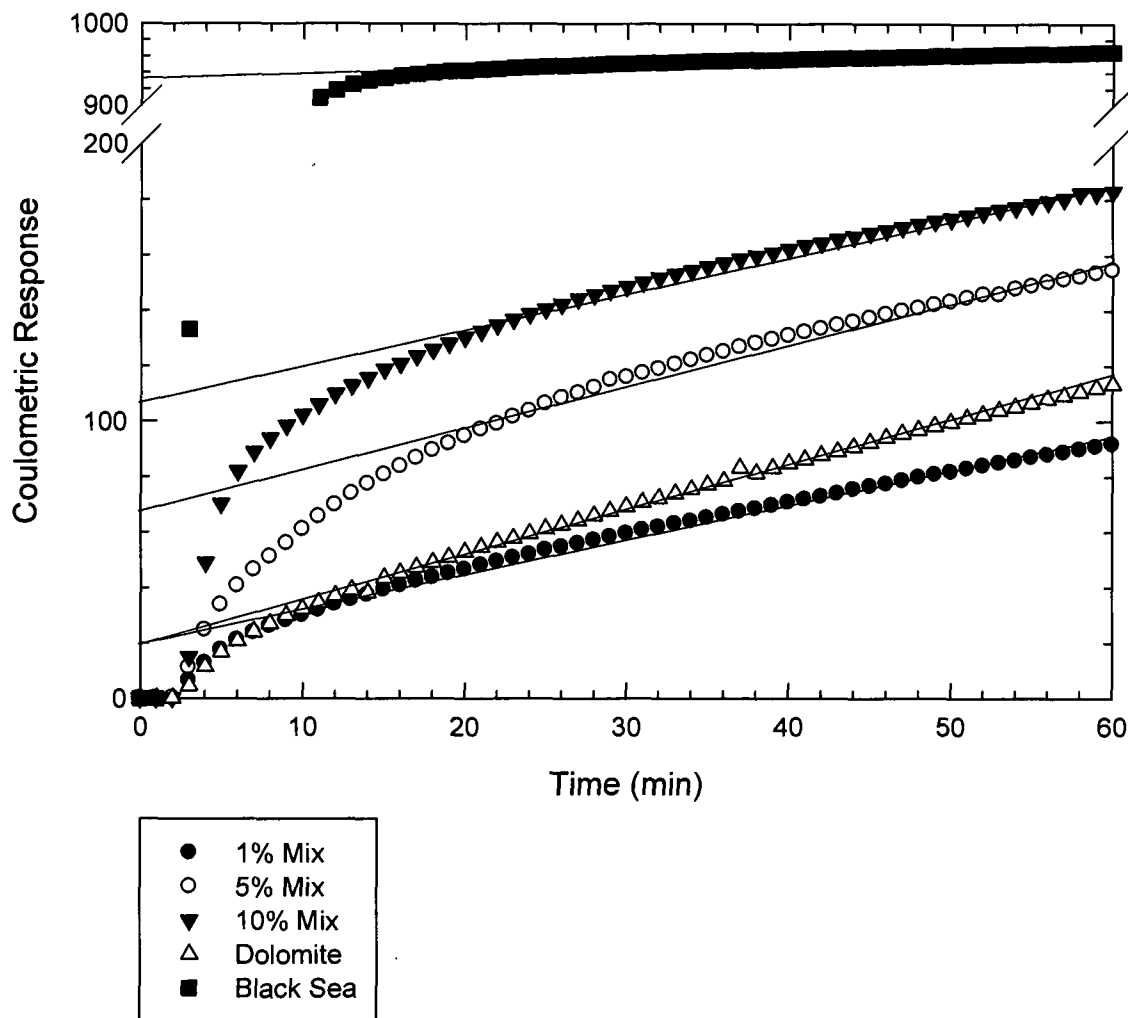


Figure 12. Responses of three Black Sea/dolomite mixtures, pure dolomite, and “pure” Black Sea sediment used in the mixtures to pH 5 and 10°C treatment. Linear regression of data from 40 to 60 min. are shown.

and 1.2% Black Sea sediment. Figure 12 shows the time evolution of CO₂ from these biogenic and refractory carbonate mixtures, with a rapid production of CO₂ for approximately 20 min and then the slowly increasing “dolomite drift” baseline for the remaining analysis time.

The Black Sea sediment used for the mixtures contains $8.7 \pm 0.2\%$ biogenic carbonate as determined using the total carbonate method. Analyzing the 10.0% Black Sea/ 90.0% dolomite for 60 min. and regressing the last 20 data points (from 40 to 60min.) yielded $0.87 \pm 0.09\%$ biogenic carbonate (Figure 13) compared to the computed value of 0.87%. The same data analysis routine was performed for the other Black Sea/dolomite mixtures. Theoretical values of the sediments and the observed recoveries based on varying analysis times are shown in Table 4. Analyzing the 5.4% Black Sea/ 94.6% dolomite mixture yielded $0.47 \pm 0.08\%$ biogenic carbonate compared to the computed value of 0.47%. The 1.2% Black Sea and 98.8% dolomite mixture yielded $0.27 \pm 0.75\%$ biogenic carbonate; which is more than double the computed value of 0.12%. However, the concentration of the 1.2% Black Sea/dolomite mixture is below the method detection limit of 0.2% (discussed in the next section).

3.3.4. Analytical Figures of Merit

The analytical figures of merit were evaluated using a minimum of four determinations of the 1.2% 5.4% and 10.0% Black Sea/dolomite mixtures. Analysis time for an individual sample is 60 minutes plus an additional 6 minutes for a “dump/rinse” cycle for the CM5240 autosampler, totaling 66 minutes per sample. Accuracy for this method is $100\% \pm 0.1\%$ at the 0.10% and 0.47% concentration (as above for BlackSea/dolomite mixtures). The precision is 10% (RSD) at 0.87% concentration and 16% (RSD) at the 0.47% level. Using the variability at the low 0.47% Black Sea mixture, the detection limit is computed to be 0.2% (3σ , $n = 5$).

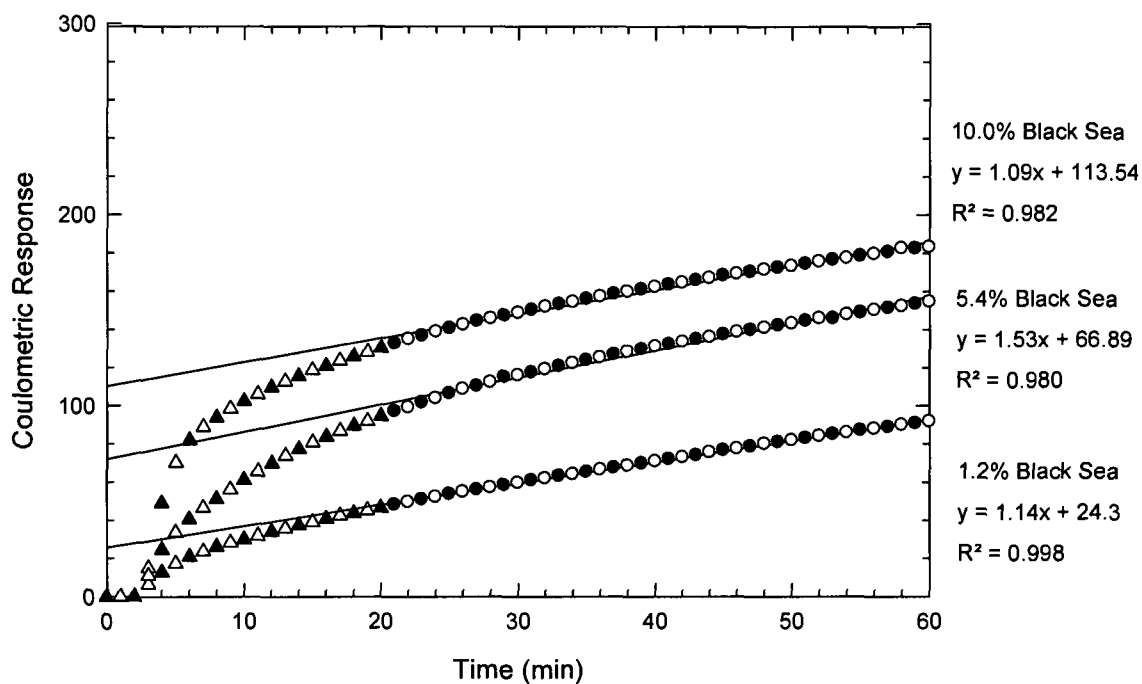


Figure 13. Analyses of three Black Sea sediment-dolomite mixtures under optimized conditions (including linear regressions of the “dolomite drift” to determine the concentration of biogenic carbonate) at pH 5 and 10°C.

3.4. Conclusions

This analytical method developed for determining biogenic carbonate in sediments has proven to be reliable and has good detection limits. The method has a wide application for a variety of sediment types and biogenic concentrations. This new analytical method will prove to be invaluable in the future for assessing contributions of calcareous organisms in regions like the Arctic Ocean and Southern Ocean where their presence in these regions are connected to climate change.

CHAPTER 4

· BIOGENIC MATTER SOURCES THROUGH THE HOLOCENE

4.1. Introduction

Recent observations of the dramatic changes that are occurring in the Arctic Ocean are receiving great attention due to the effects these changes have on this ecosystem. In order to put these current day observations into historical context and perhaps reveal mechanisms controlling them, many parameters must be constrained, such as surface water primary production, sources of biogenic and detrital materials, amounts of river discharge, surface water circulation, and amounts of carbon burial and rates of remineralization. These parameters are directly or indirectly preserved in the sediment record and thus show temporal changes in environmental conditions [cf. *Burdige, 2006*]. Nevertheless, an individual sediment record also reflects its unique environmental setting, including water depth, sedimentation rate, and proximity to external sources such as rivers. When several locations' environmental records are compared, regional trends can be established. In this case, records of the oceanographic conditions, amounts of ice cover, river inputs to the region, and changes in salinity on the Alaskan shelf during the Holocene were sought.

The sources of organic matter can help establish climatic and environmental conditions by the presence, absence, or differences in types of material. For example, recently observed climate changes have increased the ventilation of deep water with surface water, transporting nutrients from below the mixed layer to the surface layer [*Hill and Stockwell, 2005*]. With more nutrients and light available in the surface ocean of the Arctic, primary production has deepened below the stratified surface layer into

the thermocline [*Hill and Stockwell, 2005*]. Of the primary producers present in the Arctic Ocean today, typically it is dominated by diatoms [*Hill and Stockwell, 2005*]. However, recent observations in the nearby Bering Sea document blooms of coccolithophores in place of diatoms [*Jida, 2002*]. Sediment records of biogenic silica or carbonate document whether ecological shifts such as this have occurred before on the Alaskan shelf.

Inputs of organic matter from terrestrial sources are preserved in the Alaskan shelf and slope sediments [*Belicka et al., 2004*]. Geochemical clues about terrestrial organic materials, such as those from carbon and nitrogen isotopes and biomarkers differentiate these sources from marine ones. Carbon and nitrogen isotopic end members have been identified in the North Bering-Chukchi Sea as -21.2‰ for marine and -27‰ for terrestrial sources [*Naidu et al., 2000*]. Refractory carbonates eroded from the dolomite bedrock of the Canadian Shield and delivered through river discharge have a relatively short distance between source and deposition when compared to trans-Arctic transport [*Ortiz et al., 2009*]. Source material typical of the Bering Sea and North Pacific show transport through the Bering Strait and into the Barrow Canyon at different times during the Holocene [*Ortiz et al., 2009*].

The diagenetic loss of organic matter is an important aspect to understanding post-depositional changes that affect the sediment record. Undoubtedly, the signals from organic matter that has been buried for 12,000 years or longer will be compromised. Dissolution of biogenic silica, remineralization of carbon, and authigenic production of iron sulfides are all examples of diagenetic reactions that alter the sediment record. In the Chukchi Sea, there is a close association between the amount of

diagenesis that occurs and the sources of organic matter [Naidu *et al.*, 2004]. Increases in sulfate reduction and remineralization occur when greater amounts of labile organic matter are present. The intensity of sulfate reduction and organic mineralization across the shelf increase farther offshore, away from terrestrial sources and with increasing marine organic matter [Naidu *et al.*, 2004]. Rates of remineralization in the Chukchi Sea have been categorized into low productivity and high productivity zones, with approximately 44% and 52% of organic matter being remineralized within the sediments [Naidu *et al.*, 2004]. The remaining organic carbon is subsequently buried at estimated rates of $0.67 \text{ mg cm}^{-2} \text{ yr}^{-1}$ and $1.0 \text{ mg cm}^{-2} \text{ yr}^{-1}$, respectively. Thus, there is ample evidence to support that Arctic sediments document numerous relevant processes in spite of diagenetic losses; this chapter will examine these records.

4.2. Results

4.2.1. Age Model

Age models for JPC05 and JPC08 were constructed using radiocarbon dating on calcareous shells along with paleomagnetic intensities [Darby *et al.*, 2009a; Lise-Pronovost *et al.*, 2009]. Using these age models, all the biogenic and environmental parameters were plotted by relative age to resolve the timing of the major events that have taken place in the Alaskan shelf. The approximate timing of events in cores obtained at Stations 5, 8 and P1 were also compared for broader, regional trends.

Multi-Core 6 (MC 6) that is adjacent to Station 5 was found to be highly bioturbated, to about 10 cm depth, and sedimentation rate using ^{210}Pb is roughly 0.2 cm yr^{-1} [McKay *et al.*, 2008]. Sediments obtained by the trigger core (TC) and jumbo piston core (JPC) at Station 5 had a combined length of 16.3 m, which covers the entire

Station 5

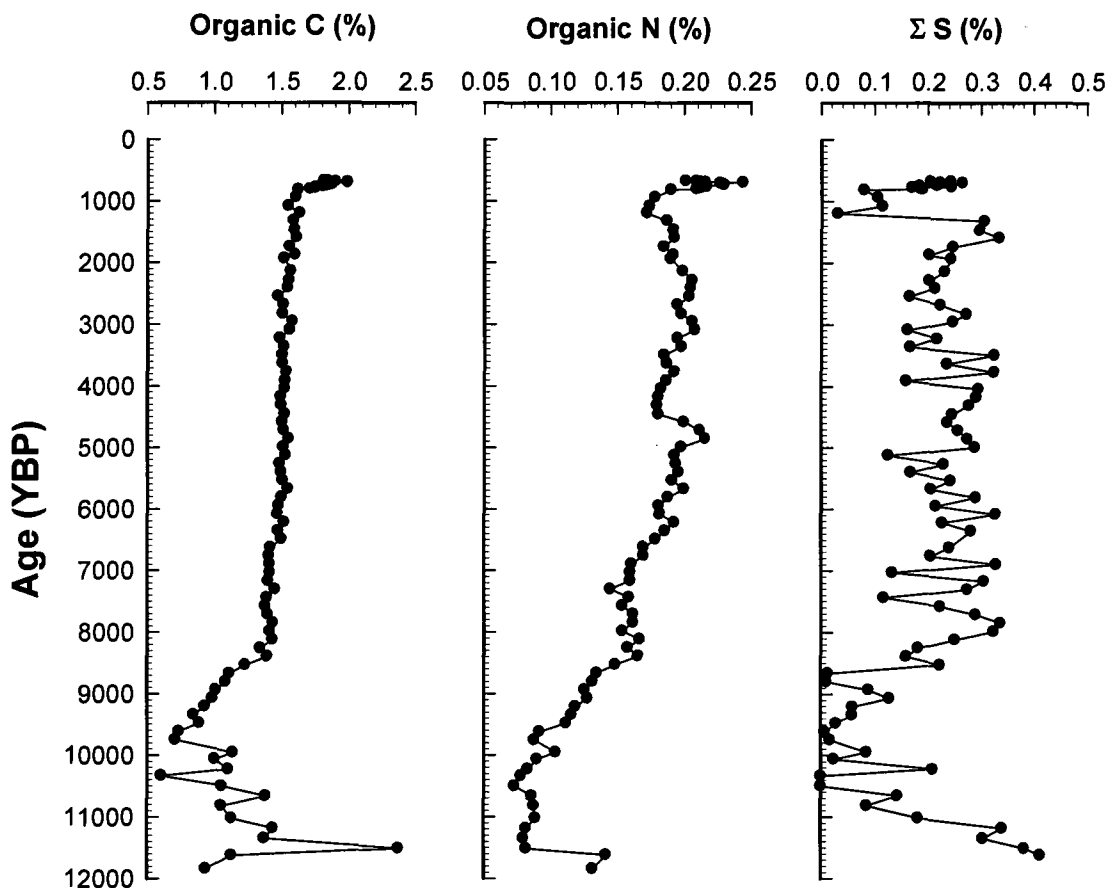


Figure 14. Organic carbon, organic nitrogen, and total sulfur versus age at Station 5.

Holocene and may extend into the late Pleistocene. The sedimentation rate at Station 5 was 1.6 m kyr^{-1} or 0.16 cm yr^{-1} . The JPC and TC obtained at Station 8 had a combined length of 13 m, which covers the Holocene record to ca. 8000 ybp. At 89 m water depth, this station was above sea level during the last glacial interval, 12,000 ybp. The sedimentation rate at Station 8 was 3.5 m kyr^{-1} or 0.35 cm yr^{-1} .

4.2.2. Carbon, Nitrogen, and Sulfur

In the earliest record obtained at Station 5, 10-12,000 ybp, organic carbon was at low concentrations, but varied between 0.5 to 2.5% (Figure 14). The organic carbon at Station 5 steadily increases from 0.5 to 1.5% from 10,000 to 7800 ybp (Figure 14). A similar transition is seen in organic carbon at Station 8 between 8400 ybp and 7600 ybp (Figure 15). Throughout most of the Holocene, 7800 to 1000 ybp, the amount of organic carbon is relatively constant at both Stations 5 and 8, ca. 1.5% (Figures 14 and 15), and increases slightly to 2% in the most recent sediments. The concentration of organic carbon on the Alaskan shelf compare well to those in sediments of the Chukchi and Bering Seas (0.1 to 2.8%), and are similar to those in most continental shelves [Naidu *et al.*, 2004].

Organic nitrogen at Stations 5 and 8 vary more than organic carbon, but have the same general features: two transitional times at the beginning of, and in the most recent Holocene and a somewhat consistent input/preservation interval spanning the mid-Holocene (Figure 14 and 15). At Station 5, from the earliest record obtained until 10,000 ybp, organic nitrogen shows some variability at lower concentrations, 0.8% (Figure 14). Over the majority of the Holocene, 10,000 ybp until 4800 ybp, concentrations of organic nitrogen slowly increase to approximately 0.21%. Between 4800 and 1000 ybp organic nitrogen concentrations slightly decrease, to 0.18%. In the most recent sediments at Station 5, 1000 ybp to present, organic nitrogen increases up to 0.25% (Figure 14). Similar trends in organic nitrogen are seen at Station 8 (Figure 15). Increasing amounts of organic nitrogen, from 0.05 to 0.17%, are seen at Station 8

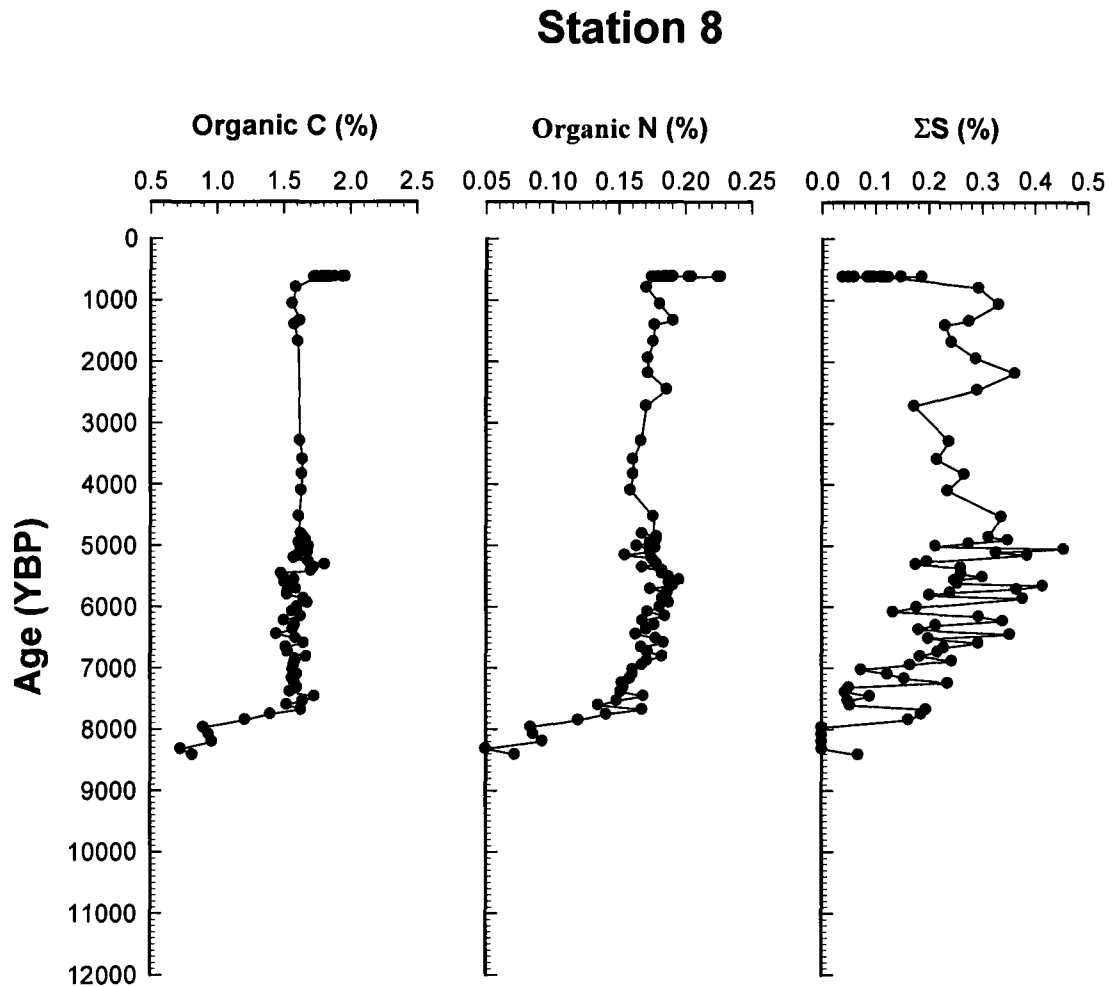


Figure 15. Organic carbon, organic nitrogen, and total sulfur versus age at Station 8.

from 8400 to 7800 ybp, followed by a relatively constant supply of organic nitrogen, ca. 0.16%, from 7800 to 1000 ybp. Surface sediments at Station 8 show a similar increase in organic nitrogen to 0.23%, slightly lower than surface concentrations at Station 5. Organic nitrogen concentrations in the Chukchi shelf have similar ranges, from 0.01% to 0.28% [Grebmeier, 1993, Feder et al., 1991].

Total sulfur in the Alaskan shelf displays a wide range of variability over relatively short time intervals of about 100-600 years (Figures 14 and 15). At Station 5,

the earliest records obtained show a decrease in total sulfur, 0.5% to 0, from 12,000 to 10,000 ybp. Between 10,000 to 9000 ybp, total sulfur is variable at generally low concentration (Figure 14). For the majority of the Holocene, 9000 to 1200 ybp, the concentration of total sulfur is quite variable, with an average value of 0.3%. A 0.2% decrease in total sulfur occurs between 1200 and 800 ybp at Station 5 (Figure 14). Most recent sediments, 800 ybp to present, increase in concentration to ca. 0.2%. Station 8 has a similar total sulfur record as Station 5 (Figure 15). A minimum in total sulfur concentration at Station 8 occurs at 8400 ybp and then total sulfur generally increases to 0.3% at 5000 ybp. Average total sulfur concentrations at Station 8 slightly decrease to 0.25% from 5000 to 600 ybp (Figure 15). Most recent sediments, 600 ybp to present, show a minimum in total sulfur concentrations, varying from 0.2 to 0.01%. No data sets for total sulfur are available for any sediments in the Chukchi Sea or the entire Arctic Ocean.

4.2.3. Biogenic Silica

Biogenic silica concentrations over the Alaskan shelf are relatively low, less than 1% by weight. When examining profiles of biogenic silica two factors must be considered: the preservation of biogenic silica and the apparent supply [*McManus et al.*, 1995]. The diagenetic loss of silica from dissolution [*DeMaster*, 1991] has attenuated its abundance in the mid- to early Holocene. Additionally, the high sedimentation rates in this region have diluted the biogenic silica to just a fraction of a percent. However, there are several events during the late Holocene that illustrate changes in the importance of biogenic sources.

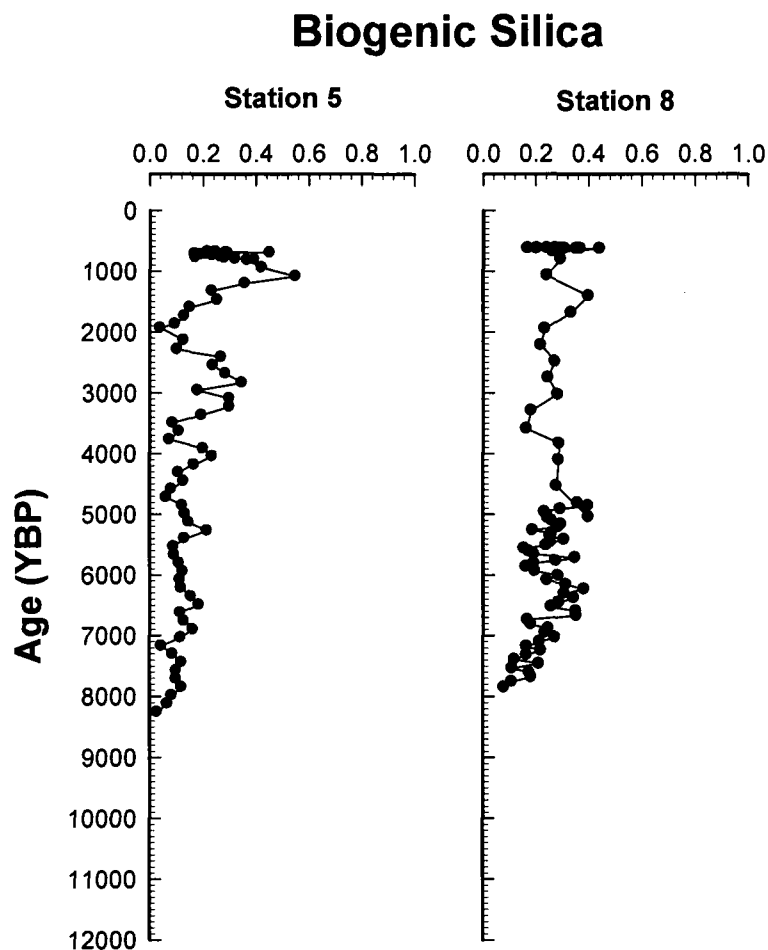


Figure 16. Biogenic silica versus age at Stations 5 and 8.

At Stations 5 and 8 (Figure 16) the earliest records obtained until 8000 ybp do not show any biogenic silica has been preserved. From 8000 to 5000 ybp, slightly increasing amounts, up to 0.1%, of biogenic silica are present at both stations. Maxima in biogenic silica then occur from 5000 to 3300 ybp to 0.22%. Second maxima in biogenic silica, 0.3%, occur between 3300 and 2000 ybp at Stations 5 and 8. In the most recent sediments, 2000 ybp to present, maxima in biogenic silica are recorded, though somewhat higher at Station 5, 0.6%, than at Station 8, 0.4% (Figure 16). Though these events have been attenuated over time due to biogenic silica dissolution

[*McManus et al.*, 1995; *Emerson and Hedges*, 2003], the mere presence of biogenic silica documents periods of higher productivity from siliceous organisms.

4.2.4. Biogenic Carbonate

No biogenic carbonate was detected at either Stations 5 or 8, but the presence of calcareous phytoplankton on the Alaskan shelf cannot be ruled out. For example, coccolithophores and other calcifying plankton have been observed in the Bering Sea [*Napp and Hunt*, 2001; *Iida et al.*, 2002]. Observations of coccolithophores and other calcifying organisms in these regions are indicators of climate change since the calcareous organism typically do not populate cold, high latitude waters [*Gradinger*, 1995]. In addition, it is possible that there are calcifying organisms prolific in this area of the Arctic, but due to the high sedimentation rates at these locations biogenic carbonate has been diluted to undetectable concentrations. The former can be confirmed by the analysis of sediments from a location with very slow sedimentation rates, such as those at Station P1. Moreover, preservation factors must be considered, and in particular, shells and tests of calcareous organisms were absent or highly corroded at both Stations 5 and 8 (Polyak, 2008 personal communication). It seems that post depositional dissolution is prevalent in these cores compared to Station P1.

4.2.5. Total Carbonate

Total Inorganic Carbonate (TIC) profiles (Figure 17) from the Alaskan shelf show a low, continuous supply of carbonate-rich detrital material, approximately 0.2%, during most of the Holocene. Although the records at Stations 5 and 8 are slightly offset in the timing of events, they are very similar in shape (Figure 17). Early Holocene records at Station 5 show variability, but increasing amounts of total

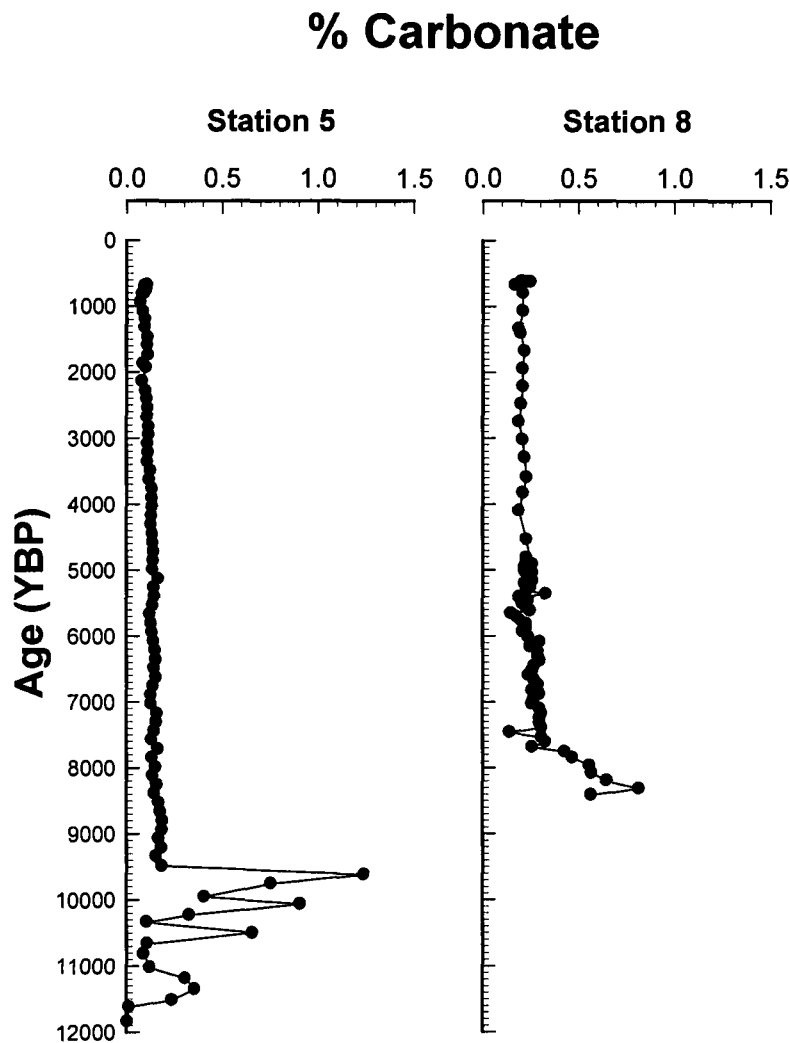


Figure 17. Total carbonate versus age at Stations 5 and 8.

carbonate, 0 to 1.5%, from 12,000 to 9500 ybp. An abrupt decrease in total carbonate occurs at 9600 ybp to low concentrations, 0.2%. From 9600 ybp to present, total carbonate remains quite low and slowly declines to 0.1%. Station 8 shows a rapid decrease in total carbonate, 1 to 0.2% from 8400 to 7700 ybp. Total carbonate concentrations at Station 8 remain constant over the majority of the Holocene, 0.2% (Figure 17). Reflectance and X-ray diffraction analyses of these sediments [Ortiz *et al.*, 2009] identify dolomite weathered from the Canadian Shield as the source of carbonate

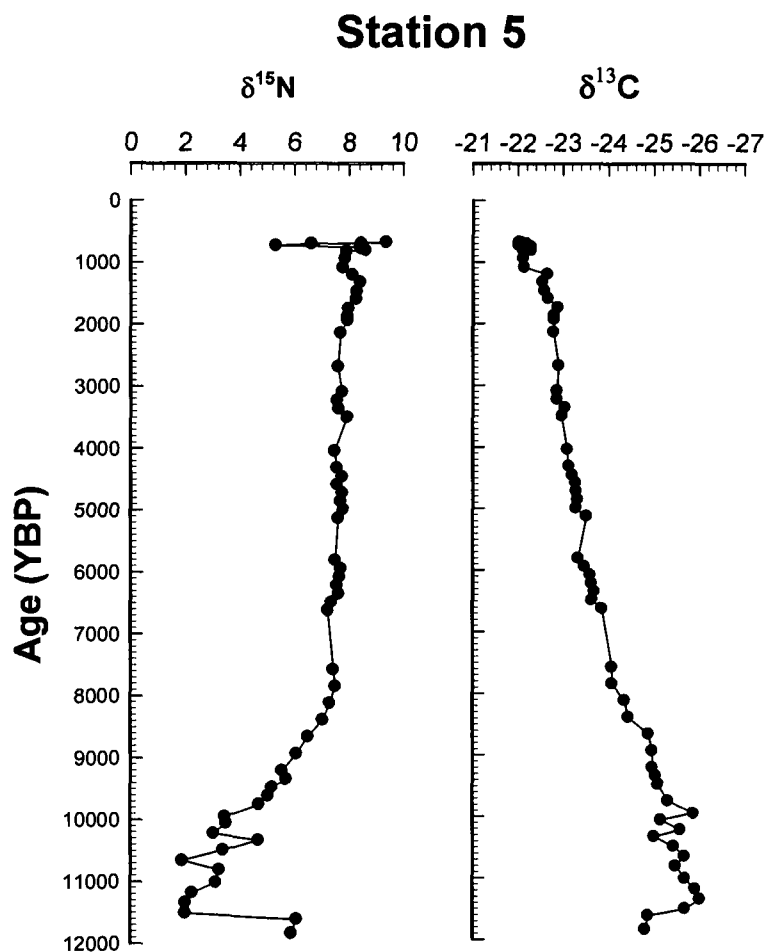


Figure 18. Organic carbon and nitrogen isotopes versus age at Station 5.

to the Alaskan shelf. The sediments deposited onto the Alaskan shelf are from nearby sources, rather than transported from great distances.

4.2.6. Carbon and Nitrogen Isotopes

Carbon and nitrogen isotope data are used to better identify sources of organic matter because marine and terrestrial organic matter have distinct isotopic signatures [Stein and Macdonald, 2004a]. ^{13}C data from Station 5 show a transition of isotopic composition over the Holocene, ranging from -26‰ in the early Holocene to -22‰ in the most recent sediments (Figure 18). This broad range encompasses both terrestrial

and marine isotopic signatures and highly degraded terrestrial matter such as soils [Burdige, 2006]. Typically, -27‰ is used as the terrestrial end member for the Beaufort Sea [Naidu *et al.*, 2000]. The marine isotopic end member is less straightforward, ranging from -15‰ to -22‰ [Stein and Macdonald, 2004a].

^{15}N data show a wide range of isotopic signatures, 2‰ to 10‰ (Figure 18). In the early Holocene, 12,000 ybp, ^{15}N is 5‰ and quickly decreases to < 2‰. From 11,500 to 8,000 ybp, the ^{15}N signature shows an increase from <2‰ to 8‰. From 8,000 to 1,000 ybp ^{15}N is constant at 8‰. From 1,000 ybp to the most recent surface sediments obtained at Station 5, there is a minimum in ^{15}N at 5‰ (Figure 18). The isotopic marine and terrestrial “end members” for ^{15}N are not as clearly defined as ^{13}C . Typically ^{15}N from terrestrial sources are generally >10‰ and marine sources are < 5‰ [Fogel and Cifuentes, 1993; Schubert and Calvert, 2001].

4.2.7. Total Sulfur and Sulfur Speciation

Sedimentary sulfur can be derived from different pools of organic, inorganic, and elemental forms and is highly affected by biogeochemical cycling in anoxic environments [cf. Cutter and Velinsky, 1987]. As organic matter is diagenetically altered by anaerobic respiration, the formation of iron sulfide compounds such as acid-volatile sulfide (AVS), greigite, and pyrite occur [cf. Cutter and Velinsky, 1987]. AVS, primarily FeS, is unstable and typically found in early stages of anoxic diagenesis [Goldhaber and Kaplin, 1974]. These amorphous, weakly crystalline iron monosulfides are soluble in weak hydrochloric acid (hence the name) and may be lost due to oxidation or transformed to greigite and/or pyrite [Sweeny and Kaplin, 1973; Berner, 1970].

Arctic 2005 HLY0501-MC6

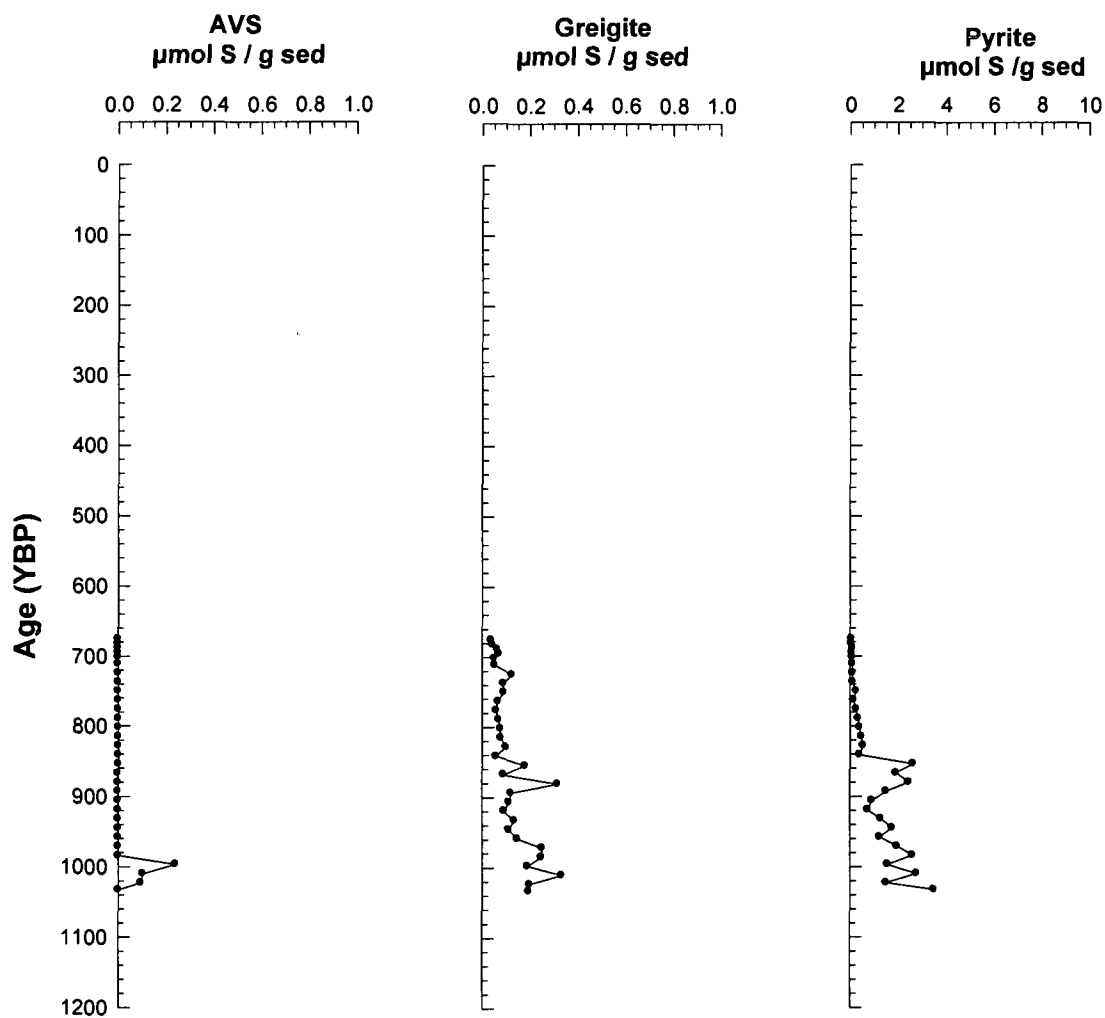


Figure 19. Acid volatile sulfide (AVS, primarily FeS), greigite (Fe_3S_4), and pyrite (FeS_2) versus age in Multicore 6 that is adjacent to Station 5.

Very little AVS is present in the surface sediments of the Alaskan shelf; at 1,000 ybp a small amount of AVS was detected (Figure 19). Greigite (Fe_3S_2), also an unstable intermediate mineral in the formation of pyrite, has very low concentration and

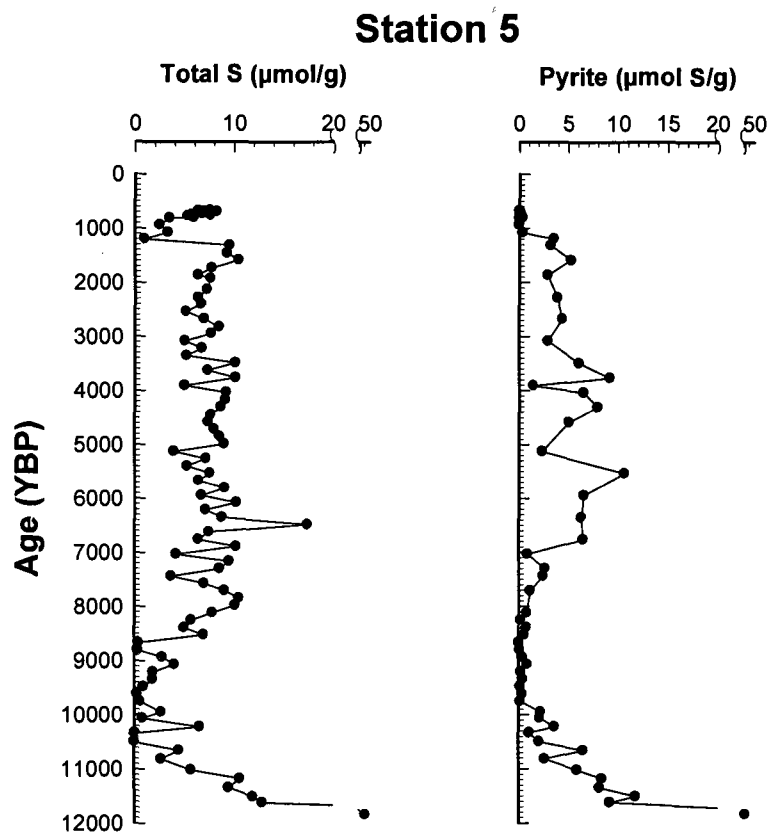


Figure 20. Total sulfur and pyrite versus age at Station 5.

generally decreases from 1,000 ypb to present (Figure 19). Pyrite (FeS_2), the thermodynamically stable iron sulfide mineral, shows a maximum of $5 \mu\text{mol g}^{-1}$ at 1000 ybp. From 1000 to 850 ybp pyrite concentrations are ca. $2 \mu\text{mol g}^{-1}$. From 850 ybp to present, pyrite concentrations decrease to undetectable level (Figure 19). Sulfur speciation in the most recent sediments in the Alaskan shelf shows that 94-99% of the total sulfur is not identified by these three constituents. This may in part be due to the well oxygenated and bioturbated sediments (Hillaire-Marcel, personal communication) that do not support sulfate reduction. Other phases, elemental sulfur and more likely organic sulfur make up the majority of sulfur delivered to the sediment surface [Matrai and Eppley, 1989; Cutter and Velinsky, 1987].

Due to storage issues with the trigger and piston cores, only pyrite was determined in these samples. Pyrite abundance at Station 5 show the highest concentrations, ca. $50 \mu\text{mol g}^{-1}$, in the earliest records (Figure 20). A rapid decrease occurs to concentrations near or below detection limits from 9800 to 7000 ybp. Wide variation in pyrite concentrations occur from 7000 to 2000 ybp, ranging from 1 to $11 \mu\text{mol g}^{-1}$ with average values around $3 \mu\text{mol g}^{-1}$. Concentrations of pyrite again decrease to near detection limit ($0.1 \mu\text{mol S g}^{-1}$) in the most recent sediments (Figure 20). Other stable phases of sulfur, elemental sulfur and more likely organic sulfur make up the difference in sulfur concentrations not accounted for by pyrite concentrations [Matrai and Epply, 1989; Cutter and Velinsky, 1987]. Currently, no known data sets are available for sulfur speciation in the Chukchi Sea or Arctic Ocean with which to compare.

4.3. Discussion

4.3.1. Temporal and Regional Trends

The organic carbon to nitrogen ratio can be used to roughly elucidate the sources of organic matter. Based on the Redfield ratio, pure marine organic matter has an atomic C/N ratio of 6.6 [Redfield *et al.*, 1963]. Terrestrial organic matter is enriched in carbon, which elevates the C/N to values of 15 or higher [Naidu *et al.*, 1993]. In North Bering-Chukchi Sea sediments, C/N ratios range from 7.5 to 12 [Naidu *et al.*, 2004].

The earliest record obtained at Station 5 has low C/N values, ca. 6 (Figure 21). Directly after these two data points, C/N values generally increase until 9800 ybp. The elevated C/N values during this time are suggestive of a decline in marine organic matter supply and an increase in terrestrial materials. For the majority of the Holocene,

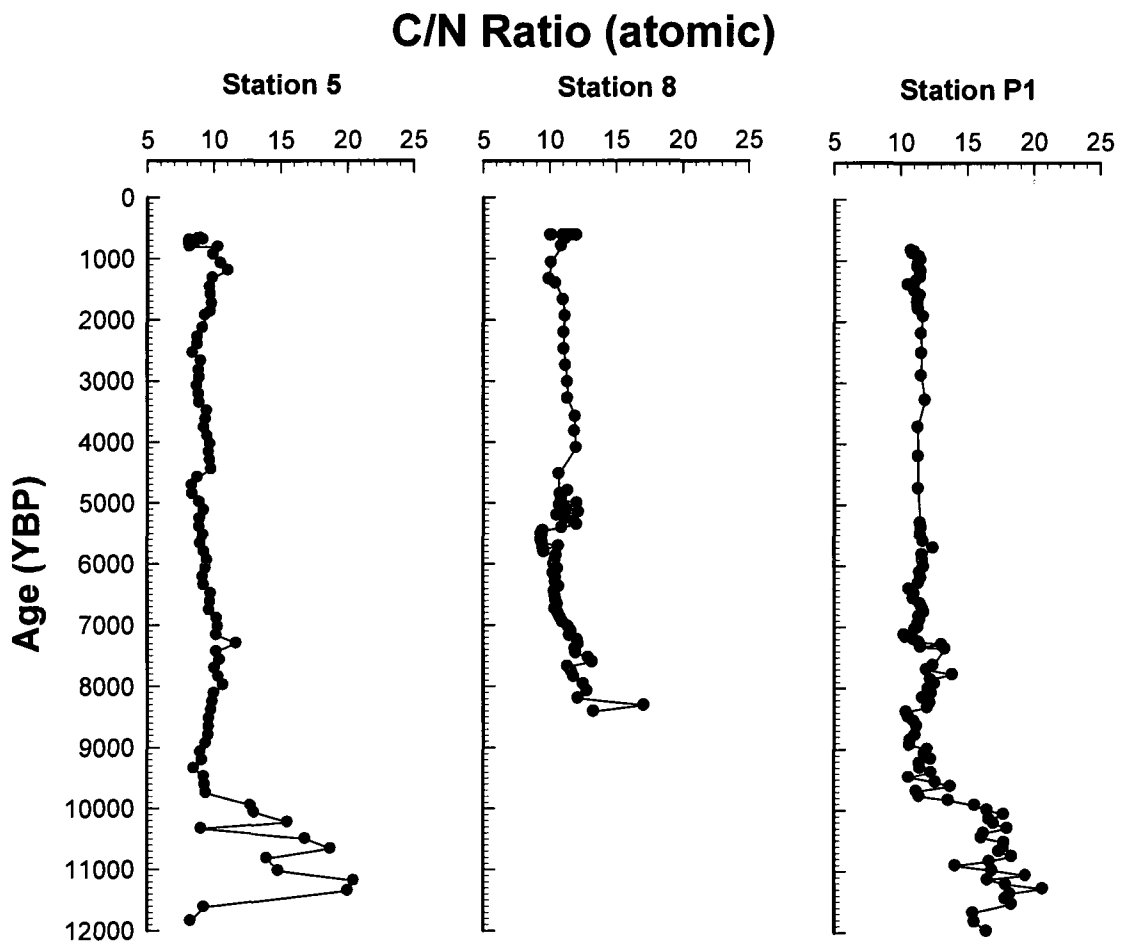


Figure 21. Atomic organic carbon:organic nitrogen ratios versus age at Stations 5, 8, and P1.

9800 ybp to present, Station 5 shows only small variations in C/N and are constant, ca. 10 (Figure 21). Most of the fluctuations in the C/N values can be attributed to the variability in nitrogen supply/preservation as the profile of organic carbon is quite constant during this time (Figure 14 and 15). The record at Station 8 is abbreviated due to its depth, but closely resembles the general trends observed at Station 5. Station P1 also shows the same trends as Station 5 and 8 (Figure 21). At 8000 ybp, Station P1 shows a small decrease in C/N that is not observed in the other profiles.

The low level of refractory dolomite over the Holocene shows a constant, but weak, background source of terrestrially-derived material (Figure 17). The source of dolomite in this region of the Arctic Ocean is weathered from the Canadian Shield [Ortiz *et al.*, 2009] and delivered to the shelf via river input, sea ice, and surface currents. In the early Holocene, 12,000 to 9500 ybp, Station 5 shows an increase in refractory carbonate which also occurs simultaneously with low sulfur and organic carbon abundances. The increase of terrestrially-derived material and decrease in sulfur and organic carbon indicates terrestrial sources of material to the Alaskan shelf delivered via river and glacial outwash during this time. From 9500 ybp to present, the low level of refractory dolomite over the majority of the Holocene is consistent with a constant, but weak, background source of terrestrially-derived material (Figure 17). Station 8 shows a slightly higher amount of dolomite than Station 5 during this time, ca. 0.2%. The increase of dolomite at Station 8 over Station 5 (Figure 17) is consistent with its closer proximity to land, indicating the source of dolomite is delivered via terrestrial sources, and not surface currents.

Combining what was previously known from Station P1 (Figure 2) and the new data from Stations 5 and 8 (Figure 14 and 15), similar trends in biogenic matter are seen over the Alaskan shelf (Figure 22). Though the sediment record is of a much lower resolution at Station P1 (only 2 m in length), it has remarkable similarities to the other stations (Figure 22) For the majority of the Holocene, there are almost identical trends in three of the four components, including the variability in sulfur, the abundance of organic carbon, and increase in nitrogen into the early Holocene.

Stations P1, 5 and 8

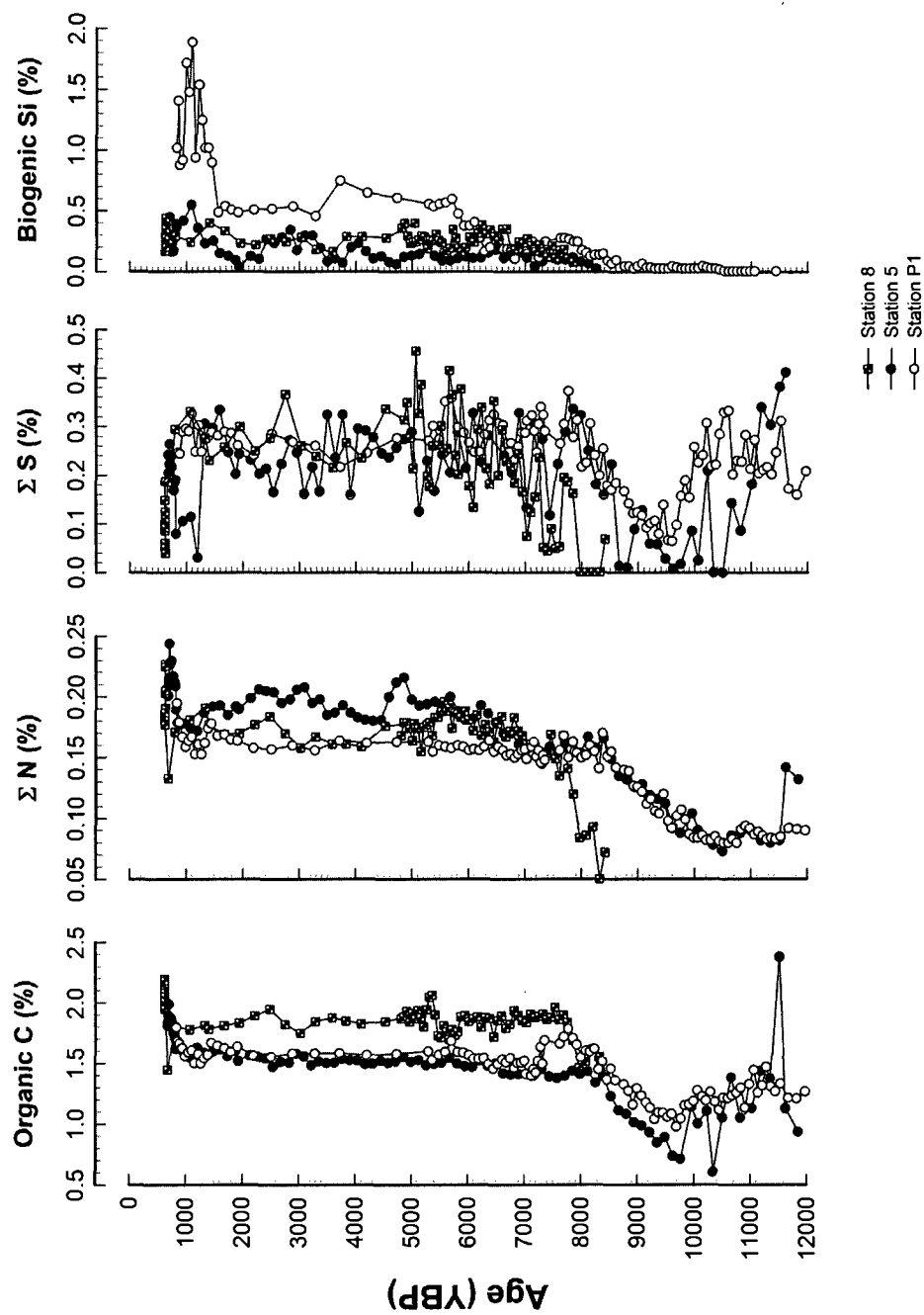


Figure 22. Overlays of organic carbon, organic nitrogen, total sulfur, and biogenic silica at Stations P1, 5, and 8.

Several events at Station 8, including a decrease in total carbonate at 8400 ybp (Figure 17), sulfur minimum at 8,000 ybp, organic carbon and nitrogen maximum at 7,700ybp (Figure 22), are equally observed at Station 5 and, P1 but separated by ca. 1000 years. The offset in the timing of these events seen at Station 8 from 5 and P1 (Figure 22) could be from a delay at Station 8 due to its location (currently 89 m) being above sea level at the beginning of the Holocene [*Kegwin, et al.*, 2006]. Thus, the environmental conditions at Station 8 went from terrestrial to very shallow, near shore conditions, to those of today. Alternatively, the age models used for these cores are incorrect after ca. 7000 ybp due to a lack of calcareous shells for ^{14}C dating. Ages beyond 7000 ybp at both Stations 5 and 8 should be considered estimates only.

The profile of pyrite is a reliable indicator of sulfate reduction under anoxic conditions [*Berner and Raiswell*, 1984]. Contributions of pyrite from external or coastal sources are discussed as part of the lithological studies by *Ortiz et al.* [2009] using reflectance and x-ray diffraction analysis. This work shows only trace amounts, ca. 0.5 %, of detrital pyrite in these and other sediment cores obtained in the Alaskan shelf.

During the early Holocene, 12,000 - 9000 ybp, the total sulfur profile is equally reflected in the abundance of pyrite (Figure 20). The early Holocene has strong characteristics of terrestrially-derived materials supported by increased amounts of dolomite (Figure 17), C/N ratios (Figure 21), and isotope data (Figure 18). Therefore, it is possible that the pyrite delivered to the Alaskan shelf in the earliest Holocene is from detrital sources. The variations in total sulfur between 9000-7000 ybp can be attributed to a supply or the preservation of elemental sulfur or more likely organic sulfur [*Matrai and Eppley*, 1989; *Cutter and Velinsky*, 1987] as pyrite values are minimal (Figure 20).

The majority of total sulfur between 7000 to 1000 ybp can be attributed to pyrite during this time (Figure 20). Pyritization in marine sediments, support by both C/N and isotope data, is indicative of anoxic conditions during these times.

To further evaluate the paleo-environmental record of the Alaskan shelf, the degree of pyritization (DOP) can be used as a unique tool. The carbon-sulfur-iron system has been used to differentiate between marine and non-marine conditions, and estimates of burial for these elements [Lyons, 1997; Berner and Raiswell, 1984]. Typically pyrite iron vs. total reactive iron is used to calculate DOP [Lyons, 1997]. However, DOP can also be calculated using pyrite sulfur vs. total sulfur (i.e., the degree of sulfur pyritization) since both are ingredients of pyrite. Though the input of organic carbon seems uniform throughout the Holocene (Figure 22), changes in the sediment biogeochemistry have occurred. Several periods during the Holocene show reducing or aerobic conditions within the sediments as documented by pyrite and DOP. In the earliest Holocene, 12,000-9500 ybp, DOP (Figure 23) and pyrite (Figure 20) values are at their highest values. However, as noted above, this period, has strong characteristics of terrestrially-derived materials; therefore it is possible that the pyrite delivered to the Alaskan shelf during this time is from detrital sources.

Subsequently, very low concentrations of total sulfur and very little pyritization (ca. 20% DOP; Figure 23) were occurring ca. 9500 to 7700ybp. The C/N and isotope data (discussed next) show that during this time organic carbon sources are highly-degraded terrestrial soils. Given these biogeochemical parameters at Station 5, it is likely that the paleo-environmental conditions in the early Holocene had strong inputs

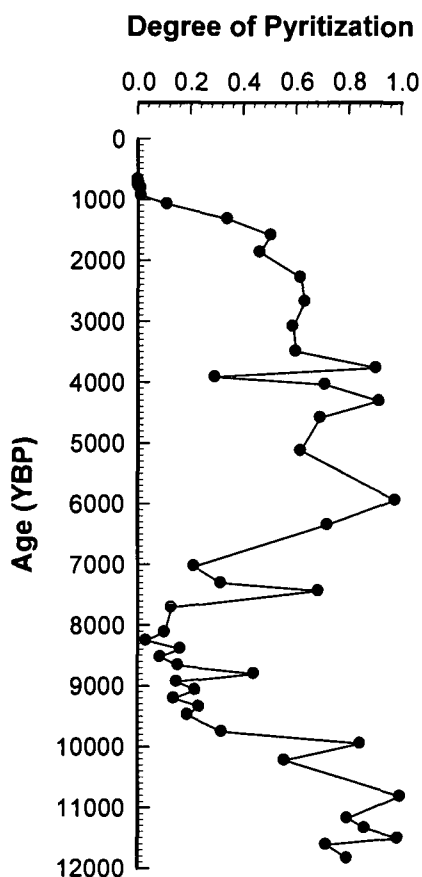


Figure 23. Degree of pyritization (calculated at the ratio of pyrite sulfur to total sulfur) as a function of age at Station 5.

of terrestrial materials and low sulfate, and therefore minimized pyrite formation. One could argue a large freshwater inputs may have occurred (low Org C/pyrite S), but it is difficult to resolve this from simple delivery of terrestrial organic matter input with low total S. Pyrite abundance and DOP values are variable and then generally increase from 7700 to 6000 ybp.

During the mid-Holocene, 6000 to 3800 ybp, the total sulfur is variable and ranges between 0.2 to 0.3%. At this time the DOP is relatively high; supporting 60-100% of total sulfur as pyrite (Figure 23). Increased DOP shows that sufficient amounts of labile organic matter were supplied to the sediments of the Alaskan shelf to support

Source materials to the western Arctic shelf

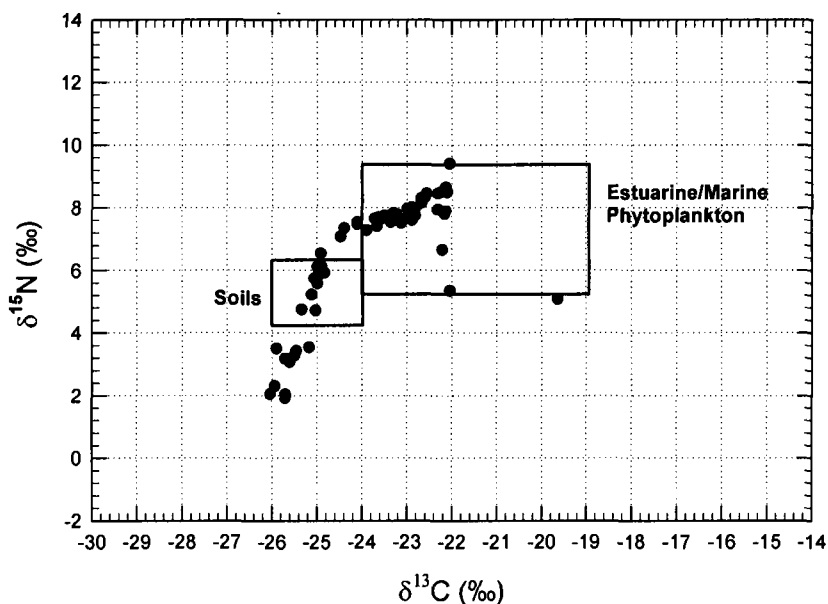


Figure 24. Known isotopic source materials (boxes) overlying organic carbon and nitrogen isotope data from Station 5

anoxic respiration and enough iron and sulfate were present to allow pyritization (Figure 22). Thus, carbon remineralization within the sediments from 6000 – 3800 ybp was driven by sulfate reduction and not oxic respiration. Between 3800 to 1000 ybp DOP slowly decreases to zero. The most recent sediments show ca. 0.2 to 0.3% total sulfur, but no pyritization has occurred due to strong bioturbation and oxygen penetration into the sediments.

4.3.2. Sources of Organic Matter

Isotopic signatures for marine/estuarine phytoplankton and highly-degraded terrestrial organic matter and soils can be separated by $\delta^{13}\text{C}$ and $\delta^{15}\text{N}$ [Cloern *et al.*, 2002]. Organic matter delivered into the Alaskan shelf from the early Holocene, 12,000 to 10,000 ybp, show a marine-like $\delta^{15}\text{N}$ isotopic signature ($< 2\text{‰}$), but it is not

supported by the depleted $\delta^{13}\text{C}$ values indicating soil organic matter. The increase in both $\delta^{13}\text{C}$ and $\delta^{15}\text{N}$ from 10,000 to 8000 ybp show a transition, or mixing, of organic matter sources from highly-degraded, terrestrial soils to more marine-like source (Figure 24). From 8000 ybp to the present, isotope data fall within the range of estuarine and marine phytoplankton (Figure 24).

Together, changes in C/N and $\delta^{13}\text{C}$ can better elucidate the sources of organic matter [Stein and Macdonald, 2004a]. The variability shown in elevated C/N values and a range of $\delta^{13}\text{C}$ from -25 to -26‰ (Figures 5 and 25) in the early Holocene, 12,000 to 9000 ybp, is consistent with terrestrial organic matter (Figures 5, 22, and 25). Low C/N values are constant for most of the Holocene (Figure 21), implying the invariant supply of organic C and N, but increasing $\delta^{13}\text{C}$ (Figure 19) shows a shift from degraded terrestrial organic matter to modern marine organic materials from 9000 to 1000 ybp (Figure 25). In the last 1000 years the source of organic matter to this area of the Alaskan shelf is consistent with marine phytoplankton, similar to what is currently found in the Chukchi shelf today [Naidu *et al.*, 1997].

Throughout the Holocene, the sources of biogenic matter transitioned between marine and terrestrial inputs. Of the marine inputs, approximately 0.2% of the bulk sediment was comprised of biogenic silica, directly confirming the importance of diatoms and other siliceous organisms as primary producers in the mid- to late Holocene (Figure 22). Small differences in biogenic silica abundances between stations indicate slightly different environmental conditions at each station over the Holocene (assuming similar preservation). P1 clearly show a maximum at 7800 ybp that is not present at the other locations (Figure 22). This additional supply/preservation of

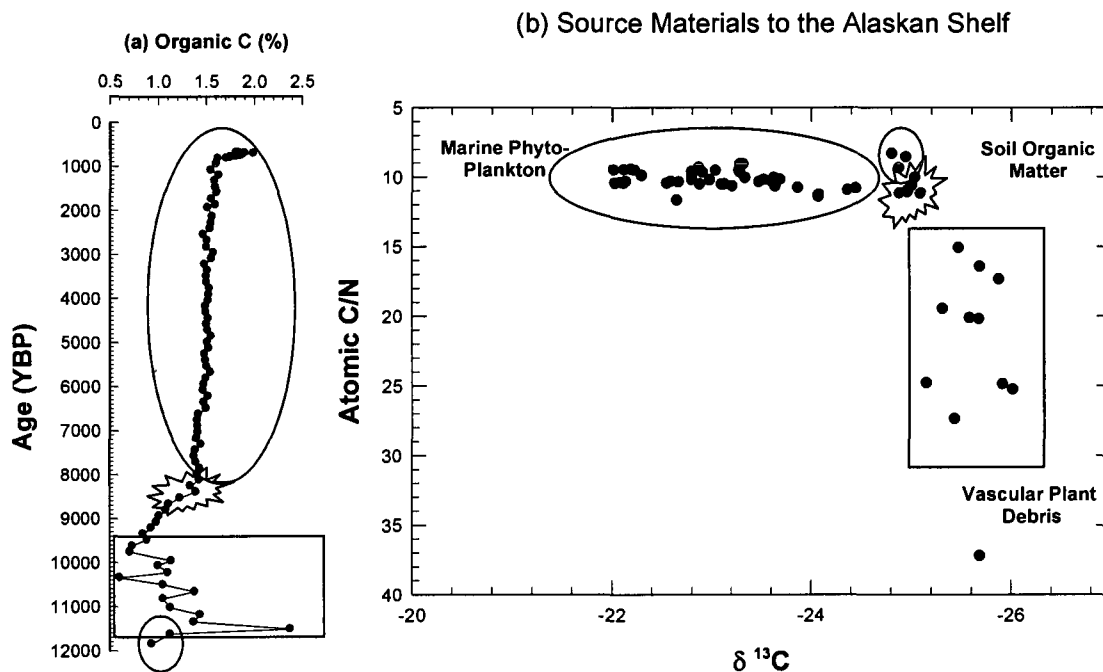


Figure 25. Plots of (a) organic carbon versus age at Station 5 and (b) Atomic C/N versus $\delta^{13}\text{C}$ from Station 5, with known organic matter sources identified.

biogenic silica could quite possibly be a sustained increase of primary production equal or greater than what is observed today in the Alaskan shelf given the known diagenetic loss of biogenic silica. Additionally, surface and subsurface biogenic silica maxima at Station P1 highlight important events in primary production that are not as pronounced at Stations 5 and 8 (Figure 22). The high sedimentation rates at Station 5 and 8, 0.15 and 0.35 m kyr^{-1} respectively, might have diluted the amount of biogenic silica to a fraction of what was preserved at Station P1. Station 5 and 8 are also closer to land and possibly subject to higher inputs of terrestrial and glacial matter. The use of biomarkers could help determine specific contributions of organic matter from diatoms from other marine sources.

4.3.3. Integrity of the Sediment Records

Biogeochemical properties of sediments are subject to reworking from oxic or anoxic metabolism. To quantify the amount of organic carbon lost due to remineralization occurring in these shelf sediments, equations (2) and (3) following the multi “G” model (Bernier, 1980; Martens and Klump, 1984) were used. Fitting the organic carbon data from the piston core at Station 5 to equation (2), using measured sedimentation rates, etc, a rate constant for remineralization, $k = 0.0027 \text{ yr}^{-1}$, was calculated. The MC data at the top of Figure 14 show more rapid remineralization, as organic carbon concentrations decrease 0.5% in less than 1,000 years. Fitting the organic carbon data from the multicore to equation (2), and using estimated sedimentation rate of roughly 0.2 cm yr^{-1} [McKay *et al.*, 2008], a rate constant for remineralization, $k = 0.006 \text{ yr}^{-1}$, was calculated. In comparison, coastal remineralization rate constants for the “G1” or more labile fraction are $1\text{-}8 \text{ yr}^{-1}$ [Burdige, 2006]. These low rates of remineralization on the Alaskan shelf, both in the surface sediments and over the entire Holocene record, are comparable to rates modeled by Tromp *et al.* [1995] as the less reactive, more refractory “G2” fraction (10^{-1} to 10^{-5} yr^{-1}). Though the comparison of coastal rates is difficult because sedimentation rates, sources, and amounts of organic carbon vary widely, little carbon is being remineralized at Station 5 after deposition.

According to Naidu *et al.* [2004], between 3-60% of organic carbon flux accumulates on the sea floor and of that portion, 40-97% is remineralized by benthic organisms or lost to resuspension and advection. Very little organic matter is actually retained below the mixed or bioturbated layer. The low rate of remineralization

calculated here implies two points: whatever carbon that was getting deposited is slowly remineralized over a long time scale (5000 yrs) much like deep sea sediments, and the “G1” organic material was rapidly lost before it was buried.

The fraction of organic matter that is buried at Station 5 can be quantified using equation (4). Sediment trap data from other investigators [Naidu *et al.*, 2004] show that the particulate organic carbon flux to these sediments is ca. 76 to 2 mg cm⁻¹yr⁻¹ (productive vs. non-productive regions) [Stein and MacDonald, 2004]. Using these estimates and organic carbon data in Figure 14 to calculate carbon burial efficiency, Station 5 has a 1.5% burial efficiency. Similarly, regions of the Chukchi Sea have burial efficiencies of 1.0 to 0.67% [Naidu *et al.*, 2004]. Estimates of burial efficiency for shelf and upper slope sediments of mid- to low latitudes are 42% [Burdige, 2006]. Thus, Station 5 has similar burial efficiency as other regions of the Alaskan shelf and Chukchi Sea, but only a fraction of burial compared to other shelf and slope systems.

4.4. Summary

The many biogeochemical parameters used in this study can be used to place the observed modern day changes occurring in the Alaskan shelf in context with past events (Figure 26). The C/N and ¹³C in the very earliest record at Station 5, 12,000 ybp, suggest marine conditions prior to the inundation of glacial outwash and terrestrial organic matter (Figures 18 and 21). From 12,000 to 9600 ybp abundant amounts of terrestrially-derived materials were delivered to the Alaskan shelf (Figure 26). These terrestrial sources are confirmed by the abundance of dolomite, high C/N ratios, heavy ¹³C signatures, and low sulfur (Figures 17, 18, 21, and 22). Immediately following these terrestrial inputs, a thousand year transition in the Alaskan shelf established

marine conditions like those found in the late Holocene (Figure 25). A decrease in dolomite supply, decreasing C/N ratio, lighter ^{13}C signature, and a return of sulfur into the system support marine sources of organic matter and a decrease of terrestrial inputs (Figures 17, 21, 22, and 25).

In the mid-Holocene, 6000 – 1000 ybp, increased concentrations of pyrite occurred at this time because enough labile organic matter was deposited for anoxic conditions to occur, and sufficient amounts of sulfate and iron were available for efficient pyritization, 60-80% (Figure 23) of the sulfur and iron available. These anoxic, sulfate-reducing conditions were present for many thousands of years during the mid-Holocene (Figure 26). The most recent record, 1000 to present (Figure 14), shows much different biogeochemical conditions than in the mid- to early Holocene. Organic carbon concentrations are 50% higher, but anoxic conditions do not appear to be present (Figure 19). This is likely the result of high amounts of bioturbation, enhancing oxygen penetration into the upper sediments of the Alaskan shelf.

In terms of the marine sources of organic matter in the mid- and late Holocene, their origin appears to be diatoms or other siliceous organisms that could be further identified by biomarkers (Figure 16). The recent observations of coccolithophores in the Bering Sea suggest that other phytoplankton species could be present in high latitude waters, but they were not found in the Holocene records examined here. With respect to other environmental changes occurring in the Arctic at present, it will be interesting to see if increased river discharges [Peterson et al., 2002] shift the Alaskan shelf to a more terrestrially-dominated system as seen in the earliest Holocene (Figure 26).

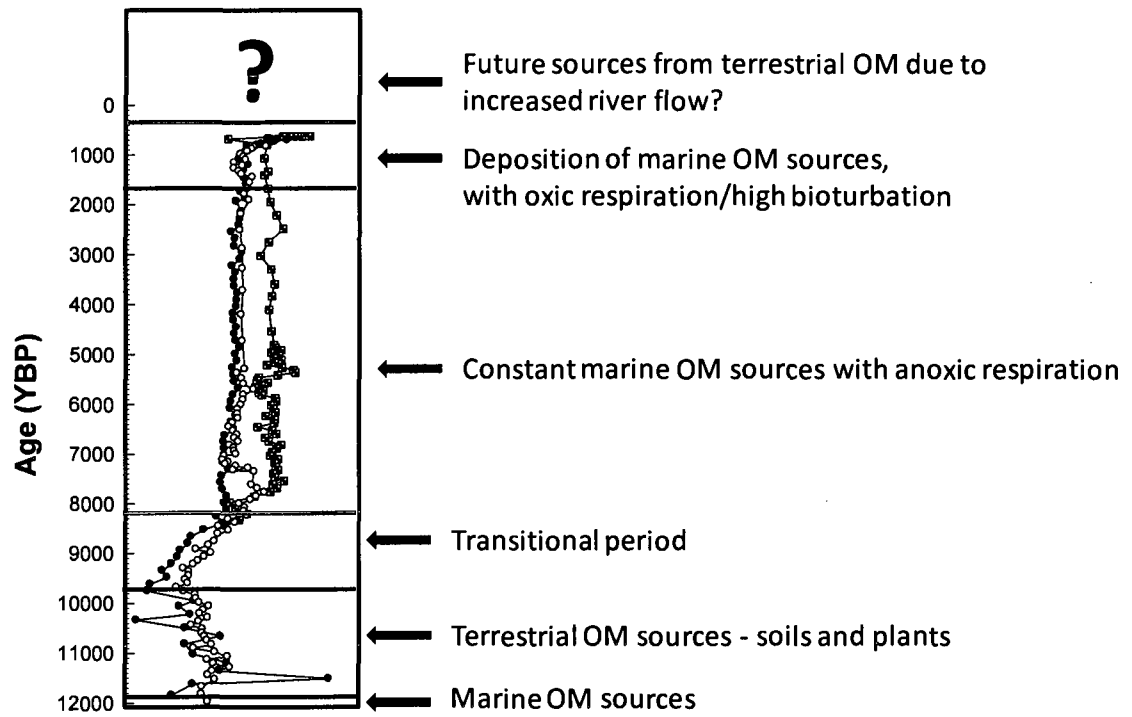


Figure 26. Sources of organic matter (OM) through the Holocene on the Alaskan shelf.

REFERENCES

- Aagaard, K., E. Fahrbach, J. Meincke, and J.H. Swift, Saline outflow from the Arctic Ocean: Its contribution to the deep waters of the Greenland, Norwegian, and Iceland seas, *J. Geophys. Res.*, 96, 20433-20441, 1991.
- Ashjian, C.J., S.M. Gallagher, and S. Plourde, Transport of plankton and particles between the Chukchi and Beaufort Seas during summer 2002, described using a Video Plankton Recorder, *Deep-Sea Res. Part II*, 52, 3109-3115, 2005.
- Baskaran, M., and A.S. Naidu, ^{210}Pb -derived chronology and the fluxes of ^{210}Pb and ^{137}CS isotopes into continental shelf sediments, East Chukchi Sea, Alaskan Arctic, *Geochem. Cosmochim. Acta*, 59, 4435-4448, 1995.
- Belicka, L.L., R.W. Macdonald, M.B. Yunker, and H.R. Harvey, The role of deposition regime on carbon transport and preservation in Arctic sediments, *Mar. Chem.* 86, 65-88, 2004.
- Bender, M.B., W. Martin, J. Hess, F. Sayles, L. Ball, and C. Lambert, A whole-core squeezer for interfacial pore-water sampling, *Limnol. Oceanogr.*, 32, 1214-1225, 1987.
- Berner, R., Sedimentary pyrite formation, *Am. J. Sci.*, 268, 1-23, 1970.
- Berner, R. A. and R. Raiswell, Burial of organic carbon and pyrite sulfur in sediments over Phanerozoic time: a new theory, *Geochim. Cosmochim. Acta*, 47, 855-862, 1983.
- Bond, G., W. Showers, M. Cheseby, R. Lotti, P. Almasi, P. deMenocal, P. Priore, I. Hajdas, and G. Bonani, A pervasive millennial-scale cycle in North Atlantic Holocene and glacial climates. *Science*, 278, 1257-1266, 1997.
- Bordovskiy, O.K., Sources of organic matter in marine basins, *Mar. Geol.*, 3, 5-31, 1965.
- Boudreau, B.P., *Diagenetic Models and their Implementation*, Springer-Verlag, Berlin, 1997.
- Burdige, D.J., *Geochemistry of Marine Sediments*, Princeton University Press, 2006.
- Cloern, J.E., E.A. Canuel, and D. Harris, Stable carbon and nitrogen isotope composition of aquatic and terrestrial plants of the San Francisco Bay estuarine system, *Limnol. Oceanogr.*, 47, 713-729, 2002.
- Codispoti, L.A., C. Flagg, V. Kelly, and J.H. Swift, Hydrographic conditions during the 2002 SBI process experiments, *Deep-Sea Res. Part II*, 52, 3109-3115, 2005.
- Comiso, J.C., C.L. Parkinson, R. Gerstern, and L. Stock, Accelerated decline in the Arctic sea ice cover, *Geophys. Res. Lett.*, 35, L01703, doi:10.1029/2007GL031972, 2008.
- Cutter, G.A., and T.J. Oatts, Determination of dissolved sulfide and sedimentary sulfur speciation using gas chromatography-photoionization detection, *Anal. Chem.*, 59, 717-721, 1987.
- Cutter, G.A., and D.J. Velinsky, Temporal variations of sedimentary sulfur in a Delaware marsh, *Mar. Chem.*, 23, 311-327, 1987.
- Cutter, G.A., and J. Radford-Knoery, Determination of carbon, nitrogen, sulfur, and inorganic sulfur species in marine particles, in *Marine Particles: Analysis and Characterization*, edited by D. Hurd and D. Spencer, pp. 57-63, American Geophysical Union, Washington D.C., 1991.

- Darby, D., J. Bischof, G. Cutter, A. deVernal, C. Hillaire-Marcel, G. Dwyer, J. McManus, L. Osterman, L. Polyak, and R. Poore, New record of pronounced changes in Arctic Ocean circulation and climate, *EOS Trans.*, AGU, 82, 603-607, 2001.
- Darby, D.A., L. Polyak, and M. Jakobsson, The 2005 HOTRAX expedition to the Arctic, *Global Planet. Change*, 68, 1-4, 2009.
- Darby, D.A., J. Ortiz, L. Polyak, S. Lund, M. Jakobsson, and R.A. Woodgate, The role of currents and sea ice in both slowly deposited central Arctic and deposited Chukchi-Alaskan margin sediments, *Global Planet. Change*, 68, 58-72, 2009a.
- DeMaster, D.J., Measuring biogenic silica in marine sediments and suspended matter, in *Marine Particles: Analysis and Characterization*, edited by D. Hurd and D. Spencer, pp. 363-367, American Geophysical Union, Washington D.C., 1991.
- Emerson, S., and J.I. Hedges, Sediment diagenesis and benthic fluxes, in *Treatise of Geochemistry*, edited by H. Elderfield, Vol. 6, 293-319, Elsevier, New York, 2003.
- Fogal, M.L., and L.A. Cifuentes, Isotope fractionation during primary production, in *Organic Geochemistry*, pp. 73-98, edited by S.A. Mako and M.H. Engel, Plenum Press, New York, 1993.
- Goldhaber, M.B., and I.R. Kaplan, The sulfur cycle, in *The Sea*, edited by E.D. Goldberg, Vol. 5, Ch. 17, pp. 569-655, Wiley, New York, 1974.
- Gradinger, R., Climate change and biological oceanography of the Arctic, *Philos. T. Roy. Soc. A.*, 352, 1699, 277-286, 1995.
- Grebmeier, J.M., Studies on pelagic-benthic coupling extended onto the Soviet continental shelf in the Bering and Chukchi Seas, *Cont. Shelf Res.*, 13, 653-668, 1993.
- Grebmeier, J.M., T.E. Whitedge, L.A. Codispoti, K.H. Dunton, J.J. Walsh, T.J. Weingartner, and P.A. Wheeler, Arctic Systems Science Ocean-Ice Interactions Western Arctic Shelf-Basin Interactions Science Plan, ARCSS/OAII Report 7, Old Dominion University, Norfolk, Va., 65, 1998.
- Grebmeier, J.M., T.E. Whitedge, K. Aagaard, M. Bergmann, W.C. Carmack, L.A. Codispoti, D. Darby, K.H. Dunton, I.A. Melnikov, S. Moore, T. Takizawa, J.J. Walsh, P. Wassman, and P. Wheeler, Arctic System Science Ocean-Atmosphere-Ice Interactions Western Arctic Shelf-basin Interactions (SBI) Phase II Implementation Plan, SBI Project Office, The University of Tennessee, Knoxville, 30, 2001.
- Grebmeier, J.M., The western Arctic Shelf-Basin Interactions, *Arctic Res. of the U.S.*, 17, 24-36, 2003.
- Grebmeier, J.M., and H.R. Harvey, The western Arctic Shelf-Basin Interactions (SBI) Project: an overview, *Deep-Sea Res. Part II*, 52, 3109-3115, 2005.
- Hay, B.J., M.A. Aurthur, W.E. Dean, E.D. Neff, and S. Honjo, Sediment deposition in the late Holocene abyssal Black Sea with climatic and chronological implications, *Deep-Sea Res.*, 38, S1211-S1235, 1991.
- Hester, K., and E.A. Boyle, Water chemistry control of the cadmium content of some recent benthic foraminifera, *Nature*, 298, 260-262, 1982.

- Hill, J.C., N.W. Driscoll, R.L. Phillips, J.P. Donnelly, J. Brigham-Grette, P.T. Gayes, and L. Keigwin, A large incised valley on the Chukchi shelf: implications for high discharge, sea level fluctuations and climatic variations since the LGM, *EOS Trans.*, AGU, 87, 36, 2006.
- Hill, V., G. Cota, and D. Stockwell, Spring and summer phytoplankton communities in the Chukchi and Eastern Beaufort Seas, *Deep-Sea Res. Part II*, 52, 3109-3115, 2005.
- Hillaire-Marcel, C., A. de Vernal, and D.J. Piper, Lake Agassiz final drainage event in the northwest North Atlantic, *Geophys. Res. Lett.*, 34, L15601, doi:10.1029/2007GL030396, 2007.
- Howarth, R.W., J.H. Dacey, and G.M. King, Carbon flow through oxygen and sulfate reduction pathways in salt marsh sediments, *Limnol. Oceanogr.*, 29, 1037-1051, 1984.
- Iida, T., S.I. Saitoh, T. Miyamura, M. Toratani, H. Fukushima., and N. Shiga, Temporal and spatial variability of coccolithophore blooms in the eastern Bering Sea, 1998-2001, *Prog. Oceanogr.*, 1-2, 165-175, 2002.
- Jakobsson, M., J.V. Gardner, P.R. Vogt, L.A. Mayer, A. Armstrong, J. Backman, R. Brennan, B. Calder, J.K. Hall, and B. Kraft, Multibeam bathymetric sediment profiler evidence for ice grounding on the Chukchi borderland, Arctic Ocean, *Quat. Res.*, 63, 150-160, 2005.
- Jones, G.S., and P.A. Kaiteris, A vacuum-gasometric technique for rapid and precise analysis of calcium carbonate in sediments and soils, *J. Sediment. Res.*, 53, 2, 655-660, 1983.
- Keigwin, L.D., J.P. Donnelly, M.S. Cook, N.W. Driscoll, and J. Brigham-Grette, Deglaciation, rapid sea-level rise, and Holocene climate in the Chukchi Sea, *Geology*, 34, 861-864, 2006.
- Keir, R.S., The dissolution kinetics of biogenic calcium carbonates in seawater, *Geochim. Cosmochim. Acta*, 62, 1347-1364, 1980.
- Kennett, J.P., *Marine Geology*, 813 pp, Prentice Hall, Englewood Cliffs, New Jersey, 1982.
- Lise-Pronovost, A., G. St-Onge, S. Brachfield, F. Barletta, D. Darby, Paleomagnetic constraints on the Holocene stratigraphy of the Arctic Alaskan margin, *Global Planet. Change*, 68, 85-99, 2009.
- Lyons, T.W., Sulfur isotopic trends and pathways of iron sulfide formation in upper Holocene sediments of the anoxic Black Sea, *Geochim. Cosmochim. Acta*, 61, 16, 3367-3382, 1997.
- Marten, C.S., and J.V. Klump, Biogeochemical cycling in organic rich marine basin- 1. Methane sediment water exchange processes, *Geochim. Cosmochim. Acta*, 44: 471-490, 1980
- Mason, O. K., and J.W. Jordan, Minimal sea level rise in the Chukchi Sea: Arctic insensitivity to global change?, *Global Planet. Change*, 32, 13-23, 2001.
- Matrai, P. A., and R.W. Eppley, Particulate organic sulfur in the waters of the southern California blight, *Global Biogeochem. Cycles*, 3, 1, 89-103, 1989.
- McKay, J.L., A. deVernal, C. Hillaire-Marcel, C. Not, L. Polyak, and D. Darby, Holocene fluctuations in Arctic sea-ice cover: dinocyst-based reconstructions for the eastern Chukchi Sea. *Can. J. Earth Sci.*, 45, 1377-1397, 2008.
- McManus, J., D.E. Hammond, W.M. Berelson, T.E. Kilgore, D.J. DeMasters, O.G. Ragueneau, and R.W. Collier, Early diagenesis of biogenic opal: dissolution rates, kinetics, and paleoceanographic implications, *Deep-Sea Res. Part II*, 42, 2-3, 871-903, 1995.

- Moran, S.B., K.M. Ellis, and J.N. Smith, $^{234}\text{Th}/^{238}\text{U}$ disequilibrium in the central Arctic Ocean: implications for particulate organic carbon export, *Deep-Sea Res. Part II*, 44, 8, 1593-1606, 1997.
- Morse, J. W., and F.T. Mackenzie, *Geochemistry of Sedimentary Carbonates*, 724 pp., Elsevier, New York, 1990.
- Morse., J.W., and R.S. Arvidson, The dissolution kinetics of major sedimentary carbonate minerals, *Earth-Sci. Rev.*, 58, 51-84, 2002.
- Mortlock, R.D., and P.N. Froelich, A simple method for the rapid determination of biogenic opal in pelagic marine sediments, *Deep-Sea Res.*, 36, 1415-1426, 1989.
- Mysak, L. A., Oceanography: Patterns of Arctic circulation, *Science*, 293, 5533, 1269-1270, 2001.
- Naidu, A.S, L.W. Cooper, B.P. Finney, R.W. Macdonald, C. Alexander, and I.P. Semiletov, Organic carbon isotope ratios of the Amerasian continental shelf sediments, *Int. J. Earth Sci.*, 89, 522-532, 2000.
- Naidu, A.S., L.W. Cooper, J.M. Grebmeier, T.E. Whitledge, and M.J. Hameedi, The continental margin of the North Bering-Chukchi Sea: concentrations, sources, fluxes, accumulation and burial rates, in *The Organic Carbon Cycle in the Arctic Ocean*, edited by R. Stein and R.W. Macdonald, 193-203, Springer-Verlag, Berlin, 2004.
- Napp, J.M., and G.L. Hunt, Anomalous conditions in the south-east Bering Sea 1997: linkages among climate, weather, ocean and biology, *Fish. Oceanogr.*, 10, 1, 61-68, 2001.
- Ortiz, J.D., L. Polyak, J.M. Grebmeier, D. Darby, S. Eberl, S. Naidu, and D. Nof, Provenance of Holocene sediments on the Chukchi-Alaskan margin based on combined diffuse spectral reflectance and quantitative x-ray diffraction analysis, *Global Planet. Change*, 68, 73-84, 2009.
- Overland, J., J. Turner, J. Francis, N. Gillett and M. Tjerström, The Arctic and Antarctic: two faces of climate change. *EOS Trans.*, AGU, 89, 19, 177-178, 2008.
- Peterson, B.J., M.R. Holmes, J.W. McClelland, C.J. Vorosmarty, R.B. Lammers, A.I. Shiklomanov, and S. Rahmstorf, S., Increasing river discharge to the Arctic Ocean, *Science*, 298, 2171-2173, 2002.
- Perovich, D. K., B. Light, H. Eicken, K.F. Jones, K. Runciman, and S.V. Nghiem, Increasing solar heating of the Arctic Ocean and adjacent seas; 1979-2005: Attribution and role in the ice-albedo feedback, *Geophys. Res. Lett.*, 34, 2007.
- Perovich, D. K., and J.A. Ritcher-Menge, Loss of sea ice in the Arctic, *Annu. Rev. Mar. Sci.*, 1, 417-441, 2009.
- Phillips, R.L., P. Barnes, R.E. Huner, T.E. Reiss, and D.M. Rearic, Geologic investigations in the Chukchi Sea, 1984, NOAA ship SURVEYOR cruise, U.S. Geological Survey Open-File Report 88-25, 1988.
- Polyak, L., D.A. Darby, J.F. Bishcof, and M. Jakobsson, Stratigraphic constraints on late Pleistocene glacial erosion and deglaciation of the Chukchi margin, Arctic Ocean, *Quat. Res.*, 67, 234-345, 2007.
- Presley, B.J., A simple method for determining calcium carbonate in sediment samples, *J. Sediment. Petrol.*, 45, 745-746, 1975.

- Radi, T., and A. de Vernal, Dinocysts as proxy of primary productivity in mid-high latitudes of the Northern Hemisphere, *Mar. Micropalaeontol.*, 68, 84-114, 2008.
- Redfield, A.C., B.H. Ketchum, and F.A. Richards, The influence of organisms on the composition of seawater, in *The Sea*, edited by M.N. Hill, Vol. 2, pp. 26-87, Interscience Publishers, New York, 1963.
- Rigor, I.G., J.M. Wallace, and R.I. Colony, Response of sea ice to the Arctic Ocean, *J. Climate*, 15, 2648-2663, 2002.
- Sakshaug, E., Primary and secondary production in the Arctic seas, in *The Organic Carbon Cycle in the Arctic Ocean*, edited by R. Stein and R.W. Macdonald, pp. 57-81, Springer-Verlag, Berlin, 2004
- Schubert, C.J., and S.E. Calvert, Nitrogen and carbon isotopic composition of marine and terrestrial organic matter in the Arctic Ocean sediments: implications for nutrient utilization and organic matter composition, *Deep-Sea Res.*, 48, 789-810, 2001.
- Seager, R., D.S. Battisti, J. Yin, N. Gordon, N. Naik, A.C. Clement, and M.A. Cane, Is the Gulf Stream responsible for Europe's mild winters?, *Q. J. R. Meteorol. Soc.*, 128, 2563-2586, 2002.
- Serreze, M. C., J. E. Walsh, F. S. Chapin III, T. Osterkamp, M. Dyrurgerov, V. Romanovsky, W. C. Oechel, J. Morison, T. Zhang, and R. G. Barry, Observational evidence of recent change in the northern high-latitude environment, *J. Climatic Change*, 46, 159-207, 2008.
- Springer, A.M., and C.P. McRoy, The paradox of pelagic food webs in the northern Bering Sea - III. Patterns of primary productivity, *Cont. Shelf Res.*, 13, 5/6, 575-599, 1993.
- Steele, M., W. Ermold, and J. Zhang, Arctic Ocean surface warming trends over the past 100 years, *Geophys. Res. Lett.*, 35, 2008.
- Stein, R., and K. Fahl, The Laptev Sea: distribution, sources, variability and burial of organic carbon, in *The Organic Carbon Cycle in the Arctic Ocean*, edited by R. Stein and R.W. Macdonald, pp. 213-236, Springer-Verlag, Berlin, 2004.
- Stein, R., and K. Fahl, The Kara Sea: distribution, sources, variability and burial of organic carbon, in *The Organic Carbon Cycle in the Arctic Ocean*, edited by R. Stein and R.W. Macdonald, pp. 237-266, Springer-Verlag, Berlin, 2004a.
- Stein, R., and R.W. Macdonald, Organic carbon in Arctic Ocean sediments: sources, variability, burial and paleoenvironmental significance, in *The Organic Carbon Cycle in the Arctic Ocean*, edited by R. Stein and R.W. Macdonald, pp. 169-177, Springer-Verlag, Berlin, 2004.
- Stein, R., and R.W. Macdonald, Geochemical proxies used for organic carbon source identification in Arctic sediment, in *The Organic Carbon Cycle in the Arctic Ocean*, edited by R. Stein and R.W. Macdonald, pp. 24-32, Springer-Verlag, Berlin, 2004a.
- Stroeve, J., M. Serezze, S. Drobot, S. Gearheard, and M. Holland, Arctic sea ice extent plummets in 2007, *EOS Trans, AGU*, 89, 13-20, 2008.
- Swift, J.H., K. Aagaard, and S. A. Malmberg, The contribution of Denmark Strait overflow to the deep North Atlantic, *Deep Sea Res.*, 27, 29-42, 1980.
- Teller, J.T., D.W. Leverington, and J.D. Mann, Freshwater outbursts to the oceans from glacial Lake Agassiz and their role in climate change during the last deglaciation, *Quat. Sci. Rev.*, 21, 879-887, 2002.

- Tromp, T.K., P. van Cappellen, and R.M. Key, A global model for the early diagenesis within organic carbon and organic phosphorus in marine sediments, *Geochim. Cosmochim. Acta*, 59, 1259-1284, 1995.
- Van Cappellan, P., and L. Qui, Biogenic silica dissolution in sediments of the Southern Ocean. II. Kinetics, *Deep-Sea Res. Part II*, 44, 1129-1149, 1997.
- Vetrov, A., and E.A. Romankevich, The Barents Sea: distribution, sources, variability and burial of organic carbon, in *The Organic Carbon Cycle in the Arctic Ocean*, edited by R. Stein and R.W. Macdonald, pp. 266-278, Springer-Verlag, Berlin, 2004.
- Woodgate, R., K. Aagaard, and T.J. Weingartner, A year in the physical oceanography of the Chukchi Sea: moored measurements from autumn 1990-1991, *Deep-Sea Res. Part II*, 52, 3116-3149, 2005.

APPENDIX A

STATION P1 DATA

Depth	Age (ybp)	% Org. N	% Org. C	% Total S	Org C/N	% Biogenic Silica	C/S	Cd:Ca ($\times 10^{-7}$)
20.5	830	0.195	1.799	0.246	11	1.02	20	
21.5	850	0.179	1.686	0.247	11	1.41	18	
23	880	0.179	1.667	0.245	11	0.88	18	3.46
24.5	930	0.167	1.627	0.29	11	0.92	15	3.61
27	990	0.159	1.563	0.296	11	1.72	14	2.34
30	1040	0.164	1.591	0.291	11	1.48	15	2.29
32.5	1100	0.167	1.609	0.327	11	1.89	13	1.91
35	1160	0.153	1.504	0.249	11	0.94	16	4.03
37.5	1220	0.161	1.579	0.303	11	1.54	14	4.58
40	1270	0.153	1.502	0.249	11	1.25	16	
42.5	1330	0.162	1.545	0.275	11	1.02	15	1.03
45	1390	0.174	1.57	0.28	11	1.02	15	1.74
47.5	1450	0.178	1.67	0.289	11	0.9	15	2.74
52.5	1560	0.168	1.646	0.282	11	0.49	16	
57.5	1680	0.169	1.625	0.29	11	0.54	15	
62.5	1790	0.165	1.596	0.287	11	0.51	15	
65	1910	0.164	1.638	0.262	12	0.49	17	1.26
67.5	2190	0.158	1.564	0.241	12	0.51	17	
70	2510	0.157	1.555	0.286	12	0.52	14	1.93
72.5	2880	0.16	1.581	0.269	12	0.54	16	1.55
75	3280	0.156	1.582	0.261	12	0.46	16	0.92
77.5	3720	0.164	1.585	0.217	11	0.75	19	
80	4200	0.162	1.569	0.246	11	0.65	17	1.24
82.5	4730	0.163	1.579	0.277	11	0.61	15	
85	5290	0.163	1.6	0.272	11	0.56	16	2.1
87.5	5370	0.155	1.529	0.302	12	0.54	14	
90	5480	0.16	1.571	0.275	11	0.56	15	1.61
92.5	5590	0.159	1.596	0.352	12	0.57	12	
95	5700	0.158	1.686	0.359	12	0.6	13	1.47
97.5	5810	0.16	1.594	0.299	12	0.48	14	
100	5910	0.159	1.59	0.288	12	0.38	15	2.45
102.5	6010	0.156	1.569	0.268	12	0.38	16	
105	6100	0.157	1.54	0.248	11	0.41	17	2.77

STATION P1 DATA CONTINUED

Depth	Age (ybp)	% Org. N	% Org. C	% Total S	Org C/N	% Biogenic Silica	C/S	Cd:Ca ($\times 10^{-7}$)
107.5	6190	0.156	1.54	0.249	12	0.28	16	
110	6280	0.159	1.544	0.284	11	0.17	15	5.53
112.5	6370	0.164	1.494	0.313	11	0.2	13	
115	6450	0.155	1.458	0.325	11	0.3	12	1.59
117.5	6530	0.159	1.497	0.308	11	0.27	13	
120	6610	0.156	1.534	0.304	11	0.19	13	2.39
122.5	6680	0.152	1.51	0.266	12	0.19	15	
125	6750	0.153	1.545	0.267	12	0.19	15	
127.5	6820	0.15	1.465	0.233	11	0.11	17	
130	6880	0.153	1.505	0.26	11	0.19	15	1.8
132.5	6940	0.156	1.508	0.289	11	0.23	14	
135	7000	0.157	1.523	0.288	11	0.22	14	
136.5	7030	0.149	1.414	0.313	11	0.25	12	1.33
140.5	7120	0.159	1.401	0.324	10	0.25	12	3.15
142.5	7160	0.163	1.452	0.292	10	0.18	13	
145	7200	0.151	1.426	0.248	11	0.17	15	11.4
147.5	7240	0.156	1.521	0.306	11	0.12	13	
150	7280	0.146	1.636	0.341	13	0.16	13	2.53
152.5	7320	0.152	1.498	0.325	12	0.2	12	
155	7350	0.148	1.69	0.291	13	0.25	15	
157.5	7620	0.156	1.664	0.266	12	0.28	17	
159.5	7690	0.168	1.72	0.306	12	0.28	15	1.42
162.5	7770	0.15	1.785	0.374	14	0.27	13	
165	7850	0.163	1.709	0.279	12	0.25	16	
167.5	7920	0.154	1.655	0.314	13	0.25	14	
170	8000	0.15	1.552	0.218	12	0.18	19	1.98
172.5	8080	0.152	1.603	0.226	12	0.16	19	
175	8150	0.16	1.595	0.307	12	0.13	14	15.2
177.5	8230	0.155	1.619	0.242	12	0.14	18	
180	8310	0.141	1.45	0.2	12	0.14	19	
182.5	8380	0.17	1.519	0.255	10	0.15	16	
185	8460	0.151	1.368	0.179	11	0.09	20	
187.5	8530	0.155	1.459	0.171	11	0.07	23	

STATION P1 DATA CONTINUED

Depth	Age (ybp)	% Org. N	% Org. C	% Total S	Org C/N	% Biogenic Silica	C/S	Cd:Ca ($\times 10^{-7}$)
190	8610	0.142	1.362	0.185	11	0.1	20	
195	8760	0.14	1.329	0.168	11	0.05	21	
197.5	8840	0.139	1.276	0.143	11	0.05	24	
200	8920	0.127	1.161	0.123	11	0.03	25	
202.5	8990	0.126	1.296	0.124	12	0.05	28	
205	9070	0.122	1.236	0.118	12	0.07	28	
207.5	9150	0.112	1.18	0.093	12	0.04	34	
210	9220	0.116	1.136	0.102	11	0.04	30	
212.5	9300	0.106	1.043	0.107	11	0.03	26	
215	9370	0.104	1.097	0.08	12	0.03	37	
217.5	9450	0.12	1.094	0.14	11	0.03	21	
220	9530	0.098	1.061	0.067	13	0.03	42	
222.5	9600	0.092	1.085	0.065	14	0.05	45	
225	9680	0.102	0.98	0.098	11	0.04	27	
227.5	9760	0.107	1.046	0.158	11	0.03	18	
230	9830	0.099	1.155	0.19	14	0.03	16	
232.5	9910	0.087	1.162	0.155	16	0.03	20	
240	10140	0.086	1.227	0.242	17	0.03	12	
242.5	10210	0.082	1.194	0.308	17	0.03	15	
245	10290	0.082	1.266	0.219	18	0.05	14	
247.5	10370	0.085	1.184	0.222	16	0.04	10	
250	10440	0.081	1.116	0.285	16	0.03	15	
252.5	10520	0.08	1.219	0.33	18	0.03	14	
255	10600	0.08	1.216	0.334	18	0.02	10	
257.5	10670	0.083	1.237	0.203	17	0.01	10	
260	10750	0.08	1.259	0.231	18	0.01	10	
262.5	10830	0.091	1.301	0.229	17	0.01	16	
265	10900	0.094	1.137	0.284	14	0.01	15	
267.5	10980	0.092	1.33	0.214	17	0.01	15	
270	11060	0.087	1.447	0.274	19	0.01	11	
272.5	11130	0.089	1.261	0.205	17	0.01	17	
275	11210	0.086	1.319	0.212	18	0.01	14	
277.5	11280	0.083	1.472	0.218	21		16	

STATION P1 DATA CONTINUED

Depth	Age (ybp)	% Org. N	% Org. C	% Total S	Org C/N	% Biogenic Silica	C/S	Cd:Ca ($\times 10^{-7}$)
280	11360	0.084	1.312	0.203	18		17	
282.5	11440	0.083	1.271	0.248	18		18	
285.5	11530	0.085	1.335	0.313	18		17	
290	11670	0.092	1.217	0.173	15	0.01	14	
295	11820	0.091	1.212	0.161	16		11	
300	11970	0.09	1.269	0.209	16		19	
305	12120	0.088	1.348	0.361	18		20	
310	12280	0.09	1.269	0.454	16		16	
315	12430	0.088	1.343	0.37	18	0.01	10	
320	12580	0.088	1.272	0.34	17		10	
325	12740	0.086	1.367	0.313	19		12	
330	12890	0.09	1.262	0.319	16	0.01	11	
335	13040	0.096	1.307	0.346	16		10	
340	13190	0.088	1.276	0.346	17		10	
345	13350	0.086	1.281	0.451	17		8	
350	13500	0.084	1.192	0.407	17		8	
355	13650	0.082	1.303	0.436	19	0.01	8	
360	13810	0.082	1.272	0.214	18		16	
365	13960	0.08	1.246	0.237	18		14	
370	14110	0.081	1.245	0.276	18		12	
375	14260	0.08	1.267	0.372	18		9	
380	14420	0.084	1.073	0.286	15	0.01	10	
385	14570	0.078	1.223	0.276	18		12	
390	14720	0.085	1.304	0.251	18		14	
395	14870	0.087	1.206	0.232	16		14	
400	15030	0.088	1.131	0.246	15		12	
405	15180					0.01		
410	15330					0.01		
415	15490					0.01		
420	15640	0.089	1.22	0.214	16	0.01	15	
429	15910	0.087	1.264	0.191	17	0.01	18	

APPENDIX B

MULTICORE 6 DATA

Depth	Age (ybp)	% Org. N	% Org. C	% Total S	Org C/N	% Biogenic Silica	% Carbonate
0.5	0	0.201	1.813	0.243	9	0.22	0.108
1.5	0	0.209	1.842	0.205	9	0.25	0.109
2.5	1	0.212	1.900	0.242	9	0.29	0.097
3.5	1	0.216	1.990	0.223	9	0.45	0.101
4.5	1	0.244	1.990	0.265	8	0.29	0.097
6	1	0.227	1.872	0.220	8	0.17	0.097
8	2	0.229	1.879	0.240	8	0.19	0.093
10	2	0.230	1.868	0.217	8	0.23	0.094
12	2	0.215	1.839	0.184	9	0.26	0.103
14	3	0.217	1.805	0.244	8	0.17	0.102
16	3	0.213	1.751	0.170	8	0.28	0.101
18	4	0.212	1.748	0.185	8	0.32	0.093
20	4	0.209	1.710	0.190	8	0.39	0.092
22	4	0.217	1.791	0.164	8	0.20	0.081
24	5	0.213	1.746	0.129	8	0.19	0.097
26	5	0.214	1.740	0.171	8	0.09	0.089
28	6	0.204	1.706	0.110	8	0.17	0.088
30	6	0.204	1.667	0.178	8	0.20	0.091
32	6	0.201	1.663	0.160	8	0.16	0.089
34	7	0.203	1.625	0.167	8	0.23	0.090
36	7	0.203	1.591	0.155	8	0.17	0.087
38	8	0.195	1.626	0.152	8	0.26	0.081
40	8	0.197	1.690	0.177	9	0.20	0.088
42	8	0.205	1.658	0.146	8	0.20	0.090
44	9	0.197	1.623	0.169	8	0.14	0.088
46	9	0.202	1.638	0.106	8	0.08	0.094
48	10	0.204	1.638	0.174	8	0.14	0.089
50	10	0.199	1.631	0.215	8	0.18	0.092
52	10	0.223	1.642	0.292	7	0.13	0.092
54	11	0.224	1.605	0.258	7	0.12	0.095
55.5	11	0.226	1.627	0.223	7	0.14	0.093

MULTICORE 6 DATA CONTINUED

Depth	AVS ($\mu\text{mol S / g}$)	Greigite ($\mu\text{mol S / g}$)	Pyrite ($\mu\text{mol S / g}$)	Org.C / Pyrite S	DOP	^{15}N (‰)	^{13}C (‰)
0.5	0.000	0.038	0.069	20	0.001	9.38	-22.03
1.5	0.000	0.043	0.064	24	0.001		
2.5	0.000	0.063	0.108	21	0.001	8.46	-22.09
3.5	0.000	0.070	0.088	24	0.001		
4.5	0.000	0.050	0.093	20	0.001	6.63	-22.19
6	0.000	0.053	0.115	23	0.002		
8	0.000	0.125	0.111	21	0.001	5.32	-22.02
10	0.000	0.089	0.124	23	0.002		
12	0.000	0.091	0.261	27	0.005	8.43	-22.3
14	0.000	0.066	0.152	20	0.002		
16	0.000	0.058	0.256	27	0.005	8.47	-22.23
18	0.000	0.068	0.335	25	0.006		
20	0.000	0.075	0.393	24	0.007	8.62	-22.12
22	0.000	0.077	0.475	29	0.009		
24	0.000	0.099	0.537	36	0.013	8.31	-22.19
26	0.000	0.057	0.392	27	0.007		
28	0.000	0.179	2.618	41	0.076	8.15	-22.17
30	0.000	0.090	1.929	25	0.035		
32	0.000	0.316	2.459	28	0.049	8	-22.16
34	0.000	0.122	1.521	26	0.029		
36	0.000	0.113	1.368	27	0.028	7.93	-22.27
38	0.000	0.091	1.265	29	0.027		
40	0.000	0.135	1.591	25	0.029	7.99	-22.27
42	0.000	0.112	2.253	30	0.049		
44	0.000	0.148	1.503	26	0.028	7.38	-22.17
46	0.000	0.250	2.405	41	0.073		
48	0.000	0.249	4.142	25	0.076	7.96	-22.21
50	0.240	0.190	2.435	20	0.036		
52	0.104	0.332	4.254	15	0.047	7.87	-22.19
54	0.095	0.199	2.489	17	0.031		
55.5	0.000	0.194	3.821	19	0.055	7.98	-22.27

APPENDIX C

MULTICORE 8 DATA

Depth	Age (ybp)	% Org. N	% Org. C	% Total S	Org C/N	% Biogenic Silica	% Carbonate
0.5	622.58	0.227	1.958	0.149	10	0.17	0.240
1.5	622.84	0.225	1.956	0.097	10	0.17	0.220
2.5	623.1	0.190	1.887	0.086	12	0.21	0.220
3.5	623.36	0.203	1.946	0.098	11	0.24	0.220
4.5	623.62	0.205	1.964	0.099	11	0.30	0.220
6	624.01	0.185	1.825	0.061	12	0.28	0.210
8	624.53	0.191	1.798	0.051	11	0.27	0.220
10	625.05	0.185	1.805	0.040	11	0.20	0.220
12	625.57	0.190	1.842	0.116	11	0.31	0.220
14	626.09	0.180	1.856	0.111	12	0.28	0.230
16	626.61	0.184	1.761	0.188	11	0.37	0.250
18	627.13	0.187	1.832	0.092	11	0.36	0.220
20	627.65	0.187	1.792	0.112	11	0.35	0.220
22	628.56	0.175	1.733	0.119	12	0.30	0.220
23.5	628.97	0.177	1.750	0.125	12	0.44	0.200

APPENDIX D

TC05 DATA

Depth	Age (ybp)	% Org. N	% Org. C	% Total S	Org C/N	% Biogenic	% Carbonate
1.5	817.4	0.198	1.751	0.112	10		0.093
19.5	939.8	0.19	1.621	0.08	10		0.082
40.5	1082.6	0.178	1.605	0.106	11	0.36	0.073
60.5	1082.6	0.174	1.549	0.115	10	0.42	0.086
82.5	1198.2	0.182	1.638	0.08	10	0.55	0.106
100.5	1320.6	0.172	1.652	0.083	11	0.32	0.066
120.5	1470.2	0.175	1.594	0.054	11	0.24	0.109
140.5	1592.6	0.167	1.579	0.046	11	0.33	0.099

Depth	Pyrite ($\mu\text{mol S/g}$)	Org.C / Pyrite S	DOP	^{15}N (‰)	^{13}C (‰)
1.5	0.04	3403	0.012	7.92	-22.3
19.5	0.03	4221	0.013	7.86	-22.12
40.5	0.37	364	0.111	7.78	-22.14
60.5				7.78	-22.2
82.5	2.37	58	0.946	7.96	-22.27
100.5	3.31	42	1.277	7.67	-22.27
120.5	3.96	34	2.345		
140.5	3.52	37	2.447	7.88	-21.17

APPENDIX E

TC08 DATA

Depth	Age (ybp)	% Org. N	% Org. C	% Total S	Org C/N	% Biogenic Silica	% Carbonate
10.5	680	0.133	1.278	0.186	11	0.26	0.17
20.5	800	0.171	1.595	0.295	11	0.29	0.21
30.5	1069	0.181	1.569	0.332	10	0.24	0.21
40.5	1338	0.191	1.625	0.276	10		0.19
50.5	1408	0.177	1.582	0.231	10	0.40	0.20
59.5	1677	0.176	1.610	0.243	11	0.57	0.19
69.5	1946	0.172	1.569	0.289	11	0.55	0.20
79.5	2189	0.172	1.577	0.362	11	0.30	0.21
89.5	2458	0.186	1.660	0.291	10	0.31	0.22
99.5	2727	0.171	1.570	0.174	11	0.25	0.24

APPENDIX F

JPC05 DATA

Depth	Age (ybp)	% Org. N	% Org. C	% Total S	Org C/N	% Biogenic	
						Silica	% Carbonate
2.5	1082.6	0.172	1.631	0.031	11	0.36	0.097
20.5	1198.2	0.187	1.587	0.306	10	0.23	0.098
42.5	1320.6	0.192	1.596	0.298	10	0.25	0.113
60.5	1470.2	0.193	1.613	0.335	10	0.15	0.111
82.5	1592.6	0.185	1.560	0.248	10	0.13	0.115
101.5	1742.2	0.192	1.602	0.203	10	0.10	0.087
110.5	1871.4	0.19	1.520	0.244	9	0.04	0.103
140.5	1932.6	0.199	1.569	0.232	9	0.13	0.081
162.5	2136.6	0.206	1.555	0.203	9	0.10	0.099
180.5	2286.2	0.205	1.546	0.214	9	0.27	0.106
200.5	2408.6	0.204	1.474	0.166	8	0.24	0.111
220.5	2544.6	0.195	1.515	0.224	9	0.28	0.110
242.5	2680.6	0.198	1.509	0.273	9	0.35	0.118
260.5	2830.2	0.206	1.580	0.247	9	0.18	0.117
280.5	2952.6	0.208	1.560	0.162	9	0.30	0.112
300.5	3088.6	0.195	1.486	0.217	9	0.30	0.114
320.5	3224.6	0.198	1.517	0.167	9	0.19	0.111
340.5	3360.6	0.185	1.505	0.325	9	0.09	0.126
360.5	3496.6	0.187	1.507	0.236	9	0.11	0.119
380.5	3632.6	0.193	1.536	0.325	9	0.07	0.134
401.5	3768.6	0.187	1.529	0.16	10	0.20	0.133
420.5	3911.4	0.183	1.526	0.296	10	0.24	0.135
440.5	4040.6	0.181	1.496	0.292	10	0.17	0.134
460.5	4176.6	0.18	1.499	0.278	10	0.11	0.131
481.5	4312.6	0.181	1.524	0.246	10	0.13	0.138
500.5	4455.4	0.2	1.506	0.237	9	0.08	0.139
520.5	4584.6	0.212	1.518	0.257	8	0.06	0.143
540.5	4720.6	0.216	1.553	0.275	8	0.12	0.141
560.5	4856.6	0.198	1.515	0.289	9	0.13	0.138
580.5	4992.6	0.193	1.530	0.126	9	0.15	0.167
600.5	5128.6	0.194	1.487	0.23	9	0.22	0.143
620.5	5264.6	0.196	1.497	0.168	9	0.13	0.147
640.5	5400.6	0.191	1.508	0.243	9	0.09	0.140
660.5	5536.6	0.2	1.547	0.206	9	0.09	0.124
680.5	5672.6	0.188	1.500	0.29	9	0.11	0.131
700.5	5808.6	0.181	1.479	0.215	10	0.13	0.135
720.5	5944.6	0.182	1.471	0.328	9	0.11	0.143
740.5	6080.6	0.193	1.523	0.228	9	0.12	0.151

JPC05 DATA CONTINUED

Depth	Age (ybp)	% Org. N	% Org. C	% Total S	Org C/N	% Biogenic	
						Silica	% Carbonate
760.5	6216.6	0.186	1.479	0.282	9	0.16	0.155
780.5	6352.6	0.179	1.503	0.559	10	0.19	0.144
800.5	6488.6	0.17	1.421	0.241	10	0.12	0.155
820.5	6624.6	0.17	1.410	0.206	10	0.13	0.140
840.5	6760.6	0.161	1.414	0.329	10	0.16	0.131
860.5	6896.6	0.16	1.417	0.134	10	0.12	0.131
880.5	7032.6	0.16	1.402	0.306	10	0.05	0.162
900.5	7168.6	0.145	1.454	0.275	12	0.09	0.158
920.5	7304.6	0.159	1.392	0.118	10	0.12	0.147
940.5	7440.6	0.154	1.381	0.224	10	0.10	0.132
960.5	7576.6	0.162	1.399	0.29	10	0.10	0.166
980.5	7712.6	0.162	1.438	0.337	10	0.12	0.134
1000.5	7848.6	0.154	1.414	0.324	11	0.08	0.152
1020.5	7984.6	0.167	1.435	0.251	10	0.07	0.137
1040.5	8120.6	0.158	1.343	0.182	10	0.03	0.161
1060.5	8256.6	0.166	1.398	0.16	10		0.148
1080.5	8392.6	0.149	1.233	0.224	10		0.171
1100.5	8528.6	0.135	1.116	0.014	10		0.180
1120.5	8664.6	0.132	1.087	0.011	10		0.189
1140.5	8800.6	0.126	1.016	0.09	9		0.188
1160.5	8936.6	0.128	0.990	0.129	9		0.169
1180.5	9072.6	0.119	0.934	0.06	9		0.186
1200.5	9208.6	0.116	0.849	0.059	9		0.156
1220.5	9344.6	0.112	0.893	0.029	9		0.187
1240.5	9480.6	0.092	0.739	0.008	9		1.243
1260.5	9616.6	0.088	0.712	0.018	9		0.760
1290	9752.6	0.104	1.140	0.086	13		0.410
1306	9953.2	0.09	1.005	0.025	13		0.910
1330	10062	0.083	1.106	0.21	16		0.330
1346	10225.2	0.078	0.607	0.001	9		0.107
1370	10334	0.073	1.056	0.001	17		0.660
1394	10497.2	0.086	1.383	0.144	19		0.110
1417	10660.4	0.088	1.055	0.087	14		0.089
1447	10816.8	0.089	1.133	0.183	15		0.124
1471	11020.8	0.082	1.441	0.341	21		0.310
1495	11184	0.08	1.375	0.305	20		0.360
1519	11347.2	0.082	2.381	0.383	34		0.240
1535	11510.4	0.142	1.130	0.413	9		0.016
1568	11619.2	0.132	0.935	1.388	8		0.010
1605	11843.6	0.128	0.926	0.737	8		0.020
1631	12095.2	0.137	1.113	0.738	9		0.016

JPC05 DATA CONTINUED

Depth	Pyrite ($\mu\text{mol S/g}$)	Org.C / Pyrite S	DOP	^{15}N (‰)	^{13}C (‰)
2.5	3.56	38	3.672	8.13	-22.66
20.5	3.25	41	0.340	8.42	-22.54
42.5				8.29	-22.59
60.5	5.29	25	0.505	8.27	-22.67
82.5				7.98	-22.88
101.5	2.94	45	0.463	7.94	-22.8
110.5				7.94	-22.8
140.5				7.71	-22.8
162.5	3.90	33	0.615		
180.5					
200.5					
220.5	4.44	28	0.634	7.61	-22.91
242.5					
260.5					
280.5	2.98	44	0.589	7.75	-22.87
300.5				7.57	-22.87
320.5				7.62	-23.04
340.5	6.09	21	0.600	7.94	-22.98
360.5					
380.5	9.19	14	0.905		
401.5	1.47	87	0.293		
420.5	6.57	19	0.710	7.48	-23.1
440.5					
460.5	7.96	16	0.916	7.57	-23.13
481.5				7.76	-23.21
500.5	5.12	24	0.692	7.57	-23.28
520.5				7.76	-23.29
540.5				7.69	-23.32
560.5				7.8	-23.29
580.5	2.43	52	0.617	7.62	-23.53
600.5					
620.5					
640.5	10.64	12	1.401		
660.5					
680.5				7.51	-23.34
700.5	6.58	19	0.979	7.71	-23.48
720.5				7.66	-23.6
740.5				7.56	-23.63

JPC05 DATA CONTINUED

Depth	Pyrite ($\mu\text{mol S/g}$)	Org.C / Pyrite S	DOP	^{15}N (‰)	^{13}C (‰)
760.5	6.34	19	0.719	7.62	-23.69
780.5				7.38	-23.64
800.5				7.25	-23.87
820.5	6.55	18	1.017		
840.5					
860.5	0.90	132	0.214		
880.5					
900.5	2.71	45	0.316		
920.5	2.53	46	0.685		
940.5				7.44	-24.08
960.5	1.17	100	0.129		
980.5				7.51	-24.08
1000.5					
1020.5	0.81	148	0.103	7.32	-24.37
1040.5	0.18	613	0.032		
1060.5	0.81	144	0.162	7.05	-24.45
1080.5	0.61	169	0.087		
1100.5	0.07	1370	0.155	6.51	-24.89
1120.5	0.15	595	0.443		
1140.5	0.42	201	0.150	6.08	-24.97
1160.5	0.89	93	0.220		
1180.5	0.26	299	0.139	5.55	-24.97
1200.5	0.43	164	0.234	5.71	-25.04
1220.5	0.17	432	0.190	5.2	-25.1
1240.5	0.40	156	1.581	5.05	-19.62
1260.5	0.18	330	0.319	4.72	-25.32
1290	2.27	42	0.845	3.47	-25.88
1306	2.16	39	2.767	3.51	-25.16
1330	3.66	25	0.558	3.05	-25.59
1346	1.08	47	34.468	4.69	-25.01
1370	2.14	41	68.462	3.4	-25.44
1394	6.58	18	1.462	1.89	-25.68
1417	2.71	32	0.996	3.25	-25.48
1447	5.97	16	1.044	3.15	-25.69
1471	8.46	14	0.794	2.27	-25.92
1495	8.21	14	0.861	2.02	-26.02
1519	11.83	17	0.988	2.01	-25.69
1535	9.24	10	0.716	6.09	-24.88
1568	34.49	2	0.795	5.89	-24.81
1605	14.24	5	0.618	5.81	-24.95
1631	26.67	3	1.156	5.89	-24.68

APPENDIX G

JPC08 DATA

Depth	Age (ybp)	% Org. N	% Org. C	% Total S	Org C/N	% Biogenic Silica	% Carbonate
9.5	1676.913	0.169	1.593	0.258	11	0.336	0.220
19.5	1946.213	0.170	1.623	0.300	11	0.236	0.210
29.5	2215.513	0.177	1.682	0.250	11	0.220	0.210
39.5	2484.813	0.184	1.749	0.277	11	0.274	0.200
49.5	2754.113	0.170	1.634	0.367	11	0.248	0.190
59.5	3023.413	0.158	1.539	0.261	11	0.284	0.210
69.5	3292.713	0.167	1.627	0.239	11	0.184	0.220
80.5	3588.943	0.161	1.647	0.216	12	0.165	0.230
89.5	3831.313	0.161	1.641	0.267	12	0.289	0.210
99.5	4100.613	0.159	1.637	0.236	12	0.289	0.190
115.5	4531.493	0.176	1.617	0.337	11	0.280	0.230
134.5	5043.163	0.178	1.638	0.892	11	0.401	0.260
150.5	4808.85	0.168	1.638	0.730	11	0.360	0.230
167.5	4858.15	0.179	1.655	0.314	11	0.400	0.230
185.5	4910.35	0.179	1.673	0.350	11	0.295	0.260
203.5	4962.55	0.174	1.622	0.277	11	0.235	0.220
220.5	5011.85	0.164	1.695	0.214	12	0.245	0.220
237.5	5061.15	0.174	1.638	0.456	11	0.248	0.230
254.5	5110.45	0.174	1.688	0.328	11	0.264	0.250
271.5	5159.75	0.155	1.619	0.387	12	0.298	0.260
288.5	5209.05	0.175	1.583	0.539	11	0.288	0.220
307.5	5264.15	0.177	1.693	0.198	11	0.190	0.250
323.5	5310.55	0.179	1.816	0.177	12	0.263	0.230
340.5	5359.85	0.168	1.733	0.261	12	0.256	0.330
358.5	5412.05	0.183	1.712	0.549	11	0.309	0.190
375.5	5461.35	0.183	1.489	0.262	9	0.258	0.240
393.5	5513.55	0.188	1.505	0.302	9	0.241	0.210
410.5	5562.85	0.196	1.585	0.249	9	0.158	0.230
427.5	5612.15	0.188	1.513	0.255	9	0.175	0.250
444.5	5661.45	0.191	1.551	0.416	9	0.195	0.150
462.5	5713.65	0.174	1.598	0.366	11	0.350	0.180
480.5	5765.85	0.187	1.534	0.241	10	0.277	0.200
496.5	5812.25	0.186	1.532	0.202	10	0.195	0.230
515.5	5867.35	0.183	1.655	0.378	11	0.164	0.230
540.5	5939.85	0.188	1.684	0.526	10	0.198	0.210
565.5	6012.35	0.181	1.606	0.178	10	0.287	0.240
591.5	6087.75	0.172	1.569	0.134	11	0.244	0.300
615.5		0.185	1.634	0.295	10	0.316	0.250

JPC08 DATA CONTINUED

Depth	Age (ybp)	% Org. N	% Org. C	% Total S	Org C/N	% Biogenic Silica	% Carbonate
641.5	6157.35	0.168	1.508	0.340	10	0.384	0.290
666.5	6232.75	0.177	1.588	0.214	10	0.309	0.290
691.5	6305.25	0.171	1.573	0.182	11	0.345	0.300
717.5	6377.75	0.163	1.45	0.353	10	0.289	0.270
741.5	6453.15	0.178	1.594	0.200	10	0.260	0.260
766.5	6522.75	0.184	1.654	0.294	10	0.353	0.240
791.5	6595.25	0.167	1.521	0.229	11	0.355	0.270
816.5	6667.75	0.172	1.534	0.218	10	0.170	0.290
842.5	6740.25	0.183	1.676	0.185	11	0.183	0.260
866.5	6815.65	0.172	1.596	0.245	11	0.249	0.300
891.5	6885.25	0.168	1.585	0.167	11	0.236	0.270
916.5	6957.75	0.161	1.577	0.075	11	0.275	0.260
941.5	7030.25	0.161	1.607	0.124	12	0.217	0.300
967.5	7102.75	0.159	1.57	0.156	12	0.168	0.310
991.5	7178.15	0.153	1.589	0.237	12	0.222	0.300
1016.5	7247.75	0.154	1.609	0.052	12	0.168	0.300
1041.5	7320.25	0.152	1.555	0.045	12	0.122	0.310
1066.5	7392.75	0.169	1.7383	0.091	12	0.215	0.143
1092.5	7465.25	0.149	1.651	0.050	13	0.113	0.310
1116.5	7540.65	0.135	1.53	0.054	13	0.178	0.330
1141.5	7610.25	0.168	1.638	0.196	11	0.185	0.260
1167.5	7682.75	0.141	1.408	0.187	12	0.111	0.430
1199.5	7758.15	0.120	1.218	0.163	12	0.081	0.470
1241	7850.95	0.084	0.904	0.001	13		0.56
1281	7971.3	0.086	0.945	0.001	13		0.57
1321	8087.3	0.093	0.969	0.001	12		0.65
1361	8203.3	0.050	0.733	0.001	17		0.82
1395	8319.3	0.072	0.822	0.069	13		0.57

VITA

Carie Curry

Department Ocean Earth and
Atmospheric Sciences
4600 Elkhorn Ave
Norfolk, VA 23529
757-683-4929

1229 Graydon Ave #2
Norfolk, VA 23507
757-963-7344

EDUCATION

Old Dominion University, Norfolk, Virginia

Masters of Science, Ocean and Earth Science, December 2009
Concentration in Chemical Oceanography
GPA 3.4

Old Dominion University, Norfolk, Virginia

Bachelor of Science, Ocean and Earth Science, December 2006
Concentration in Geological Oceanography
Minor- Environmental Health
GPA 3.3

Austin Community College, Austin, Texas

Associate of Science, Geology, August 2004
GPA 3.5

WORK EXPERIENCE

Water Quality Specialist

Supervisor: Jessie DeLuna
Hampton Roads Sanitation District, Virginia Beach, Virginia

05/09 – Present

Graduate Research Assistant

Supervisor: Dr. Gregory Cutter
Department of Ocean Earth and Atmospheric Sciences, Old Dominion University

09/06 – 05/09

FIELD EXPERIENCE

Sea Going:

R/V Knorr- GEOTRACES: 35 day oceanographic expedition for trace metal sampling.
North Atlantic Ocean; June 6- July 12, 2008

R/V Slover- SERDP: 4 days sediment box coring.
Elizabeth River, Virginia; May 2006 and Baltimore Harbor, Maryland; June 2007

PUBLICATIONS

Lingle, C.A., Gipson, B.R., Cutter, G.A., and Cutter, L.S. 2007. Biogenic tracers through the Holocene on the western Arctic shelf. *Eos Trans. AGU*, 88(52), Fall Meet. Suppl., Abstract PP51A-0190.

Lingle, C.A., Gipson, B.R., and Cutter, G.A. 2008. High Resolution Holocene Records of Biogenic Fluxes to the Western Arctic Shelf. *Eos Trans. AGU*, 89(53), Fall Meet. Suppl., Abstract PP11C-1413.